

## PROTEIN REPELLENCY OF GRAFTED PVP AND PEO SURFACES

THE COMPARATIVE PROTEIN REPELLENCY STUDY OF POLYVINYL  
PYRROLIDONE AND POLYETHYLENE OXIDE GRAFTED TO PLASMA  
POLYMERIZED SURFACES

By

SAL THOMAS, BSc (Eng.)

a Thesis

Submitted to the School of Graduate Studies

in Partial fulfillment of the Requirements

for the Degree

Master of Applied Science

©Copyright by Sal Thomas, April 2003

Master of Applied Science  
(Chemical Engineering)

McMaster University  
Hamilton, Ontario

Title: Comparative Protein Repellency Study of Polyvinyl  
Pyrrolidone and Polyethylene Oxide Grafted to  
Plasma Polymerized Surfaces

Author: Sal Thomas, BSc (Eng.) (Queen's University)

Supervisors: Professors Heather Sheardown and John L. Brash

Number of Pages: xiii, 169

## **Abstract**

The objective of this work was to investigate the potential of poly(vinyl pyrrolidone) (PVP) as a protein resistant biomaterial. Two types of PVP surface were studied: (1) plasma polymerized N-vinyl pyrrolidone monomer on polyethylene (PE), and (2) grafted PVP surfaces formed by reaction of the activated polymer with plasma polymerized allyl amine on PE. Surfaces were also prepared by grafting polyethylene oxide (PEO), a known protein repellent, to plasma polymerized allyl amine and for comparison to PVP. The surfaces were characterized chemically by water contact angle and X-ray photoelectron spectroscopy (XPS). Protein interactions were studied using radiolabeled fibrinogen in PBS buffer.

Plasma polymerized N-vinyl pyrrolidone surfaces were prepared in a microwave plasma reactor. Reactions were carried out both at room temperature and at 50°C (increased vapour pressure) in an attempt to increase the extent of plasma polymer deposition. The resulting surfaces showed structures chemically different from conventional linear PVP. XPS analysis suggested the presence of a variety of functional groups, including amines, amides, hydroxyls, carbonyls and urethanes. Mechanisms for the reactions occurring could not be ascertained but it appeared that the monomer was extensively fragmented in the plasma. Although these surfaces were hydrophilic (contact angles of 20 to 30°), they did

not resist fibrinogen adsorption: in fact they showed adsorption levels approximately 10% greater than unmodified polyethylene.

Methods for direct grafting of polyvinyl pyrrolidone and polyethylene oxide to plasma polymerized allyl amine (PPAA) surfaces were designed on the assumption that the PPAA surfaces would be rich in amino groups for reaction with appropriate polymer chain ends. Although there was 8-12% of nitrogen on the surfaces, the C1s high resolution showed that amide and urethane functionalities are also present in addition to amines. The hydroxyl end groups of preformed PEO and PVP chains were activated by reaction with either 1-[3-(dimethylamino) propyl], 3-ethylcarbodiimide and N-hydroxy succinimide (EDC/NHS), and N-N-disuccinimidyl carbonate (DSC). NMR spectra of the products of these reactions showed that for PEO, the yields were moderate, and for PVP, the yields were low. Surfaces grafted using polymers activated with EDC/NHS were more hydrophilic than surfaces grafted with DSC-activated polymers. XPS data did not provide clear evidence that significant polymer grafting had occurred in any of the systems. It was concluded that changes in the allyl amine plasma polymer in different environments following plasma polymerization may affect the efficiency of grafting subsequently. XPS data suggested that the allyl amine plasma surfaces undergo oxidation over time in air. Also the films may be partly removed from the polyethylene surface when placed in buffer as suggested by XPS and contact angle data. Various

parameters were examined in an attempt to improve the allyl amine plasma polymerization process for greater stability of the film. Increasing the treatment time from 10 to 30 minutes gave surfaces that showed a slower change in contact angle when stored in air.

Despite the lack of strong chemical evidence of extensive polymer grafting, all of the grafted surfaces were found to be significantly protein repellent, with reductions of 10 to 36 % compared to unmodified polyethylene. The PEO surfaces were more repellent than the PVP, although the differences were not significant. Surfaces grafted using polymers activated with EDC/NHS were more protein repellent than those grafted with DSC-activated polymers. Protein adsorption was not affected by PVP molecular weight in the range 2,500 to 10,000. Since there is considerable overlap of the molecular weight distributions (MWD) of these two polymers, it is speculated that the MWDs of the grafted polymers may be more similar than those of the polymers themselves, possibly due to "selection" of similar, presumably optimal molecular weights.

Discussion of the possible reasons for the better protein resistance of PEO compared to PVP is given in terms of chain structure in relation to the steric exclusion and water barrier theories of protein repulsion.

## **Acknowledgements**

First, I would to thank my supervisors Dr. Sheardown and Dr. Brash for the opportunity to learn about the biomaterials field, their guidance and patience during the course of this work. I would also like to thank Rena Cornelius, Glenn McClung, Jiahong Tan, Larry Unsworth, Brandi Meeks, Zhangxu Jia, Hong Chen and Lina Liu for their help and encouragement. I would like to thank Brian Sayer and Donald Hughes for help with NMR. I would like to thank Gerry Pleizier and Rana Sodhi for the XPS analysis, especially Rana Sodhi's guidance in understanding XPS. I would like to thank the friends I have made at my time at McMaster, especially Ed Kolodka, Ed Irving and Nadia Scantlebury for their support for my work. Lastly, I owe deep gratitude for the completion of this work to my parents and my sister Cynthia whose endless love and support strengthened me each step of the way.

## Table of Contents

<b>Abstract</b>	<b>iii</b>
<b>Acknowledgements</b>	<b>vi</b>
<b>Table of Contents</b>	<b>vii</b>
<b>List of Figures</b>	<b>x</b>
<b>List of Tables</b>	<b>xiii</b>
<b>Chapter 1. Introduction</b>	<b>1</b>
<b>Chapter 2. Literature Review</b>	<b>5</b>
2.1 Protein Adsorption	6
2.2 Hemostasis	7
2.2.1 Coagulation	7
2.2.2 Fibrinolytic System	9
2.3 Thrombogenicity of Blood Contacting Biomaterials	10
2.3.1 Protein Repellent Surfaces	11
2.3.2 Polyethylene Oxide (PEO) Protein Repellent Surfaces	13
2.3.3 Mechanisms of Protein Repellency by PEO	13
2.4 Poly N-vinyl Pyrrolidone	19
2.4.1 Properties of PVP	19
2.4.2 Applications of PVP in Medicine	21
2.4.3 PVP as a Surface Modifier in Biomaterial Applications	23
2.5 Plasma Polymerization	24
2.5.1 Theory on Plasma Polymerization	24
2.5.2 Plasma Polymerization of Allyl Amine	30
2.5.3 Plasma Polymerization of N-vinyl Pyrrolidone	32
2.6 Project Rationale	36
<b>Chapter 3. Experimental</b>	<b>38</b>
3.1 Preparation of Polyethylene Surfaces for Plasma Modification	38
3.2 Monomer Purification	38
3.3 Plasma Polymerization	39
3.3.1 Microwave Plasma Reactor	39
3.3.2 Plasma Polymerization of Allyl Amine	40
3.3.3 Plasma Polymerization of N-vinyl Pyrrolidone	42
3.4 Polymer Activation for Surface Coupling	42
3.4.1 Polymer Activation with EDC and NHS Chemistry	44
3.4.2. DSC Activation of Polymers	46
3.4.3 Surface Reaction of Aminated Surfaces with Activated Polymers	48



3.5 Nuclear Magnetic Resonance _____	48
3.6 Water Contact Angles _____	49
3.7 X-ray Photoelectron Spectroscopy (XPS) _____	51
3.8 <sup>125</sup> I Radiolabeling of Fibrinogen _____	54
3.9 Protein Adsorption Experiments _____	55
<b>Chapter 4. Results and Discussion: Plasma Polymerization of N-Vinyl Pyrrolidone on Polyethylene (PPNVP) _____</b>	<b>57</b>
4.1 Water Contact Angles _____	58
4.2 XPS Characterization of the PPNVP Surfaces _____	60
4.2.1 Low Resolution XPS Analysis of the PPNVP Surfaces _____	60
4.2.2 High Resolution Analysis of Plasma Polymerized NVP Surfaces _____	65
4.3 Fibrinogen Adsorption on PPNVP Surfaces _____	73
<b>Chapter 5. Results and Discussion: Grafted PVP and PEO surfaces _____</b>	<b>77</b>
5.1 Allyl Amine Plasma Treated Surfaces _____	79
5.1.1 Water Contact Angles of Allyl Amine Plasma Polymerized Surfaces _____	80
5.1.2 X-ray Photoelectron Spectroscopy Analysis of Allyl Amine Surfaces _____	82
5.1.3 General Discussion _____	85
5.2. Aging of Plasma Polymerized Allyl Amine Surfaces _____	90
5.2.1 Surface Analysis of Aged Allyl Amine Surfaces _____	90
5.2.2 Discussion of Changes in Surface Physical and Chemical Properties with Time in Air after Plasma Treatment. _____	94
5.3 Discussion of Changes in Surface Physical and Chemical Properties on Exposure of Plasma Polymerized Surfaces to Buffer. _____	97
5.4 Chemical modification of the polymer chain ends for grafting _____	102
5.4.1 Chemical Modification of PVP and PEO with EDC and NHS _____	103
5.4.2 Chemical Modification of PVP and PEO with DSC _____	111
5.5 Surface Properties of PVP and PEO Modified PE Surfaces _____	114
5.5.1 Water Contact Angles _____	115
5.5.2 XPS Analysis of the Grafted Surfaces Using EDC/NHS-activated Polymers _____	118
5.5.3 XPS Analysis of the Grafted Surfaces Using DSC-activated Polymers _____	124
5.5.4 General Discussion of PEO and PVP Grafting _____	130
5.6 Fibrinogen Adsorption onto the PEO and PVP Surfaces _____	133
5.7 General Discussion of Protein Resistance _____	137
5.7.1 Steric Exclusion Mechanism of Protein Resistance _____	137
5.7.2 Water Barrier Theory _____	141
<b>Chapter 6. Conclusions _____</b>	<b>146</b>
<b>Chapter 7. Recommendations for Future Studies _____</b>	<b>149</b>

<b>References</b>	<b>150</b>
<b>Appendix A. Calculation of the Vapour Pressure of NVP</b>	<b>167</b>
<b>Appendix B. Preparation of PBS Buffer</b>	<b>169</b>
<b>Appendix C. Determination of Free Iodide Content</b>	<b>169</b>

## List of Figures

Figure 2.2.1: Formation of crosslinked fibrin, the basis of a thrombus, as propagated through the coagulation cascade after contact with a material surface.	8
Figure 2.2.2: The fibrinolytic cascade.	10
Figure 2.3.1: Repeat structure of poly(ethylene oxide)	12
Figure 2.3.2: Forces that contribute to the repulsive interactions between a protein and terminally-attached PEO surface with respect to distance.	15
Figure 2.4.1: Repeat unit structure of PVP.	20
Figure 2.4.2: The mesomerism of PVP in water.	21
Figure 2.5.1: Effect of energy parameter on the deposition and physical properties of the plasma polymer obtained.	29
Figure 3.3.1: Simplified schematic of the microwave-cold plasma system containing samples (ex. polyethylene sheets) when in operation.	40
Figure 3.4.1: EDC and NHS activation of PEO and PVP and conjugation with amines.	45
Figure 3.4.2: Reaction scheme of DSC-activation of PEO and PVP, and conjugation with amines	47
Figure 3.6.1: Definition of a contact angle	50
Figure 3.7.1: Dependence of sampling depth in XPS on take-off angle.	53
Figure 3.8.1: Radiolabeling of the tyrosine residue in proteins using the ICI method.	54
Figure 4.1: Water contact angles of surfaces obtained by the plasma polymerization of NVP on polyethylene.	59
Figure 4.2.1: C1s Low resolution XPS results for PE, argon plasma treated PE, and plasma polymerized NVP at room temperature and 50°C.	62
Figure 4.2.2: O1s low resolution XPS results for PE, argon plasma treated PE, and plasma polymerized NVP at room temperature and 50°C.	63
Figure 4.2.3: N1s low resolution XPS results for for PE, argon plasma treated PE, and plasma polymerized NVP at room temperature and 50°C.	64
Figure 4.2.4: C1s High Resolution Spectra at 20° take-off angle of A) Argon; B) PPNVP heated to 50°C; C) PPNVP; D) theoretical PVP.	66

Figure 4.2.5: Composition of the C1s envelope among the argon-treated, and PPNVP surfaces as compared to the theoretical PVP surface.	68
Figure 4.2.6: N1s high resolution spectra of a) PPNVP surface prepared by heating the monomer at 50°C; and b) theoretical PVP.	69
Figure 4.3.1: Fibrinogen adsorption from PBS (pH 7.4) on PPNVP and PE surfaces.	73
Figure 5.0.1: The chemical structure of the repeat unit of PVP	77
Figure 5.0.2: Structures of EDC and NHS.	78
Figure 5.0.3: Structure of DSC.	78
Figure 5.1.1: Water contact angles of allyl amine plasma polymerized surfaces formed under different conditions.	82
Figure 5.1.2: Elemental composition of the allyl amine surface and under its various modifications.	84
Figure 5.2.1: Surface composition of plasma polymerized allyl amine surfaces (10 min treatment) aged for 3 and 11 days.	91
Figure 5.2.2: Water contact angles of plasma polymerized allyl amine surfaces versus time elapsed after plasma treatment.	93
Figure 5.2.3: Composition of the C1s envelope for aged allyl amine plasma polymers.	96
Figure 5.3.1: Composition of C1s peak of allyl amine plasma polymers immersed in buffer.	99
Figure 5.4.1: Proton NMR spectrum of PEO following reaction with succinic anhydride.	104
Figure 5.4.2: Proton NMR spectrum of PVP 2500 following reaction of hydroxy-terminated polymer with succinic anhydride.	106
Figure 5.4.3: Proton NMR spectrum of the carboxylated-PEO after reaction with EDC/NHS.	109
Figure 5.4.4: Proton NMR spectrum of carboxylated-PVP after reaction with EDC and NHS.	110
Figure 5.4.5: Proton NMR spectrum of PEO after reacting with DSC.	112
Figure 5.4.6: Proton NMR spectrum after PVP 2500 reacts with DSC.	113

Figure 5.5.1: Grafting of EDC/NHS activated polymers to allyl amine plasma layer via amide bond formation.	115
Figure 5.5.2: Grafting of DSC-activated polymers to allyl amine plasma layer via carbamate bond formation.	115
Figure 5.5.3: Water contact angles of PEO and PVP modified surfaces (a) polymers activated with EDC/NHS; (b) polymers activated with DSC.	116
Figure 5.5.4: XPS elemental analysis of PEO- and PVP-grafted surfaces. Polymers activated with EDC/NHS.	120
Figure 5.5.5: High Resolution C1s spectra of allyl amine, PEO and PVP (activated by EDC/NHS) surfaces at the 20° take-off angle.	123
Figure 5.5.6: Composition of the C1s envelope of the allyl amine, PEO- and PVP-grafted surfaces activated with EDC/NHS at the 20° take-off angle.	124
Figure 5.5.7: XPS Elemental analysis of PEO and PVP-grafted surfaces. Polymers activated with DSC.	126
Figure 5.5.8: High Resolution C1s spectra at 20° take-off angle of Allyl amine, PEO and PVP (DSC activation).	128
Figure 5.5.9: Composition of the C1s envelope for DSC-activated polymers and allyl amine.	129
Figure 5.6.1: Fibrinogen Adsorption to PEO and PVP surfaces a) EDC/NHS coupling system b) DSC activation system.	134
Figure 5.6.2: Reduction in fibrinogen adsorption compared to PE for both chemical-activating systems at 1mg/mL fibrinogen concentration of PEO and PVP	136
Figure 5.7.1: Space filling structures of left) PEO right) PVP.	143
Figure A1: Determination of the Clausius-Clapeyron relationship for N-vinyl Pyrrolidone.	168

## List of Tables

Table 2.4.1 : PVP's many applications in medicine.	22
Table 5.7.1 Root mean square end-to-end distance and radius of gyration of PEO and PVP.	139
Table A1 Vapour pressures and temperatures for N-vinyl pyrrolidone.	167

## 1. Introduction

A biomaterial's success in the body depends on appropriate interactions, or lack of interaction with the surrounding biological environment. In blood-contacting biomaterials this may entail preventing thrombus formation, immune responses or bacterial colonization from occurring. The initial and precipitating event in all of these phenomena is the adsorption of proteins. Once adsorbed, the proteins change configuration, and may attract cells or may themselves lead to adverse reactions. While biomaterials have seen some success, the adverse reactions that occur following contact of the materials with blood remain in most cases and the need for improvements in blood compatibility remains.

Many types of materials have been used as biomaterials. Metals, ceramics, and polymers have been used in applications ranging from contact lenses to hip and joint replacements and as drug delivery matrices. Polymers are of particular interest due to the widespread availability of materials with different properties including reasonable mechanical properties, good processability and fabricability (Lamba and Cooper, 2001). However, polymers with the greatest mechanical strength are generally hydrophobic and have been shown to cause adverse reactions in the body. Hydrophilic polymers are generally known to reduce protein adsorption and to show greater

“biocompatibility”, but mechanically, tend to be less desirable (Lamba and Cooper, 2001; Tunney et al., 2002). Since protein adsorption is a surface phenomenon, altering the surface of hydrophobic materials has been suggested as a solution to address the improvement of the biocompatibility of polymeric biomaterials.

In theory, surface modification can improve biocompatibility of materials without changing their bulk properties. Surface modification with hydrophilic polymers such as polyethylene oxide (PEO) has been shown in many studies to reduce protein adsorption and cellular interactions. Attachment of antithrombotic agents or cell adhesion molecules for promoting endothelial cell adhesion had also been studied to make a more blood-compatible surface (Lamba and Cooper, 2001). Coatings, blends, and self-assembled monolayers are three techniques used to modify surfaces.

Plasma polymerization is a useful tool in modifying surface properties without changing bulk properties. It is a solvent-free process that can produce thin (a few  $\mu\text{m}$ ), pinhole free films (d'Agostino, 1990; Yasuda, 1990). Plasma polymerization can be used to modify a variety of surfaces with organic or inorganic compounds that cannot be used through other conventional means (d'Agostino, 1990; Yasuda, 1990; Grill, 1994). The plasma polymer can introduce functional groups that can be further coupled to hydrophilic polymers or biological moieties. Plasma polymers can also serve as an interface and have been used



as a surface that supports cell adhesion (Murugesan et al., 2000; Sanborn et al., 2001; Tseng and Edelman, 1998).

Poly N-vinyl pyrrolidone (PVP or PNVP) is known for its biocompatibility and has been widely used in biomaterials applications as a drug delivery system (Kamada et al., 1999; Torchilin et al., 2001) or as a component in hemodialysis membranes (Radovich, 1995; Hoenich and Stamp, 2000). Many studies have focused on its use as an antimicrobial surface (Bridgett et al., 1993; Francois et al., 1996). In the majority of these studies graft polymerization was used to attach polymer chains to a surface. Surfaces produced this way show reduced protein adsorption and bacterial adhesion (Francois et al., 1996; Rovira-Bru et al., 2001; Tunney and Gorman, 2002). Furthermore, plasma polymerized NVP monomer (PPNVP) has been studied as a hydrophilic surface that can support endothelial cell growth (Johnson et al., 1996; Murugesan et al., 2000; Sanborn et al., 2001; Sagnella et al., 1999). However, neither these surfaces, nor those with terminally attached PVP have been extensively studied compared to other polymers that are known to reduce protein adsorption. PEO is the “gold-standard” in reducing protein adsorption due to its flexible chains, and hydrophilicity, and has shown good performance when terminally attached (Brash, 2000; Leckband et al., 1999). There have been many studies to examine how terminally-attached PEO repels protein adsorption, although the mechanism still remains unclear (Leckband et al., 1999; Morra, 2000). Since PVP is a hydrophilic polymer, it is of

interest to study the interactions of PVP surfaces with plasma proteins to better characterize the properties of this material.

In the present work, plasma polymerization of NVP and the covalent coupling of polyvinyl pyrrolidone (PVP) to polyethylene were explored. The plasma polymerization of N-vinyl pyrrolidone on a polyethylene substrate using a continuous microwave plasma reactor was studied to examine the potential of this method for generating surfaces with desirable properties in biomaterials applications, including physicochemical properties and protein adsorption behaviour. These surfaces were compared with covalent grafting of chains of PVP to polyethylene surface. The grafted surfaces were also compared with polyethylene oxide grafted surfaces. Sessile drop contact angles and X-ray photoelectron spectroscopy (XPS) were used to study the physicochemical properties of the modified materials. Fibrinogen adsorption was used to examine the biological properties.

## 2. Literature Review

Biomaterials, defined as “nonviable materials used in medical devices and intended for interactions with biological systems” (Williams, 1987), are widely used in a variety of applications including as prosthetics, as stents, and as drug delivery devices. Crucial to the design and long term success of the device is the biocompatibility of the material or its *ability to perform with an appropriate host response in a specific application* (Williams, 1987). Ratner (1993) further suggests that the biocompatibility of a material should involve the exploitation of proteins and cells in the body, allowing the material to meet a specific performance goal. In essence, the material should interact with the biological system through the cells and other components, resulting in the same reactions that would occur in the native tissue (Ratner, 1993). These interactions occur in response to the chemical and physical characteristics of the material surface. Undesirable responses to the material may lead to such conditions as blood vessel occlusion or infection (Janatova, 2000; Ratner, 1993; Horbett and Brash, 1995; Lamba and Cooper, 2001). The manipulation of these interactions can be used to generate more biocompatible materials.

## 2.1 Protein Adsorption

Protein adsorption, the first dynamic event in material-tissue interactions occurs mainly at the surface. The type of host response depends on the nature of the biological system. In the case of blood-material applications, one of the most important potential results is thrombus formation. However, adsorption of and activation of plasma proteins may also initiate subsequent events, including formation of a biofilm by bacteria (Janatova, 2001), inflammation, and cellular interactions such as adhesion, spreading and growth (Lamba and Cooper, 2001; Horbett and Brash, 1995).

Proteins are large amphipathic molecules that perform many functions including acting as structural elements (in the extracellular matrix), facilitating the transport of ions, hormones, gases etc., acting as nutritional sources, and as catalysts in biochemical reactions. When proteins adsorb to a surface, they often change conformation. The properties of the surface then become dependent on the properties of the adsorbed layer, in particular the composition, surface coverage, and biological status of the protein (Brash, 2000). This new surface may trigger many additional biological phenomena. The adsorption of proteins can be reversible and is generally more extensive on hydrophobic surfaces than on hydrophilic ones (Horbett and Brash, 1995; Brash, 2000). Competition also exists between proteins due to differences in affinity for various surfaces and the protein's inherent instability (Brash, 2000). The three major proteins studied in the field of biomaterials are albumin, fibrinogen and immunoglobulin G (IgG),

primarily due to their high relative concentrations in blood. IgG is an immune protein and plays a role in the complement cascade, a process activating the body's defense mechanisms (Janatova, 2001). Fibrinogen plays an important role in thrombosis and hemostasis, and its adsorption is associated with thrombogenicity and platelet activity (Lamba and Cooper, 2001). Albumin, the most abundant protein, has been suggested to passivate surfaces; surfaces that adsorb high levels of albumin have been shown to display lower platelet adhesion (Lamba and Cooper, 2001).

## **2.2 Hemostasis**

Hemostasis, the stoppage of blood flow, is primarily responsible for maintaining the integrity of the vasculature following damage until healing can occur. It is accomplished through two synergistic processes: fibrin formation and platelet aggregation (Davie et al., 1991). In sealing a wound, fibrin connects platelets in the evolving thrombus (Colman, 2001). Fibrin formation is propagated through coagulation and regulated by fibrinolysis.

### **2.2.1 Coagulation**

Coagulation results in the formation of a fibrin plug, maintaining the flow of blood during the healing period. This cascade, depicted in Figure 2.2.1, consists of a series of inactive proenzymes that are converted to active forms, ultimately in the conversion of the proenzyme prothrombin to the active form, thrombin. Thrombin is a pivotal protein in the cascade, mediating the conversion of soluble fibrinogen to insoluble fibrin, which polymerizes and is crosslinked by active

factor XIII, to form a stable clot. Thrombin also plays a feedback role in the cascade, amplifying the response (Carmeliet and Collen, 1997) and can activate platelets. The cascade can be initiated by two mechanisms either by contact of the plasma proteins with a damaged subendothelium or by contact with a foreign substance, including a biomaterial.

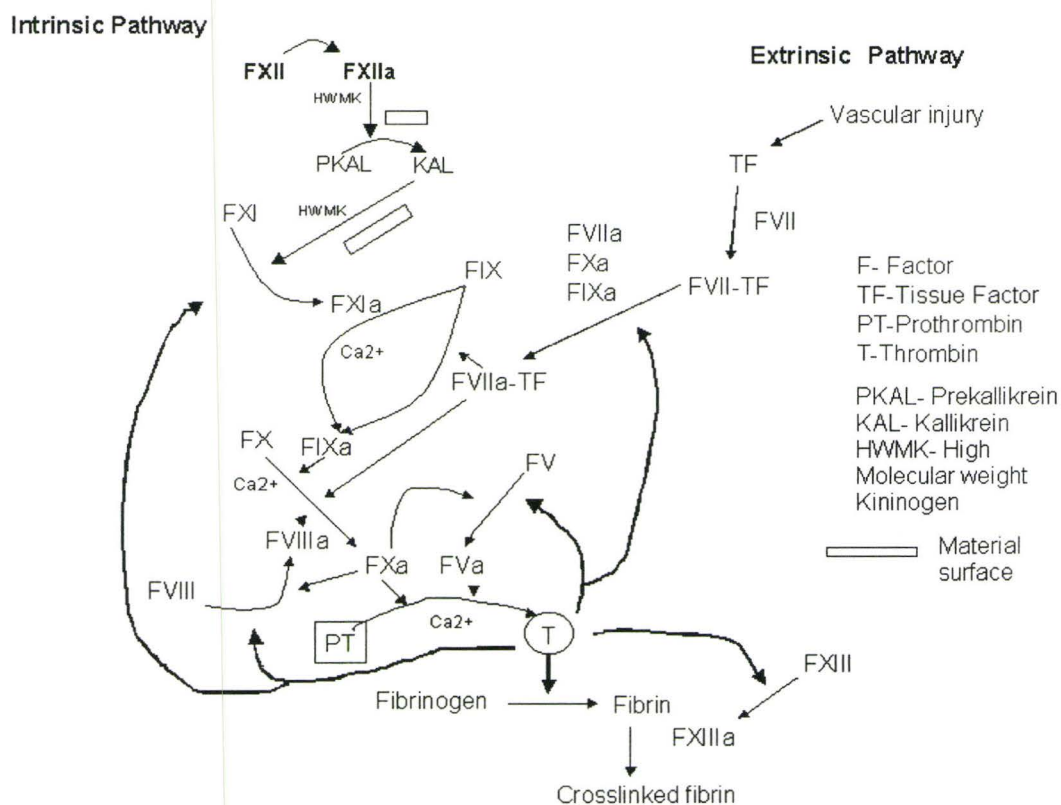


**Figure 2.2.1: Formation of crosslinked fibrin, the basis of a thrombus, as propagated through the coagulation cascade after contact with a material surface. Adapted from Davies et al., (1991). Thrombin (T) is pivotal as it activates fibrinogen to the clot material fibrin, amplifies the coagulation process, and initiates some regulatory processes.**

In biomaterials science, the intrinsic pathway or contact phase activation is of greater importance since it can be initiated when blood contacts an artificial

surface. Factor XII (Hageman factor), high molecular weight kininogen (HMWK) and plasma prekallikrein are among the first proteins adsorbed (Lamba and Cooper, 2001; Davies et al., 1991) and subsequently activate the other proteins in the intrinsic pathway. Tissue Factor activates the extrinsic pathway, but is primarily present at sites of injury (McVey, 1999).

To regulate coagulation, thrombin also stimulates its inhibitors, particularly antithrombin (AT). Thrombin is also involved in regulating the amplification of the coagulation cascade, binding thrombomodulin to activate protein C which, along with protein S inactivates factors X and V that promote thrombin activation (Carmeliet and Collen, 1997).

### **2.2.2 Fibrinolytic System**

The fibrinolytic system is responsible for limiting the extent of coagulation by breaking down fibrin and removing dispensable clots (Carmeliet and Lijnen, 1991). The critical step in fibrinolysis occurs with the activation of plasminogen to plasmin which degrades fibrin to soluble fibrin degradation products (Angles-Cano, 1994). Two types of activators, tissue-type plasminogen activator (t-PA) and urokinase plasminogen activator, are both potentiated by fibrin and catalyse the conversion of plasminogen. Figure 2.2.2 illustrates the mechanism of fibrinolysis. Inhibitors, including plasminogen activator inhibitor (PAI), which inhibits t-PA, and anti-plasmin, which inhibits plasmin, control this process both through the activators and more directly through plasmin (Collen and Lijnen, 1991). As well, thrombin bound to thrombomodulin can activate thrombin-

activated fibrinolytic inhibitor (TAFI), which prevents premature dissolution of a newly-formed fibrin plug (Nesheim et al., 1997).

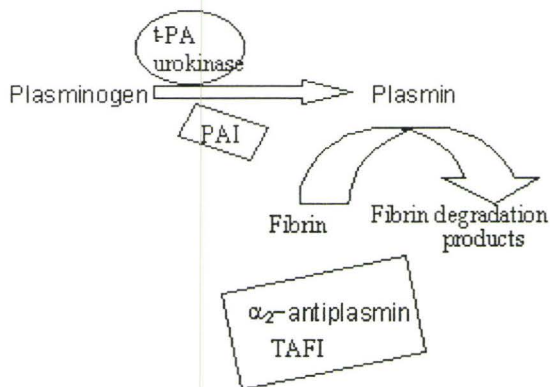


Figure 2.2.2: The fibrinolytic cascade. Adapted from Collen and Lijnen, 1991.

### 2.3 Thrombogenicity of Blood Contacting Biomaterials

The success of a material used in blood contacting applications is determined in most cases by the thrombogenic response initiated by plasma protein adsorption, which can lead to such deleterious effects as infection (Janatova, 2000) and blood vessel occlusion (Lamba and Cooper, 2001). Since biocompatibility is primarily determined by interactions of the material surface with the surrounding tissue (Brash, 2000; Lamba and Cooper, 2001; Horbett and Brash, 1995; Ratner, 1993; Ratner et al., 1990), surface modification of materials is widely used to improve biological properties. Since protein adsorption has been touted as the initial and fate-determining step in blood-biomaterials interactions, methods of developing surfaces that repel the non-specific adsorption of proteins have been widely studied.



### 2.3.1 Protein Repellent Surfaces

A number of factors have been suggested to play a role in repelling nonspecific protein adsorption to surfaces (Jeon et al., 1991; McPherson et al., 1998, Szleifer, 1997a; Leckband et al., 1999, Morra, 2000). It has been suggested that surfaces with a higher degree of hydrophilicity tend to be more protein repellent (Horbett and Brash, 1995). Hydrogels and hydrophilic polymers including poly (vinyl alcohol) (Rabinow et al, 1994, Ratner et al., 1978), poly (ethylene glycol) (Du, 2001; Sofia et al., 1998; Antonsen and Hoffman, 1992), poly (hydroxyethyl methacrylate) (Ratner et al., 1978), and poly (vinyl pyrrolidone) (Higuchi et al., 2001; Rabinow et al., 1994) have been shown to have reduced protein adsorption relative to more hydrophobic materials (Rabinow, 1994; Bohnert et al., 1988). While hydrogels in their pure form are mechanically weak (Tunney and Gorman, 2002; Rabinow et al, 1994), surfaces with terminally attached hydrophilic polymers and hydrogels have shown promising results in limiting the nonspecific adsorption of proteins (Leckband et al. 1999; Kingshott et al., 2002, Rovira-Bru et al., 2001; Sofia et al., 1998). Factors including polymer chain length, flexibility, and graft density have been cited as important determinants of the degree of passivation (Brash, 2000; Leckband et al., 1999; Szleifer, 1997a,b; Jeon et al., 1991; Jeon and Andrade, 1991; Harder et al., 1998).

### 2.3.2 Polyethylene Oxide (PEO) Protein Repellent Surfaces

Polyethylene oxide (PEO) or polyethylene glycol (PEG) has been shown to have particular promise in this capacity and as such may be considered the “gold-standard” in resisting protein adsorption (Morra, 2000). PEO is formed by anionic polymerization of ethylene oxide (Harris, 1992). Its chemical structure is shown in Figure 2.3.1. PEO has an inverse solubility-temperature relationship in which the PEO clouds on heating; temperatures between 95-135°C cause precipitation of PEO at molecular weights between 7 million and 5000 respectively in water. The addition of salts may lower this precipitation temperature (Bailey and Koleske, 1976).

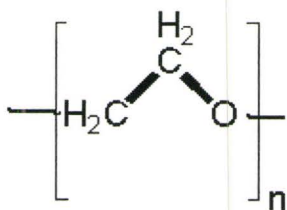


**Figure 2.3.1 Repeat structure of polyethylene oxide**

PEO has been widely used both as a coating and for the surface modification of many materials for use in medical and other applications where protein resistance is desired (e.g. Du et al., 2001; Harris, 1992; Kingshott et al., 2002). PEO-modified surfaces have also been cited in many patents as having protein repulsive properties (e.g. Timmons et al., 2002; Yang et al., 2001; Winters et al., 1993). Various factors including PEO chain length and surface density have been cited as affecting these protein repulsive properties. Dense

oligoethylene oxide chains with as few as three ethylene oxide segments have been found to resist protein adsorption effectively (Harder et al, 1998). PEO molecular weights of up to 10,000 (Sophia et al., 1998) have been examined and found to reduce the adsorption of plasma proteins. Most studies agree that a high density of PEO chains is necessary for a high degree of protein repellency (Morra, 2000; Leckband et al., 1999; Szleifer, 1997a; Lopez et al., 1992; Harder et al., 1998). However, it must be noted that complete inhibition of protein adsorption may not be achievable, since some protein adsorption has been found on all surfaces prepared to date (Tsai et al., 1999, Tsai et al., 2002). It has been suggested that if fibrinogen adsorption is less than 5 ng/cm<sup>2</sup>, platelet adhesion may not be significant. As such, this level may be considered a design criterion for blood compatibility (Tsai et al., 1999, Tsai et al., 2002).

### **2.3.3 Mechanisms of Protein Repellency by PEO**

A number of models have been proposed to understand the mechanisms by which PEO modified surfaces inhibit the adsorption of proteins. The adsorption of proteins to surfaces is thermodynamically and kinetically controlled. Attractive forces for protein adsorption include van der Waals and electrostatic forces. These forces contribute to a decrease in enthalpy as the protein approaches the surface. Furthermore, as the protein approaches the surface, the ordered surface water layers are disrupted, resulting in an increase in entropy (Leckband et al., 1999). Thermodynamically, the balance of enthalpic and entropic terms drives protein adsorption. The kinetics of protein adsorption are

believed to be diffusion controlled in many situations (Leckband et al., 1999; Jeon et al, 1991; Szleifer, 1997a).

When surfaces are modified with hydrophilic polymers such as PEO, it is believed that steric repulsive and osmotic forces can overcome the attractive interactions (Jeon et al., 1991; Szleifer, 1997a; Halperin, 1999; Leckband et al, 1999). Figure 2.3.2 illustrates the short and intermediate-range forces that are important when a protein approaches a surface with attached PEO chains. As can be seen in Figure 2.3.2, a protein far from the surface experiences no net force. As the protein approaches the surface, attractive forces including van der Waals and the electrostatic forces are driving forces for protein adsorption. Depending on the interface, at some distance from the surface, the protein will experience a repulsive force due to the presence of the PEO, inhibiting further movement toward the surface (Leckband et al., 1999; Jeon et al., 1991; Szleifer, 1997a). This occurs when a surface has a high graft density of PEO chains where the distance between chains is smaller than the Flory radius (brush regime) (Leckband et al, 1999; Jeon et al., 1991).

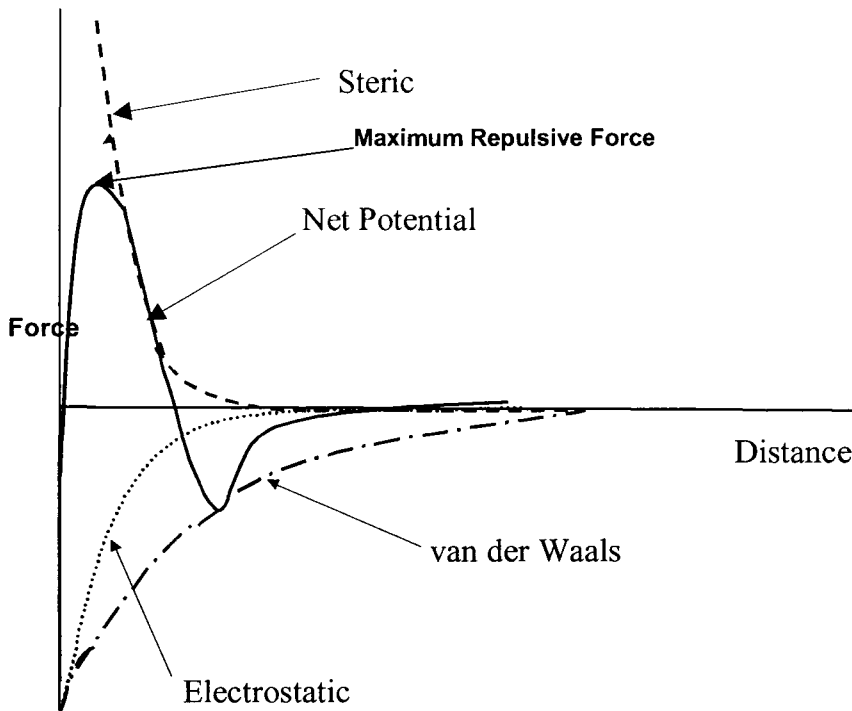


**Figure 2.3.2: Forces that contribute to the repulsive interactions between a protein and terminally-attached PEO surface with respect to distance. The repulsive forces, thought to be mainly the steric barrier, contribute to a protein repellent surface. The maximum of the net potential represents the point where the compressed chain exhibits the greatest repulsive force. The minimum of the net potential occurs at the edge of PEO brush. Adapted from Leckband et al., 1999.**

Steric repulsion is thought to play a crucial role in controlling of protein adsorption on PEO surfaces (Leckband et al., 1999; Jeon et al., 1991). It has been shown that altering the PEO molecular weight or the grafting density can substantially reduce this steric energy barrier (Efremova et al., 2001). It is thought that long grafted polymer chains prevent the protein from approaching the surface, thus limiting the attractive forces. Polymer chain compression and osmotic repulsion are the major factors involved as the protein moves toward the surface (Leckband et al., 1999, Halperin, 1999). Through the presence of the polymer chains, the attractive forces for protein adsorption are believed to be

overcome by an osmotic penalty due to the increase of polymer segment concentration and loss of water molecules that result to an increase in osmotic pressure (Szeleifer, 1997a; Halperin, 1999; Leckband et al., 1999). At high graft density, the polymer chains extend into solution, thus creating a brush-like layer of PEO (McPherson et al., 1998; Halperin et al., 1999, Jeon et al., 1991).

The kinetic factors for protein adsorption, related to polymer chain length and chain density, are also important. Polymer chains of high molecular weight increase the local viscosity. Relatively long polymer chains are believed to inhibit the diffusion of the protein toward the surface, although a high density is required to achieve an effective PEO layer. A high density of long chains may slow the protein's approach to the surface (Leckband et al., 1999).

This steric barrier is affected by polymer architecture. To resist protein adsorption, it has been suggested that the polymer should be flexible (able to adopt many conformations), not fully compressible, and relatively small to allow for packing constraints (Szeleifer 1997b, Leckband et al., 1999; Halperin, 1999). PEO is a flexible molecule due to its carbon-carbon-oxygen backbone, and its small monomer size (0.3 nm) facilitates achievement of high graft density on a material surface (Szeleifer, 1997b; Morra, 2000). In addition, PEO is considered to have the weakest van der Waals interactions with proteins among water-soluble polymers (Jeon et al., 1991).

It has been suggested that this model may explain the protein repellency of PEO with a molecular weight of 2000 or higher (Antonsen and Hoffman, 1992;

Szleifer, 1997a). However, adsorption may be independent of these factors for higher molecular weight polymer chains (Szleifer, 1997a, Sofia et al., 1998). The use of higher molecular weight polymer may limit the graft density due to kinetic barriers (Halperin, 1999, Sofia et al., 1998). As a result, a low graft density may allow smaller proteins to cross the PEO barrier and adsorb to the material surface. However in light of the work of Sofia et al. (1998), it may be that high surface coverage by the polymeric units blocks potential protein adsorbing sites (Szleifer, 1997a, McPherson et al., 1998; Sofia et al., 1998).

The major limitations of the above model are related to its overly simplified approach to complex systems. An important limitation is the assumption the polymers are structureless flexible chains (Leckband et al, 1999). This model may not suitably explain the repulsion of proteins by more rigid polymers such as dextran (De Sousa Delgado et al., 2001; Fournier et al., 1998). Additionally, the chemical interactions of the polymer moieties with the surface and with the environment, as well as polymer specific behaviour (for PEO, the upper and lower critical solution temperature and the ability to self-assemble into helices) are not accounted for by this model. Furthermore, the model all but dismisses the role of water, which has been suggested to be important with PEO in particular (Morra, 2000; Leckband et al., 1999, Halperin, 1999). While the protein resistance of these materials cannot be attributed uniquely to their ability to bind water, water may play an important role in the protein resistant properties of PEO surfaces (Morra, 2000; Vogler, 1998; Halperin, 1999). The water structure may

vary around materials with varying hydrophilicity, therefore adding an additional repulsive hydration force that may contribute to protein repellency (Vogler, 1998). Finally, the model assumes that proteins are simple colloidal particles and overlooks their complex structure. These factors may also contribute to protein repellent behaviour (Morra, 2000; Leckband et al., 1999; Halperin, 1999; Szleifer, 1997a,b).

A variety of studies illustrate the inadequacy of this model. Plasma polymerization of tetraglyme (Lopez et al., 1992), triethylene glycol monoallyl ether (Beyer et al., 1997) and diethylene oxide vinyl ether (Wu et al., 2000) also produced surfaces that were nonfouling. Similarly, self-assembled monolayers of oligomeric PEO (3-6 ethylene oxide units) on gold were shown to be highly protein repellent (Harder et al, 1998), demonstrating that high molecular weights are not necessary for protein rejection to occur. Conformation has not been fully addressed by the models previously discussed (Harder et al., 1998; Efremova et al., 2001). Harder et al. (1998) compared conformations of these oligomers, and found that the amorphous and helical conformations were more resistant than the trans conformation. The helical conformation was postulated to bind water more tightly. The steric repulsion model ignores possible attractive interactions between PEO (or other potential macromolecules used for grafting) and proteins although some such interaction has been reported (Abbott et al., 1992; Sheth and Leckband, 1997; Xia and Dubin, 1993). Szleifer (1997b) and McPherson et al. (1998) reported that after an initial drop in protein adsorption, the amount of



protein adsorbed on PEO brush-type surfaces seemed to approach a lower limit at high surface coverage of PEO. It is believed that this “irreducible” adsorption may occur at the outer surface of the brush due to the interactions of the protein with PEO (McPherson et al., 1998; Halperin, 1999).

## **2.4 Poly N-Vinyl Pyrrolidone**

### **2.4.1 Properties of PVP**

Poly N-vinyl pyrrolidone (PNVP or PVP) (Figure 2.4.1) has been used in both the pharmaceutical industry and in the biomedical field in drug delivery and biomaterials applications, and has been suggested to have protein repellent properties. Poly N-vinyl pyrrolidone (PVP) is synthesized from the monomer, N-vinyl pyrrolidone (NVP), by radical polymerization using such initiators such as hydrogen peroxide (Haaf et al, 1985, Rovira-Bru et al 2001) and azo bis-isobutyronitrile (Mu et al. 1999, Raghunath et al., 1985). Since solvent participates in the initiation step, the solvent moieties are incorporated into the resulting polymer as the end group (Haaf et al., 1985). Radiation, persulphate, hydrazine and hydrogen peroxide are commonly used to crosslink the polymer. More densely crosslinked PVP can be obtained by co-polymerizing the monomer with multiple unsaturated compounds (Haaf et al. 1985). PVP can be obtained with molecular weights between 1000 and 1 million Da.

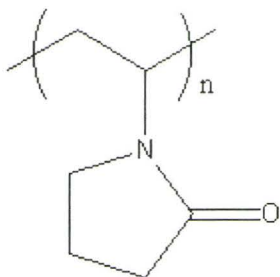


**Figure 2.4.1: Repeat unit structure of PVP**

PVP interacts with many ions (Guner, 1996; Guner and Ataman, 1994) and organic compounds (Eliassaf and Eriksson, 1960; Lerner et al, 1968). It is known to complex with iodine (Schenck et al, 1979), and in this form has been used in antiseptis applications. Also, aqueous solutions of PVP demonstrate a lower critical solution temperature, and tend to 'cloud' at temperatures between 15°C and 65°C (Guner 1996; Guner and Ataman 1994). PVP binds to many dyes (Takagishi and Kuroki, 1973), and to surfactants including SDS (Arora et al, 1998; Bauduin et al., 2001; Majhi et al, 2001; Fishmann and Eirich, 1971; Klotz and Shikama, 1967).

In hydrogel form, PVP has high oxygen permeability ( $9 \pm 0.4 \times 10^{-10}$  cm<sup>2</sup>/s for M<sub>w</sub> of 40 000 at 30% humidity [Pettrak and Pitts, 1980]), high water absorption (18% moisture content at 50% humidity [Robinson et al., 1990]), and low cytotoxicity (Higa et al.; 1999). The lactam moiety contributes to hydrophilicity and stability (Garrett et al., 2000) and to the possibility of a complex hydrogen bonding network with water (Guner, 1996; Sun and King, 1996). Takagishi and Kuroki (1973) proposed a mechanism for interaction with water as shown in

Figure 2.4.2. Many studies (Guner, 1996; Sun and King, 1996; Guven and Eltan, 1981) have added to the understanding of the lactam's interaction with water.

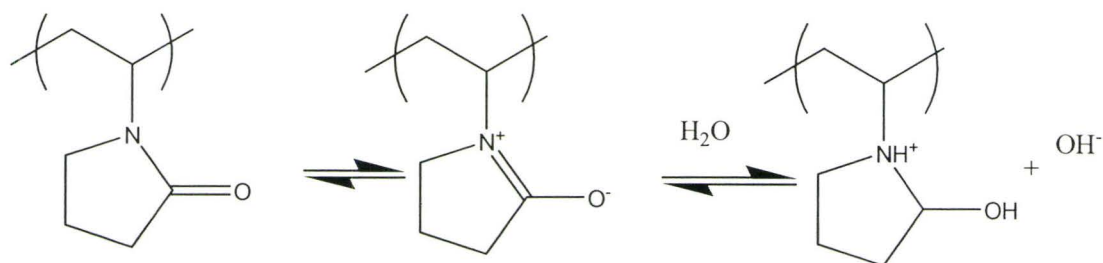


**Figure 2.4.2: The mesomerism of PVP in water. Adapted from Guner, 1996**

### 2.4.2 Applications of PVP in Medicine

As shown in Table 2.4.1, polyvinyl pyrrolidone has been used in many applications in medicine. As a result of its application as a blood substitute and plasma expander, the interactions of PVP with blood and other fluids have been widely studied. High molecular weight PVP, like PEO has been shown to prolong the activated partial thromboplastin time (aPTT), decrease factor VIII activity and prolong thrombin time in solvent/detergent treated plasma (Bakaltcheva et al, 2000). The former two are a measure of a fibrin clot forming via the intrinsic pathway while the latter is a measure of functional fibrinogen (Bakaltcheva et al. 2000). PVP has also been reported to interfere with the fibrin polymerization process (van Gelder, 1996). While these measurements of coagulation are crude, the results seem to suggest that PVP has potential for use as a biomaterial with a low level of thrombogenicity.

In drug delivery applications, the covalent attachment of PVP to peptides results in longer plasma half-lives similar to PEO (Mu, 1999; Kamada et al,

1999). Tumor necrosis factor- $\alpha$  (TNF- $\alpha$ ) coupled to PVP showed a longer blood residency time and higher activity in the body than the PEO-conjugated growth factor (Kamada et al., 1999). Covalent attachment of PVP ( $M_n$  6000) to YIGSR, a laminin-related peptide was found to increase blood residency time relative to either native YIGSR or YIGSR-PEO  $M_n$  5000 (Mu et al., 1999). The authors suggest that these PVP and PEO effects result from inhibition of protease attack and that the effects are similar for the two polymers.

**Table 2.4.1: Applications of PVP in medicine**

Reference	Application	Purpose
Malet et al 1998	Prosthetics	Prosthesis for epiphora Coatings for Cardiac pacing leads
Garrett, 2000 Matteo and Ratner (1989)	Eyes	Soft contact lenses Intraocular lenses
Kao et al. (1997)	Adhesives	Bioadhesives, wound dressings
Mu et al., (1999) Torchilin et al. (2001)	Drug delivery tools	Stabilizer for peptides Liposomes
Wiese et al. (2000) Raghunath et al. (1985) Bakaltcheva et al., 2000	Fluid substitute	Tissue expander Blood expander Blood substitute Cryoprotectant
Radovich et al, (1996) Chen and Belfort (1999) Higuchi et al. (2001) Rovira-Bru et al.(2001) Pieracci et al. (1999 ) Hoenich and Stamp (2000)	Dialysis/filtration	Component of the membrane (by covalent bonding or blending) Dialysate

### **2.4.3 PVP as a Surface Modifier in Biomaterials Applications**

Because of its relative biocompatibility and hydrophilicity, PVP has been incorporated into biomaterials as coatings or as terminally attached chains. The bipolar nature of the lactam, which is thought to contribute to hydrogen bonding interactions with water (Garrett et al., 2000; Guven and Eltan, 1981), is believed to modulate the interactions of PVP with proteins. Using PVP as a component in surfaces has been found to reduce bacterial cell adhesion (Tunney and Gorman, 2002; Francois et al., 1996; Bridgett et al., 1993) and protein adsorption (Higuchi et al., 2002; Francois et al., 1996; Rovira-Bru et al., 2001, Chen and Belfort, 1999; Desai and Hubbell, 1991, Robinson and Williams, 2002). The surface density was found to be the key factor determining the performance of the surfaces.

PVP has been graft-polymerized onto surfaces photochemically (Pieracci et al.1999), using  $\gamma$ -ray irradiation (Boffa et al, 1977), by chemical modification (Higuchi et al. 2002; Rovina-Bru et al, 2001), and using plasma-induced polymerization (Chen and Belfort, 1999) to reduce protein adsorption. Poly(ether sulphone) dialysis membranes incorporating PVP show improved performance, maintaining the same solute flux (Higushi et al. 2002, Chen and Belfort, 1999) with up to 50% reductions in protein fouling (Pierracci et al., 1999). Some of the protein was reversibly adsorbed, since cleaning with water helped to maintain the flux of the modified membranes (Chen and Belfort, 1999; Pieracci et al., 1999).

Higuchi et al. (2002) reported a significant reduction in fibrinogen adsorption as well as platelet adhesion on PVP modified membranes.

Steric repulsion has been commonly used in explaining the protein repellency of PVP. Rovira-Bru et al. (2001) modified zirconia particles with PVP with an estimated molecular weight of 15 000, and obtained a “brush” structure that reduced the adsorption of lysozyme. Decreases in lysozyme adsorption occurred with increasing graft density in accordance with the steric repulsion mechanism. Robinson and Williams (2002) examined albumin adsorption on layers of high molecular weight (10 000 to 1 200 000) PVP adsorbed to silica. Significant reductions in albumin adsorption were seen, attributed to steric repulsion and the blocking of protein adsorption sites.

## **2.5 Plasma Polymerization**

### **2.5.1 Theory on Plasma Polymerization**

Plasma polymerization uses cold plasmas to modify surfaces to form, under optimal conditions, thin, pinhole-free crosslinked films (Yasuda, 1976). The advantage of this technique is that the surface properties of a material may be altered without changing the properties of the bulk. Plasma deposited layers range in thickness from under hundred to a few thousand angstroms, even with low exposure times (Hollahan and Stafford, 1969). In comparison, ionizing,  $\beta$ - or  $\gamma$ -irradiation procedures penetrate more deeply into the bulk (Grill, 1994; Hollahan and Stafford, 1969). Because of these characteristics, the plasma

deposition process is important to microcircuit technology, treatment of metals (Beamson et al., 1985), and the focus of this work, biomaterials.

Plasma is defined as the fourth state of matter, and is made up of ions, radicals, photons and molecules (Grill, 1994; Boenig 1982; Yasuda, 1976). Plasmas exist in many forms in nature (Grill, 1994; Beamson et al., 1985) and can be either hot (thermal) or cold. Hot plasmas exist when all species are highly energetic ( $10^6$ - $10^8$  K), and the electrons and heavier particles reach the same thermodynamic equilibrium. Cold plasmas exist at low pressures and the system is not in equilibrium. The electrons are at a higher energy level than heavier particles and are therefore at higher temperatures ( $10^4$ - $10^5$  K), than the rest of the plasma which is at room temperature (Beamson et al., 1985; Grill, 1994; Boenig, 1982). Cold plasmas can be used to cause chemical reactions with gases at relatively low temperatures.

Sources available for the generation of cold plasmas include direct current, radio-frequency, and microwave frequency generators. These sources can be operated at a variety of different conditions. Radio-frequency, the most frequently used generators for cold plasmas, operates at a frequency 13.56 MHz. Microwave frequency generators operate at high frequencies, typically 2.45 GHz. Although only a few studies are available comparing microwave- and radio-frequency generated plasmas, it is believed that the chemical structure of the “monomer” fed to the plasma is better preserved with microwave plasmas (Wickson and Brash, 1999; Sodhi et al., 2001; Moisan and Wertheimer, 1993;

Beamson et al, 1985; Chun et al., 2000; Keil et al, 1998). Additionally, microwave plasma systems have been reported to generate surfaces of greater uniformity, and give better control of the generation of ions and radicals, as well as higher better deposition rates (Chun et al., 2000; Beamson et al., 1985, Moisan and Wertheimer, 1993). Plasma polymers produced from microwave-generated plasmas seemed to have more effective barrier properties than those produced from radio-frequency-generated plasmas (Sodhi et al., 2001).

Plasmas can be used to modify surfaces in two ways: plasma treatment and plasma polymerization. In plasma treatment, the plasma is used to break bonds on the surface of the substrate resulting in etching of the surface and removal of surface material such as contaminants. Free radicals can also be formed. Gases such as ammonia, nitrogen, or helium can accomplish plasma treatment by crosslinking the substrate in the near surface region (Chan et al, 1996). While plasma treatment does not create a polymer film, it may be used to introduce functional groups onto the bare substrate.

In plasma polymerization, a film is deposited onto the substrate using an organic monomer (Yasuda, 1976; Yasuda, 1990). Plasma polymerization can occur via two methods: plasma-induced polymerization and direct plasma polymerization. Plasma-induced polymerization occurs after the plasma reaction of argon or other gases introduces radicals at the surface. After the plasma is extinguished, the monomer reacts with these radicals on the surface, absorbing radiation emitted from the plasma and undergoing conventional polymerization



(Yasuda, 1976; Epailard and Brosse, 1989). Plasma-induced polymerization can be used as a means to 'lock-in chemistry' while in direct plasma polymerization, surface properties can be lost (Chen and Belfort, 1999). Direct polymerization occurs when the polymerization of the desired monomer occurs in the vapour phase upon creation of the plasma; the polymer is subsequently deposited on the surface. However, the plasma-induced polymerization process contributes to the production of plasma polymers from direct plasma polymerization when the plasma is extinguished if available monomer remains (Yasuda, 1976). The result of direct polymerization is the formation of a mixed and often chemically ill-defined surface.

While mechanisms of plasma polymerization have been proposed, the reactions that lead to polymer formation remain unclear (Yasuda, 1976; O'Toole et al., 1997). Similar to other polymerization processes, there are 4 steps: initiation, propagation, termination and reinitiation (Yasuda, 1990). Initiation occurs when free radicals or ions from the plasma collide with each other in the gas phase or by adsorption on the surface of the substrate. Propagation occurs when these radicals and ions form growing polymers with reactive ends. This can occur both in the gas phase and on the modified surface. Termination is similar to propagation (Grill, 1994), but the collisions result in the formation of neutral non-radical species. Reinitiation results from the formation of new radicals/ions in the plasma bombarding a terminated molecule (Grill, 1994).

Hydrogen abstraction can also occur, terminating living radicals (Fally et al., 1995; Li and Netravali, 1992; Gengenbach and Griesser, 1999).

Many radicals become trapped in the plasma polymer affecting the kinetics of plasma polymerization as well as the final chemistry and the stability of the plasma polymers (Yasuda, 1990). Attempts to track the lifetime of the radicals suggested that they may penetrate deeply through the substrate (Yasuda, 1976; Tseng and Yasuda, 2002). Radicals remaining on the surface can react with atmospheric oxygen as soon as the surfaces are removed from the reactor (Tseng and Yasuda, 2002) and may form peroxides (Mas et al., 1997). The duration of radical quenching can be from 1 hour following removal (Tseng and Yasuda, 2002) to many days or weeks (Boenig, 1982; Jama et al., 1996). This process is controlled by the diffusion of air and water (Wrobel, 1985; Gengenbach and Griesser, 1999) and may be dependent on the plasma operating conditions and monomer structure (Yasuda, 1990).

The operating conditions of the plasma reactor also affect the physical and chemical properties of plasma polymers, resulting in polymers very different from those expected based on the chemical structure of the monomer (Yasuda, 1976; Yasuda, 1990). Reactor geometry including substrate position, temperature, and power are few of the parameters that can be varied to alter the composition of the resultant surface. Yasuda (1976, 1990) determined that the rate of deposition ( $R$ ) varies linearly with time and depends critically on three

parameters: input power (W), flow rate of monomer (F), and monomer molecular weight (M) according to the following relationship that is valid for most reactors:

$$R \propto \frac{W}{FM} \quad (2.5.1)$$

The properties of the film and the rate of deposition depend on the value of the W/FM energy parameter. The energy parameter affects the tendency of the plasma polymer to be produced as a powder, oil or film. Figure 2.5.1 illustrates the relationship between this parameter and deposition rate and indicates the processes that dominate as W/FM varies (Beamson et al., 1985). The use of low flow rates or high power levels cannot support the plasma and can fragment the monomer greatly (Beamson et al., 1985, Dilsiz and Akovali, 1996) resulting in plasma etching or ablation. This competes with film formation and results in a polymer completely unlike the starting monomer.

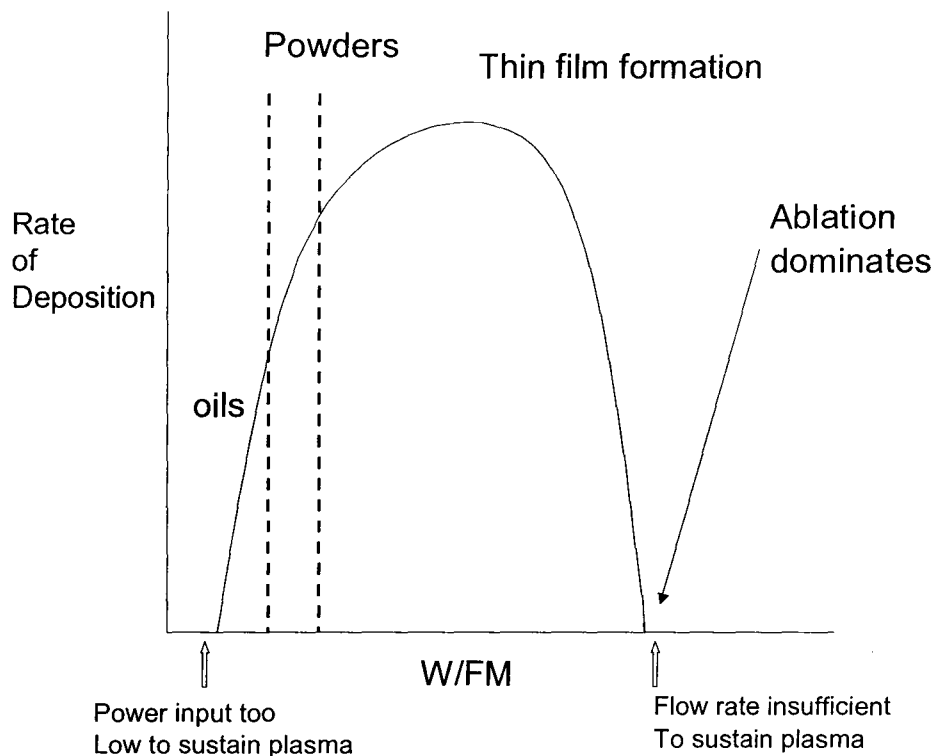


**Figure 2.5.1: Effect of the energy parameter on the deposition and physical properties of the plasma polymer obtained. At high W/FM values, etching dominates over the plasma polymerization process and the film chemistry becomes less predictable. Adapted from Beamson et al., 1985.**

Under pulsed plasma conditions an additional factor, the duty cycle, must be considered. The duty cycle, or the ratio between 'on'-time and 'off'-time of the plasma, is a critical parameter in developing plasma polymers (Han and Timmons, 1998). Many studies using pulsed plasma reactors showed that the film chemistry is better controlled with the pulsed method of operation (Han and Timmons, 1998; Hynes et al., 1996; Rinsch et al., 1996; Rinsch et al. 1995). Plasma polymers generated showed a greater retention of the mer structure (including mers containing hydroxyl, amine, fluorinated or lactam groups) with a low total power input.

Unlike conventional polymerization, many types of monomers, including saturated compounds and other nonpolymerizable gases, can be used for plasma polymerization. However, similar to conventional polymerization methods, the characteristics of the monomer (e.g. presence of triple bonds, aromatic structures, double bonds, cyclic structures) can influence both the polymerization rate and the properties of the resultant plasma polymers (Yasuda and Lamaze, 1973). For example, secondary-ion mass spectrometry, infrared reflection spectroscopy and X-ray photoelectron spectroscopy data demonstrated that although the polymerization mechanism for propanoic and propenoic acid were similar (Yasuda, 1976; Yasuda, 1990), unsaturation in the monomer was found to result in a higher deposition rate (Fally et al., 1995, O'Toole et al., 1996).

### **2.5.2 Plasma Polymerization of Allyl Amine**

One of the important applications of plasma polymerization is the introduction of a plasma polymer containing functional groups that can be used for further reaction with other species including polymers or biological moieties. There have been studies examining plasma polymers containing carboxyl groups (O'Toole, 1996; Ko et al. 1993), hydroxyl groups (O'Toole, 1997; Wickson and Brash, 1999), and silicon-containing functional groups (Tang et al., 1998). However, plasma polymers containing amine groups have been most frequently studied (Griesser et al., 1994; Fally et al., 1995; Krishnamurthy et al., 1989). This is due to the interest in the immobilization of biological moieties including polysaccharides (Dai et al., 2000), anticoagulants such as heparin (Hollahan and

Stafford, 1969; Favia et al., 1997), or antibiotics (Sodhi et al., 2001), which can be readily reacted with an aminated substrate. Ammonia (Dai et al., 2000), and mixtures of nitrogen and hydrogen (Hollahan and Stafford, 1969) were used initially to introduce the amino groups. However, aminated surfaces resulting from the plasma treatment of ammonia were found to be unstable due to restructuring (Griesser et al. 1994), and there have been reports that ammonia plasma treatment can lead to ammonia leaching from the substrate in aqueous media (Calderon et al., 1998, Griesser et al., 1994). Therefore, organic monomers (Fally et al, 1995) such as allyl amine have been widely employed more recently. Allyl amine, as well as other carbon-based monomers, can form a carbon backbone polymer that can bond to the surface of the substrate. The resultant plasma polymer shows less restructuring and loss of surface properties than from the plasma treatment of surfaces with nitrogen-containing gases (Griesser et al., 1994, Krishnamurthy et al., 1989).

The mechanism of the allyl amine plasma polymer formation has been widely studied. It is believed that radicals may play a role in both chain growth and crosslinking (Li and Netravali, 1992). Recently Beck et al. (2001) proposed, based on mass spectrometry data that the reactions in the gas phase are between cations and intact neutral molecules. Although the correlation between ion mass flux, mass deposition and power is complex, Beck et al. (2001) showed that the ion mass flux accounted for the deposit.

Plasma polymers of allyl amine have been widely used for the study of biological interactions. Nitrogen-rich plasma polymers that contain amides promoted surface cell adhesion under constant and pulsatile flow conditions in 10% fetal bovine serum (Tseng and Edelman, 1998), and in 10% fetal bovine serum under static conditions (Griesser et al., 1994). Both studies acknowledged that plasma protein adsorption may contribute to the cell adhesion. However, Tseng and Edelman (1998) noted no differences in cellular adhesion between collagen precoated surfaces of polytetrafluoroethylene and its plasma modified counterpart. Allyl amine coated polyethylene terephthalate (PET) was found to adsorb greater amounts of fibrinogen than uncoated PET and denatured fibrinogen, defined as protein remaining following surface cleaning with sodium dodecyl sulfate, adhered in significantly greater amounts to allyl amine coated samples (Tang et al., 1998).

### **2.5.3 Plasma Polymerization of N-vinyl Pyrrolidone**

Direct plasma polymerization of N-vinyl pyrrolidone (NVP) has been used to generate PPNVP surfaces. Although these surfaces may have gel-like properties (Marchant et al., 1989), they do not have the properties of the conventional polymer. Radio-frequency plasmas generated most of the PPNVP surfaces reported in the literature. Yasuda determined the deposition rate in radio-frequency plasma polymerization of NVP to be  $7.75 \times 10^{-4} \text{ cm}^{-1}$  compared to  $2.86 \times 10^{-4} \text{ cm}^{-1}$  for allyl amine (Yasuda, 1976). Matteo and Ratner (1989) prepared PPNVP films for coatings on intraocular lenses, but provided no details.

Marchant's group has studied plasma polymerized NVP and its use as a biomaterial extensively. Using a continuous radio-frequency glow discharge, they polymerized NVP on many substrates ranging from silicon wafers and other inorganic materials including gold (Marchant et al, 1989, Marchant et al, 1990, Kamath et al, 1996; Murugesan et al, 2000), polyethylene and other polymeric materials (Johnson et al, 1992; Kottke-Marchant et al, 1996). The contact angles of the resultant surfaces ranged from 25-40°. The plasma polymers seemed to be stable when deposited on organic substrates (Marchant et al, 1990). Plasma polymerization of hexane was carried out prior to NVP when the substrate was a silicon wafer (Marchant et al., 1990). On glass coverslips, a dimethyldichlorosilane coating was used prior to the plasma polymerization process (Kamath et al., 1996; Murugesan et al., 2000). Otherwise, the NVP plasma polymer could be removed from glass when sonicated in water (Marchant et al 1989).

Pulsed radio-frequency plasma polymerization of NVP on silicon, potassium chloride and PET surfaces was reported by Han and Timmons (1998). The authors reported that control over the chemistry was greater using this method than the continuous method. Infrared spectra and high resolution C1s XPS data showed increased retention of the lactam group with a lower duty cycle.

Marchant's plasma polymers have shown interesting properties in biomaterial applications. The PPNVP surfaces were found not to be cytotoxic



and showed both extensive attachment and proliferation of human fibroblasts compared to other surfaces studied including PVC, tissue culture polystyrene (TCPS), glass coverslips and surfaces plasma polymerized using  $\gamma$ -butyrolactone, hexane, and hexamethyldisilazane (Johnson et al., 1992). Endothelial cell growth was also examined on these surfaces. The results showed that the PPNVP surfaces supported endothelial cell growth for at least a week and more importantly did not stimulate interleukin-1 production (Johnson et al., 1992). PPNVP, the most hydrophilic polymer in the study, showed the greatest cell growth by day four of incubation (Kottke-Marchant et al., 1996) even without preadsorption of fibronectin. Endothelial cells seeded on the plasma polymers showed extensive cytoskeletal networks, and overall endothelial cell function was retained to a greater extent on the more hydrophilic PPNVP than on the more hydrophobic surfaces examined (Sanborn et al., 2002). In all cases, the cells were grown in medium containing between 10 and 15% serum and protein adsorption was not examined. It was therefore likely that the patterns of protein adsorption and potentially the preferential adsorption of certain proteins on the PPNVP surfaces resulted in the enhanced adhesion noted. Surfaces seeded with endothelial cells also showed a slight decrease in platelet activation due to slight decreases in platelet factor-4 release (Sagnella et al., 1999). Endothelial cells grown on PPNVP released both t-PA (40 ng/mL for 10 000 cells) and PAI (450 ng/mL for 10 000 cells), and released the lowest amounts of von Willebrand factor (Kottke-Marchant et al., 1996) compared to other surfaces in the study.

Tissue factor and thrombomodulin expression were also examined in these cells (Murugesan et al., 2000). While the ratio between the t-PA to PAI for PPNVP was the highest in the study, it was less than 10%, implying that cells were procoagulant rather than profibrinolytic on these surfaces. The authors attributed these cellular interactions to the ability of the surfaces having high oxygen and nitrogen content to support cellular attachment (Kotte-Marchant et al, 1996). The PPNVP surfaces in Marchant's study most likely have complex chemical structures that may not resemble linear PVP.

In another study, it was found that platelet adhesion and activation increased on plasma polymerized NVP surfaces and plasma polymerized EO surfaces compared to controls with adsorbed PEO-containing block copolymers (Kamath et al, 1996; Sagnella et al., 1999). Plasma polymerized PEO-like surfaces in other work showed decreased thrombogenic behaviour (Lopez et al., 1992; Beyer et al., 1997; Wu et al., 2000).

## **2.6 Project Rationale**

Protein adsorption onto surfaces initiates such adverse responses as thrombus formation and inflammation. Since protein adsorption is a surface phenomenon, surface modifications are commonly used to improve biological interactions. Many hydrophilic polymers, including PEO and PVP have been used previously to modify surfaces and change the resultant biological response. It has been clearly shown that surface modification with PEO can result in a dramatic decrease in the level of protein adsorption. Some studies suggest that

surfaces modified with PVP may show reduced protein adsorption as well. However, these results conflict with cell adhesion data in the presence of serum that suggest plasma polymerization of NVP onto surfaces results in higher levels of protein adsorption in general or that there is some specificity for the adsorption of cell adhesion proteins.

It is of interest to study these phenomena further. In this work, PVP-modified surfaces were prepared in two ways: (1) by the continuous microwave plasma polymerization of NVP monomer, (2) by grafting linear poly NVP to surfaces formed by plasma polymerization of allyl amine, presumed to give surfaces rich in amino groups. Similarly, grafted PEO surfaces were also prepared. The surfaces were characterized chemically and compared for protein resistance by studying fibrinogen adsorption from buffer.

### **3. Experimental**

Polyethylene (PE) surfaces were modified with plasma polymerized NVP and grafted with PVP and PEO polymer chains using a microwave plasma reactor. This chapter describes the experimental procedures used for modifying the polyethylene surfaces including details of the microwave plasma reactor, the reaction procedures the characterization methods, and the protein adsorption experiments.

#### **3.1 Preparation of Polyethylene Surfaces for Plasma Modification**

Polyethylene sheets (Uniplast Inc., Barrie ON) with a thickness of 0.025 cm were cut into rectangles 2 cm by 1 cm. The PE surfaces were cleaned by heating to 56°C in acetone for 5 minutes followed by ultrasonication for 15 minutes. Samples were dried under vacuum for 1 hour at room temperature and used immediately.

#### **3.2 Monomer Purification**

The monomers allyl amine and N-vinyl pyrrolidone (Aldrich, Milwaukee, WI) were purified using a series of freeze-thaw cycles for degassing. While the purification and reaction procedures used for the two monomers were similar, several minor changes were made when NVP was used in order to optimize the plasma polymerization. The base inhibitor present in the NVP monomer was not removed prior to the plasma polymerization since the removal could result in spontaneous polymerization of the monomer (Marchant, 1989; Han and Timmons, 1997). Following connection of the monomer (NVP or allyl amine)

reservoir to the monomer inlet tube on the plasma reactor (see Figure 3.3.1), degassing, to remove air, and equilibration of the system were performed. For degassing, the flask was submerged in liquid nitrogen until the monomer was completely frozen (approximately 2 minutes). Once the monomer was frozen, with the vacuum pump on, the rotameter valve and the flask valve were opened. The flow rate of gas, as determined using the rotameter, decreased as a function of time. When the system was steady state (judged by the absence of fluctuations in rotameter reading), the rotameter valve and flask valve were closed, and the flask was placed in acetone to thaw the monomer. When N-vinyl pyrrolidone was used, the acetone was heated to speed the thawing process. Several (7-10) such freeze-and-thaw cycles were performed. Volume of 2 mL was used for NVP and allyl amine for all reactions.

### **3.3 Plasma Polymerization**

#### **3.3.1 Microwave Plasma Reactor**

The remote plasma was generated using an electrode-less 2.45 GHz microwave discharge reactor (Ophthos MPG 4 power supply with McCarrol cavity; Ophthos Instruments, Rockville MD, USA) with a maximum power output of 120 W. Gas flows were controlled by flow rotameters (Model 406 and 300, Matheson, Whitby, ON). The pressure (controlled by the gas flow) was measured using a thermocouple gauge controller (TGC-200, Huntington Laboratories Inc, Mountain View, CA). The vacuum was maintained by a Trivac dual-stage rotary pump (model D4A, Leybold Vacuum Products Inc, Woodbridge,

ON), capable of displacing 125 L/min. The discharge propagated through a glass chimney, 6mm in diameter on top and 38 mm directly below the glow discharge region. The configuration of the plasma reactor is shown in Figure 3.3.1. Ultra high purity argon (Vitalaire, Brampton, ON) was used as purchased. The argon pressure was maintained at 20 psi.

### 3.3.2 Plasma Polymerization of Allyl Amine

For two-sided plasma modification of the surfaces, a maximum of three cleaned PE samples were placed vertically in Teflon or stainless steel holders in the after-glow position 6 cm from the McCarrol cavity (Wickson and Brash, 1999). The setup of the plasma reactor is depicted in Figure 3.3.1.

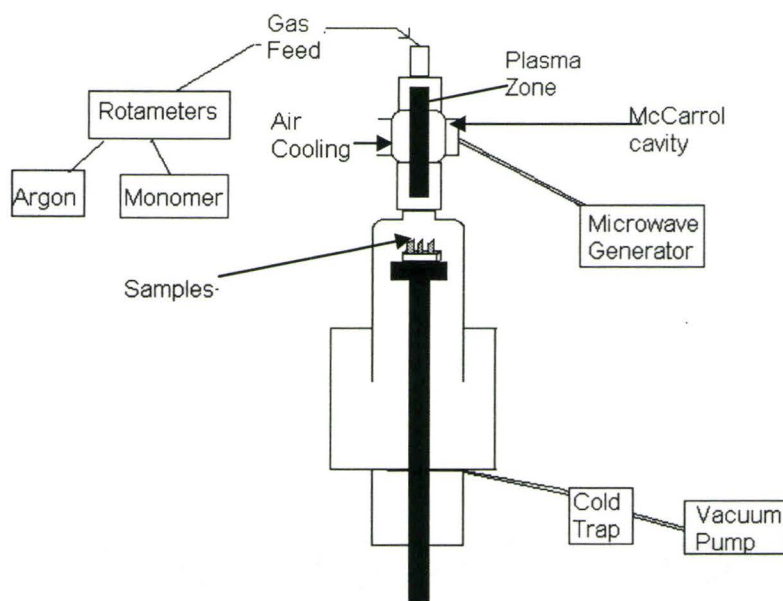


**Figure 3.3.1: Simplified schematic of the microwave-cold plasma system containing samples (ex. polyethylene sheets) when in operation. Monomer was allyl amine or N-vinyl pyrrolidone. Modified from Sodhi et al., (2001) and Wickson and Brash (1999)**

After the system was evacuated to a pressure less than 45 mTorr, argon was allowed to flow at 234 cm<sup>3</sup>/min. Once the system was equilibrated to a pressure of approximately 60 mTorr, the plasma was ignited. The forward power was set at 20 W and the reflected power was minimized (<2 W). At this time, the pressure increased to between 80 and 100 mTorr. The argon plasma, which is characterized by a magenta glow, was continued for a period of 5 minutes. Without extinguishing the plasma, allyl amine was allowed to flow at 0.90 cm<sup>3</sup>/min. The allyl amine plasma emitted a white-pink glow. The polymerization was generally continued for 10 minutes under normal operating conditions. To examine the effects of plasma polymerization time on the resultant polymer layer, samples were removed after times of 30 minutes. After the plasma polymerization was completed, the power was reduced and the high voltage and monomer flow were discontinued. To minimize the potential for surface contamination by reaction of the remaining active species, e.g. free radicals with airborne species and to flush the system of volatile components, argon was again allowed to flow through the reactor at 234 cm<sup>3</sup>/min for 10 seconds before closure of the cold trap. Following closure of the cold trap, the flow rate of argon was continued for a period of 45 seconds at the maximum rate. This allowed the reactor to reach pressures greater than 200 mTorr. Air was reintroduced to the system slowly, bringing the system back to atmospheric pressure.

### 3.3.3 Plasma Polymerization of N-vinyl Pyrrolidone

The procedure for plasma polymerization with NVP was similar to that for allyl amine. However, there were several important differences. The NVP flow rate was set at 2.2 cm<sup>3</sup>/min in order to achieve a pressure between 60-80 mTorr in the reactor when the plasma was on. While the plasma polymerization time (10 minutes) was the same as that used for allyl amine, it was noted that the flow of NVP and the pressure in the reactor dropped continuously throughout the polymerization, and it was necessary to partially close the valve to the cold trap in order to hold the monomer in the reactor.

In order to compensate for the low vapour pressure of the monomer, the monomer reservoir was heated in a silicone oil bath to a temperature of 50°C to increase the vapour pressure, with the expectation of improving the monomer flow rate and the properties of the subsequent plasma polymer layer. Heating to this temperature increased the vapour pressure by a factor of approximately 5 (See Appendix A). While pressure remained between 50-70 mTorr, the flow continued to drop from 2.2 to 0.05 cm<sup>3</sup>/min in the three runs in which this heating technique was used. Furthermore, with heating, NVP condensation occurred. It was anticipated that such condensation could damage the system, so this approach was discontinued after a few experiments.

### 3.4 Polymer Activation for Surface Coupling

Polyethylene oxide, of molecular weight 2000 (PDI = 1.04) terminated at one end with a hydroxyl group and at the other with a methoxy group was



purchased from Aldrich (Milwaukee, WI). Polyvinyl pyrrolidone, with terminal methyl and hydroxyl groups was obtained from Polysciences Inc (Warrington, PA). The PVP with a molecular weight of 2500 (also known as PVP K-12) had a reported polydispersity of 1.9 while the PVP of molecular weight 10 000 (PVP K-17) had a polydispersity of 3.9. All polymers were used as received without further purification.

### **3.4.1 Polymer Activation with EDC and NHS Chemistry**

N-hydroxy succinimide (NHS) and 1-[3-(dimethylamino)propyl]-3-ethyl dicarbodiimide hydrochloride (EDC) are commonly used in peptide and protein chemistry (Hermanson, 1996). This chemistry has also been used previously to conjugate peptides to PVP  $M_n$  6000 (Mu et al., 1999; Kamada et al., 1999) under mild conditions (i.e. in buffer). In the current work, the EDC and NHS coupling system was used to covalently link the polymer chains to the aminated surfaces based on the reaction shown in Figure 3.4.1. This conjugation system gives the polymer chains a better leaving group (the N-hydroxy succinimide moiety) in the reaction with amino groups in the surface. Since the polymers as purchased were hydroxy-terminated, they were reacted with succinic anhydride (Figure 3.4.1) to convert to carboxyl end groups that would react with amino groups in the surface.

The reaction protocol used for the conversion of the hydroxyl groups to carboxyl groups was based on the work of Du (2001). Prior to reaction, all polymers were dried under vacuum at 50°C for a period of 20 minutes. The

polymers (1-3 mmol) were dissolved in an appropriate solvent. For PEO, dry THF was used, as described by Du (2001). However, due to the relative insolubility of PVP in this solvent, DMF was selected for the PVP reactions. To the dissolved polymers, a stoichiometric excess (20 mmol) of succinic anhydride (Aldrich, Milwaukee, WI) and DMAP (dimethylamino pyridine) (Aldrich, Milwaukee, WI) (1 mmol), as a catalyst, were added. In the case of PVP, slightly higher concentrations were used to compensate for the lower recovery of this polymer in the purification steps. Reactions were carried out at room temperature for a period of 8 hours with stirring. Following reaction, the PVP polymers were extracted with cold (refrigerated for 20 minutes) diethyl ether (5-7 volumes), while isopropyl ether was used to extract the PEO (5 volumes). Polymers were further purified by redissolution twice in dichloromethane, with precipitation into diethyl ether (PVP) or isopropyl ether (PEO) between dissolutions. Unreacted succinic anhydride and DMAP were removed by filtration, and the polymers were precipitated using diethyl ether or isopropyl ether. Yields varied for the reaction, but were typically on the order of 25% for both PVP samples, and 50% for the PEO. Polymers were characterized by NMR to confirm reaction.

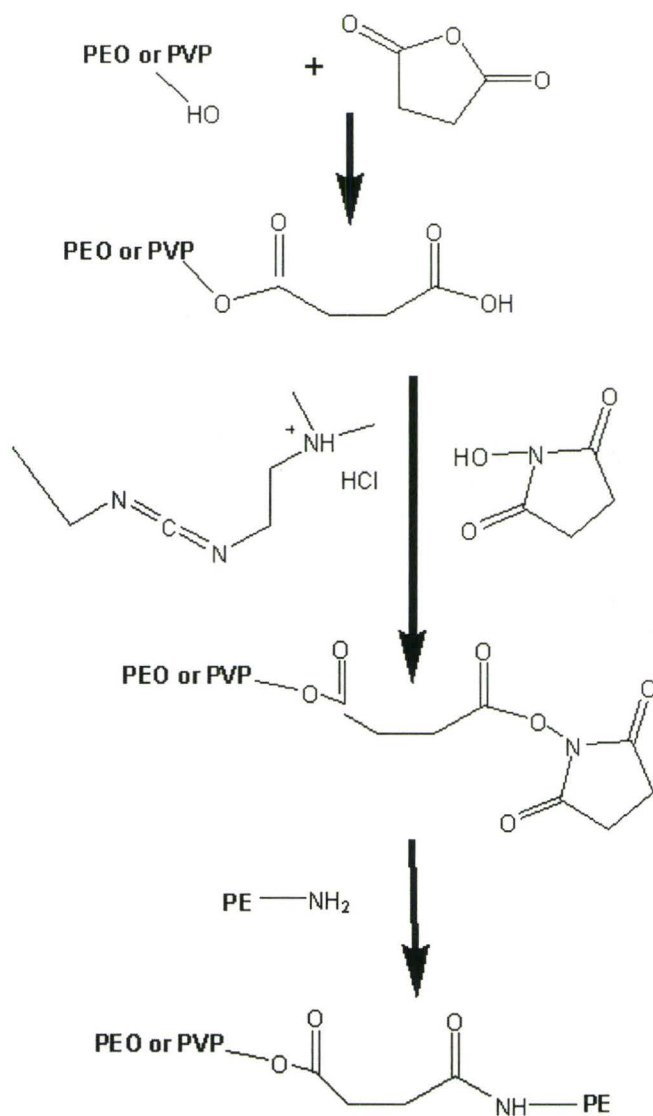


**Figure 3.4.1: EDC and NHS activation of PEO and PVP and conjugation with amines**

The carboxylated polymers were subsequently incubated with 2-molar equivalents of EDC (0.22-0.27 g) and NHS (0.15-0.2 g) in 40 mL in DMF for 5 hours at room temperature to incorporate a succinimide leaving group (Figure 3.4.1). The polymers were then extracted using cold diethyl ether (for PVP) or isopropyl ether (for PEO), and redissolved in dichloromethane to remove impurities. The polymers were placed under vacuum at room temperature for 1

hour to remove any remaining solvents. Reaction yields varied, but were typically 20% for PVP 2500, 30% for PEO, and 20% for PVP 10 000. Polymers were characterized by NMR to confirm that the desired reaction had occurred.

### 3.4.2. DSC activation of polymers

N,N-Disuccinimidyl carbonate (DSC) can also be used to activate hydroxyl groups for reaction with amino groups (Ghosh et al., 1992). The advantages of using DSC for activation over the EDC/NHS method include a reduction of the number of reaction steps, which may reduce losses, and minimize side reactions. Ghosh et al. (1992) and Boden et al. (1998) reported yields greater than 85% for xylofuranose to L-ephedrine and diacryl-glycerophosphatidylethanolamine to bis- $\omega$ -hydroxypolyethylenoxy disulphide respectively. The expected reaction of the polymers with DSC is illustrated in Figure 3.4.2. Following drying under vacuum at 50°C for 20 minutes, 1.5-2.5 mmol of the polymer was dissolved in acetonitrile (40mL) under nitrogen. Again, a higher concentration of PVP 2500 was used to compensate for possibly low recovery of the polymer in the purification steps. A 50% excess of DSC was added at once, the reactor was purged with nitrogen and placed in a 50°C oil bath. A low flow of nitrogen was continued for 20 minutes, the vessel capped and the reaction was allowed to proceed overnight. Following reaction, the acetonitrile was evaporated using a rotary evaporator in a water bath at 40°C for 5 minutes (Buchi model RE 120) and the activated polymers were subsequently purified by precipitating in toluene for PEO or chloroform for the PVP. The polymers were further purified by redissolution in

acetonitrile and reprecipitation in cold diethyl ether. Yields were typically 25% for PVP 2500, 15% for PEO, and 25% for PVP 10 000.

This procedure was also performed using triethyl amine as a catalyst. Prior to adding the DSC, a 2 molar excess of triethyl amine was added (0.40 mL, 3mmol). The purification steps remained the same. Yields were typically 34% for PVP 2500, 70% for PEO, and 25% for PVP 10 000.

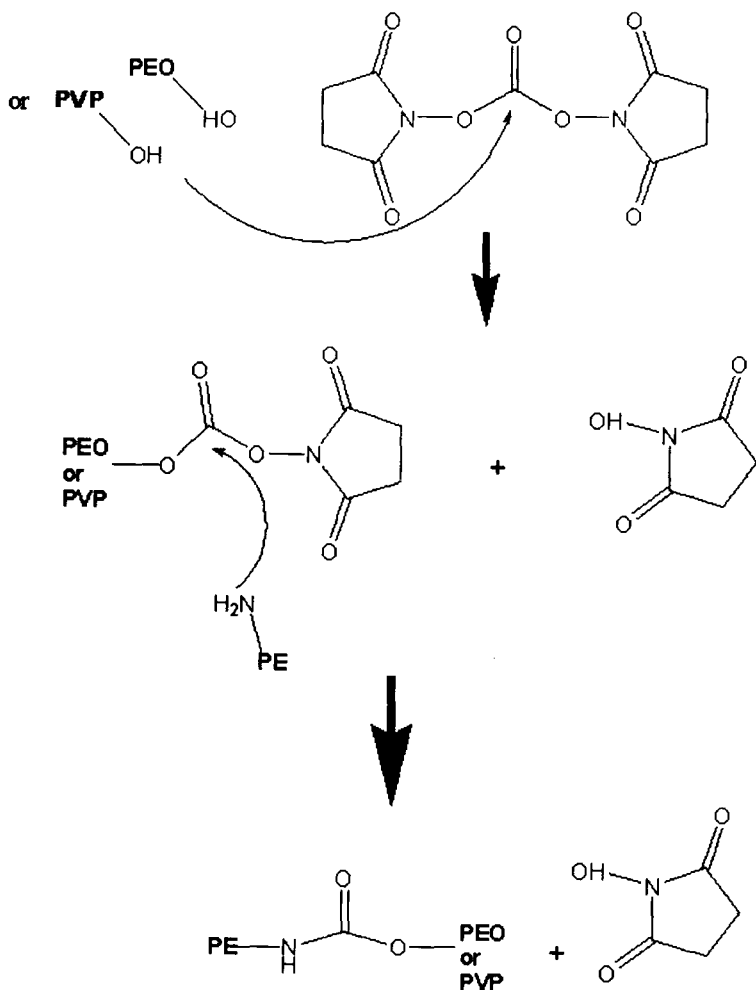


**Figure 3.4.2: Reaction scheme of DSC-activation of PEO and PVP and conjugation with amines**

### **3.4.3 Surface Reaction of Aminated Surfaces with Activated Polymers**

The procedure used to modify the aminated surface was the same for both the DSC and EDC/NHS activated polymers. The activated polymer was dissolved in 30 mL of phosphate buffered saline (pH 7.4) (see Appendix B for preparation) at a concentration of 5  $\mu\text{mol/mL}$ . Plasma polymerized allyl amine surfaces (2 by 1 cm) were immersed in the solution and left to react at room temperature with continuous shaking (wrist-action shaker, Model 75, Burrell Corporation, Pittsburgh) overnight. From previous work, the estimated maximum amino group concentration on the polyethylene surfaces following allyl amine plasma treatment was 80  $\mu\text{mol/m}^2$  (Jia, personal communication, 2001). The concentration of the activated polymers was thus in excess by a factor of 100. This high level of excess was chosen to ensure reaction between the surface and polymers. Following reaction, the surfaces were rinsed well with Milli-Q water and dried in vacuum for 2 hours at 40°C. When possible, surfaces were characterized immediately. Otherwise, surfaces were stored in a closed glass container for a maximum period of 3 days prior to characterization.

### **3.5 Nuclear Magnetic Resonance**

Nuclear Magnetic Resonance (NMR) was used to characterize the activation reactions of PEO and PVP with EDC/NHS and DSC. Proton NMR was performed on a 200 MHz spectrophotometer (Bruker Avance 200) using a 5-mm broadband inverse probe with triple axis gradient capability. Spectra were obtained at ambient temperature in 16 scans in 16 K data points over a 2.604

kHz spectral width (3.146 s acquisition time). The FID (free induction decay) was also zero-filled to 32K before Fourier transformation. The samples were prepared as 1.5 % wt/wt solutions in deuterated chloroform. The chemical shifts are reported in ppm relative to the solvent in which the signal is 7.24 ppm (chloroform).

### 3.6 Water Contact Angles

The measurement of contact angles is a convenient method that provides information about the wettability of a surface (Whitesides and Laibinis, 1990). The definition of contact angle is illustrated in Figure 3.6.1. A force balance at the 3-phase contact line gives Young's equation relating the contact angle to the interfacial tensions:

$$\gamma_{liquid-vapour} \cos \theta = \gamma_{solid-vapour} - \gamma_{solid-liquid} \quad (3.6.1)$$

Contact angles are sensitive to different functional groups, chemical heterogeneity, surface roughness and other factors. They are useful for quickly detecting global changes in surface configuration (Miyama et al., 1997). Different methods are available for measuring contact angles in both dynamic and static systems. The sessile drop technique is the most commonly used method. Water is used as the liquid for determination of relative hydrophilicity.

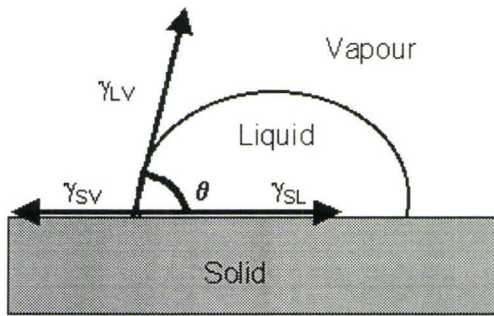


**Figure 3.6.1: Definition of contact angle**

Advancing and receding water contact angles can be obtained using this technique. The advancing angle is the angle obtained when the liquid moves forward on a virgin surface. The receding angle is the angle observed as water is withdrawn and the liquid front recedes. A difference usually exists between the two measurements and is termed hysteresis. This hysteresis is caused by surface roughness, chemical heterogeneity and impurities (Miyama et al., 1997).

Advancing and receding sessile-drop water contact angles were measured on the modified and unmodified PE surfaces using a goniometer (Model 100-00115, Rame-Hart Inc, Mountain Lakes, New Jersey). Droplets (20  $\mu\text{L}$ ) of distilled water were placed on the surface for measurement of the advancing angle and 10  $\mu\text{L}$  was withdrawn from the drop to measure the receding angle. The advancing and receding angles were measured for both sides of the drops, and the average angle was determined from measurements made on multiple areas of the surfaces ( $n>6$ ).



### 3.7 X-ray Photoelectron Spectroscopy (XPS)

X-ray photoelectron spectroscopy is a surface characterization technique that determines the elemental composition of the upper 20 –100 Å of a sample. It is a relatively precise technique with a random error between 1-5%. The error is higher for low atomic concentrations (Kingshott et al., 2002). XPS is commonly used to determine the chemistry of a plasma polymer that has a thickness of a few  $\mu\text{m}$  (O'Toole et al. 1996). XPS operates by using X-rays to bombard the surface. The X-rays eject inner electrons from the core and valence orbitals of the elements (except hydrogen and helium) found on a surface. The common X-ray sources are  $\text{MgK}\alpha$  (1253.6 eV) and  $\text{AlK}\alpha$  (1486.6 eV). These X-rays may be monochromatized or unmonochromatized. An electrostatic field separates the emitted electrons by allowing electrons with a specific energy (or the pass energy) to flow through a detector. Their kinetic energy and abundance are subsequently measured. The kinetic energy is unique for each element, thus allowing for the identification and quantification of the elemental composition. The kinetic energy of electrons ejected from the surface of the sample ( $E_{\text{kinetic}}$ ), is related to the known X-ray energy  $h\nu$  and the binding energy ( $E_{\text{bindingenergy}}$ ) according to:

$$E_{\text{Kinetic}} = h\nu - E_{\text{bindingenergy}} \quad (3.7.1)$$

XPS provides useful information from both high and low resolution scans. Low resolution scans over a 1000 eV range, identify and quantify atomic compositions. High resolution scans, over a smaller range (20-50 eV), give

information about the chemical environment of the emitted electron and thus bonding information about the element in question (Merrett et al., 2002). By varying the take-off angle, or the angle between the detector and the plane of the sample, as shown in Figure 3.7.1, it is possible to alter the depth resolution of the instrument and obtain more surface sensitive measurements (Watts, 1990). As shown in Figure 3.7.1, when the sample is oriented normal to the analyzer, electrons from a depth  $D$  (approximately 100 Å) can be detected. Changing the angle alters this depth according to:

$$D' = D \sin \theta \quad (3.7.2)$$

where  $\theta$  represents the angle between the electron trajectory to the detector and the plane of the sample surface (Ratner, 1996). While X-rays have infinite penetration depth, the mean free path of the emitted electrons is on the order of 0 to 100 Å, making it a surface sensitive technique.

In the current work, take-off angles of 90 and 20° were used, with the 20° angle providing more surface sensitive information. Analyses were performed by the Institute for Chemical Process and Environmental Technology (ICPET) at the National Research Council (NRC) of Canada and at Surface Interface Ontario (SIO) at the University of Toronto. Binding energies were referenced to the hydrocarbon C1s binding energy set to 285 eV at SIO, and 283.6 eV at ICPET. At ICPET, a Kratos AXIS HS X-ray photoelectron spectrophotometer was used for the analysis. At SIO, the machine was a Leybold Max 200. Both instruments use Al-Mg  $\alpha$ K radiation as the source of excitation. The ICPET

instrument uses monochromatized X-rays. The pressure in the analyzer chamber was reduced to  $10^{-8}$  to  $10^{-9}$  mbar. The spectra were collected using pass energies of 192 eV (SIO) or 160 eV (ICPET) for the low resolution analysis and 20 eV (ICPET) or 48 eV (SIO) for the high resolution analysis. Low-resolution spectra and high-resolution spectra for carbon, oxygen, and nitrogen were obtained for each sample. Sensitivity factors of 0.25 for C1s, 0.66 for O1s and 0.42 for N1s were used for analysis of the ICPET data. The corresponding factors used for the SIO data were 0.34 for C1s, 0.72 for O1s and 0.51 for N1s. All samples were washed in 1,1,2-trichlorotrifluoroethane immediately prior to analysis to remove any adsorbed silicone components.

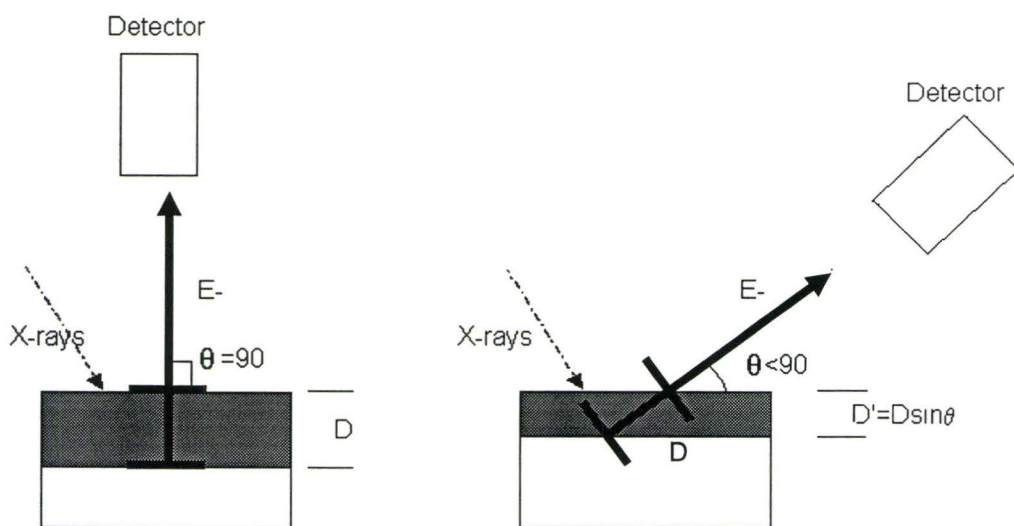


**Figure 3.7.1: Dependence of sampling depth in XPS on take-off angle. Depth of analysis (shaded area) decreases with take-off angle. Take-off angle is defined as the angle between the plane of the sample surface and the electron trajectory to the detector.**

### 3.8 <sup>125</sup>I Radiolabeling of Fibrinogen

Fibrinogen adsorption was used as a measure of the interactions of proteins with the various modified surfaces. Fibrinogen was labeled with Na<sup>125</sup>I (ICN Pharmaceuticals, Montreal, PQ) using the ICl method. In this procedure, the radioactive iodide undergoes exchange with ICl, which then reacts with tyrosine or histidine residues in proteins by an electrophilic substitution. In the case of fibrinogen, labeling occurs mainly through tyrosine residues (Yu and Brash, 1993). Figure 3.8.1 illustrates the reaction schematic for labeling of tyrosine.

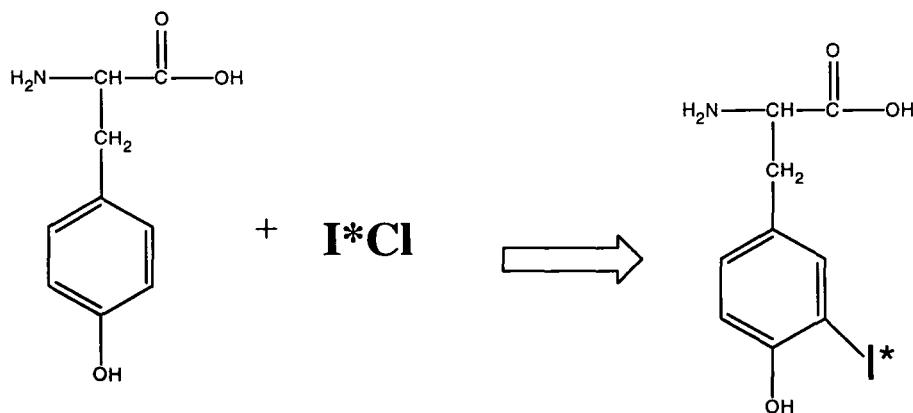


**Figure 3.8.1: Radiolabeling of the tyrosine residue in proteins using the ICl method**

Typically, 2 mg of fibrinogen (Calbiochem, La Jolla, California) was mixed with 100  $\mu$ L of glycine buffer (pH 8.3). A mixture of 0.5 mCi of Na<sup>125</sup>I, 4.5mL of 0.0353 mol/L ICl and 60  $\mu$ L of glycine buffer was added to the fibrinogen solution and stirred for 2 minutes. Following reaction, the radioactive protein solution was removed from the vial and placed in a Slide-a-Lyzer® dialysis cassette (0.5mL-3.0 mL capacity, 10 000 MW cutoff, Pierce Chemicals) to remove any

unreacted iodide. The solution was dialyzed against phosphate buffered saline (pH 7.4) for a period of 6-24 hours with two or three changes of buffer. The radiolabeled fibrinogen was either used immediately or frozen at  $-70^{\circ}\text{C}$  for use in protein adsorption studies within two days. The free radioactive iodide concentration was determined by trichloroacetic acid precipitation (see Appendix C) of the fibrinogen. In all protein adsorption studies performed, the free iodide concentration was below 2%.

### 3.9 Protein Adsorption Experiments

Films in the form of 0.6 cm diameter disks were placed in the individual wells of a 96-well microtitre plate containing 250  $\mu\text{L}$  of PBS (pH 7.4) and allowed to equilibrate overnight at room temperature. Labeled fibrinogen was added to a solution of unlabeled fibrinogen of concentration 10mg/mL such that the labeled protein content in the final solution was 6%. The solution was then serially diluted with PBS to give 5 different concentrations, ranging from 0.001 to 1 mg/mL. The surfaces ( $n=3$  for each modification) were incubated in the fibrinogen solutions (250 $\mu\text{L}$ ) for a period of 3 hours at room temperature. Subsequently, the surfaces were rinsed 3 times for 5 minutes each in 250  $\mu\text{L}$  of PBS buffer, and then counted for radioactivity using a gamma counter. The fibrinogen adsorption ( $\Gamma$ ) was assessed using the following equation:

$$\Gamma(\mu\text{g} / \text{cm}^2) = \frac{(CPM_{\text{surface}})(C_{fg}(\mu\text{g} / \text{mL}))}{(CPM_{\text{solution}}(\text{cpm} / \text{mL}))(Area(\text{cm}^2))} \quad 3.9.1$$

where  $CPM_{\text{surface}}$  is the radioactivity of the surface in counts per minute (cpm),  $C_{\text{fg}}$  is the concentration of fibrinogen, and  $CPM_{\text{solution}}$  is the radioactivity of the reference fibrinogen solution.

Data were obtained prepared at different times and the results pooled to give an estimate of the interactions of the surfaces with fibrinogen.

#### **4. Results and Discussion: Plasma Polymerization of N-Vinyl Pyrrolidone on Polyethylene (PPNVP)**

Surfaces prepared by plasma polymerization of N-vinyl pyrrolidone (NVP) have been previously used in biological and biomedical applications (Johnson et al., 1992; Kottke-Marchant et al., 1996; Sanborn et al., 2001). This chapter is focused on the chemical and biological characterization of surfaces prepared by the microwave-frequency plasma polymerization of N-vinyl pyrrolidone on polyethylene.

The N-vinyl pyrrolidone monomer has a much lower vapour pressure at room temperature than the monomers traditionally used in plasma polymerization (0.114 mm Hg versus 26.1 mm Hg for allyl alcohol and 242 mm Hg for allyl amine at 25°C for example). This resulted in fluctuations in the flow of monomer in the plasma reactor, and variability between runs. It was often noted that the pressure in the system dropped below the base pressure of 30 mm Hg. In an attempt to correct this problem, the monomer was heated to 50°C. While heating increased the vapour pressure by approximately a factor of 6 (See Appendix A for calculation), flow instability and low pressure problems remained. Furthermore, at higher temperatures, the monomer condensed in the connecting tubing and in the rotameters. These pressure and flow variations made it difficult to generate surfaces of consistent quality. Nevertheless, the PPNVP surfaces were characterized by water contact angles and by XPS to assess the differences in the chemistry on the various surfaces resulting from these

pressure and flow variations. The biological behavior of the surfaces was examined via studies of the adsorption of fibrinogen.

#### **4.1 Water Contact Angles**

While water contact angles do not give specific information about the chemistry of modified surfaces, they can be used to assess whether a modification has occurred. Figure 4.1 shows the advancing and receding water contact angles for the various surfaces, including those which were plasma polymerized with different monomers and those modified by plasma treatment with argon.

It was clear that plasma polymerization of NVP or allyl amine increased the hydrophilicity of surfaces. The cleaned polyethylene (PE) samples had advancing and receding water contact angles of  $93.0 \pm 3.4^\circ$  and  $84.3 \pm 3^\circ$  respectively. These results are comparable to data reported previously (Lee et al., 1991; Ko and Cooper, 1993). Plasma treatment with argon alone resulted in a decrease in both the advancing and receding angles to  $54.1 \pm 10.1^\circ$  and  $45.6 \pm 10.1^\circ$  respectively. The large scatter may be due to the oxidation process after plasma treatment, which depends on the storage time and environment. The change in the water contact angles relative to PE was dependent on the monomer, as expected. The allyl amine data are consistent with those previously reported values (Jia, 2001; Jaaba et al., 1997). Surfaces that were plasma polymerized with NVP showed an advancing angle of  $19.8 \pm 5.9^\circ$  and a receding angle of  $13.7 \pm 4.5^\circ$ . These values are slightly lower than those



obtained by Marchant et al. (1989) for radio-frequency plasma polymerized NVP on glass surfaces. The differences in contact angles between the argon-treated surfaces and surfaces polymerized with NVP were statistically significant ( $\alpha < 0.05$ ), suggesting that plasma treatment of the surfaces with N-vinyl pyrrolidone altered the surface chemistry in some way.

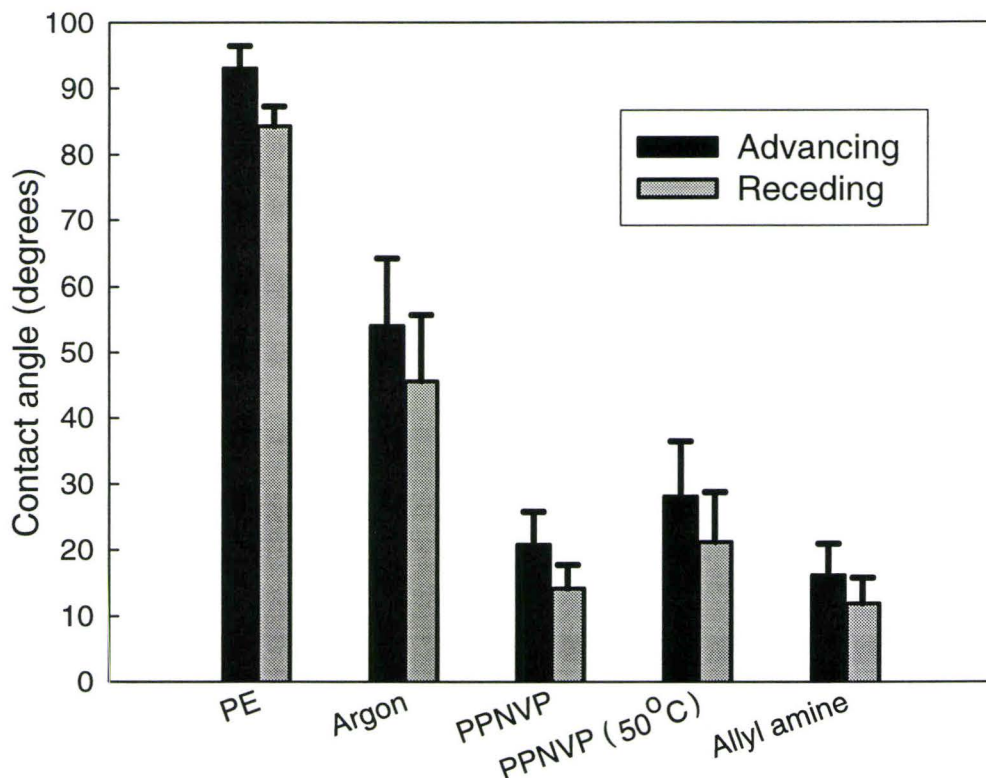


**Figure 4.1: Water contact angles of surfaces obtained by the plasma polymerization of NVP on polyethylene. All plasma modified surfaces showed a considerable increase in hydrophilicity, with the plasma polymerized surfaces showing the lowest contact angles. The allyl amine surface is shown for comparison to PPNVP. Data are mean  $\pm$  1 S.D.,  $n > 9$ .**

To overcome the instabilities in NVP flow, thought to be the result of the relatively low vapour pressure, contact angles were measured on surfaces prepared using heated (50°C) monomer. The water contact angles measured on

these surfaces, at  $28.9 \pm 8.1^\circ$  and  $21.8 \pm 8.1^\circ$ , were significantly higher ( $\alpha < 0.05$ ) than those on surfaces prepared at room temperature, and were closer to those reported by Marchant et al. (1989).

## **4.2 XPS Characterization of the PPNVP Surfaces**

### **4.2.1 Low Resolution XPS Analysis of the PPNVP Surfaces**

XPS was used to determine the elemental composition and to obtain information on the chemical structure of the various surfaces. The analysis was performed at Surface Interface Ontario, University of Toronto. Take-off angles of both  $90^\circ$  and  $20^\circ$  were used to determine compositional variations as a function of depth in the sample. Figures 4.2.1-4.2.3 summarize the low resolution carbon, oxygen, and nitrogen data for the PE control and the various modified surfaces at both  $90^\circ$  and  $20^\circ$  take-off angles.

These data indicate the variation in the elemental compositions of the various modified surfaces. As expected, the polyethylene sample was composed primarily of carbon, but contained low amounts of oxygen and nitrogen, likely due to atmospheric contamination. Argon treatment resulted in a significant increase in oxygen and nitrogen in these surfaces. The argon-treated surfaces had a nitrogen content of approximately 4% at both take-off angles; the oxygen content measured on these surfaces was 16% and 17.5% at  $20^\circ$  and  $90^\circ$  take-off angles, respectively. Argon treatment is believed to remove surface contamination by bombarding the substrate with radicals and other species, often resulting in a hydrophilic surface (Krishnamurthy et al., 1989). When argon pretreatment is

combined with plasma polymerization, it is believed to result in a more adherent plasma polymer film (Mas et al., 1997). However, the radicals produced at the polymer surface by this treatment are highly reactive and can react with atmospheric oxygen and nitrogen upon removal from the plasma reactor (Chen and Belfort, 1999). This, therefore, is likely the source of the nitrogen and oxygen observed on these argon-treated surfaces.

Surfaces modified by the plasma polymerization of N-vinyl pyrrolidone showed interesting chemistry. If the plasma polymer of NVP resembles conventional linear PVP, the carbon content is not expected to change much compared to that of the argon-treated PE surface. The measured carbon contents were highest when the system was at room temperature at a take-off angle of  $90^\circ$ . At this take-off angle, the contribution of the PE substrate to the XPS signal will be significant. At a  $20^\circ$  take-off angle, the C1s signal was lower when the monomer was at room temperature than when it was heated to  $50^\circ\text{C}$ . In general, the data for the " $50^\circ\text{C}$ " surfaces were closer to the values expected for conventional PVP. Regardless of those contributions, it is difficult to confirm the presence of the plasma polymer from the C1s data.

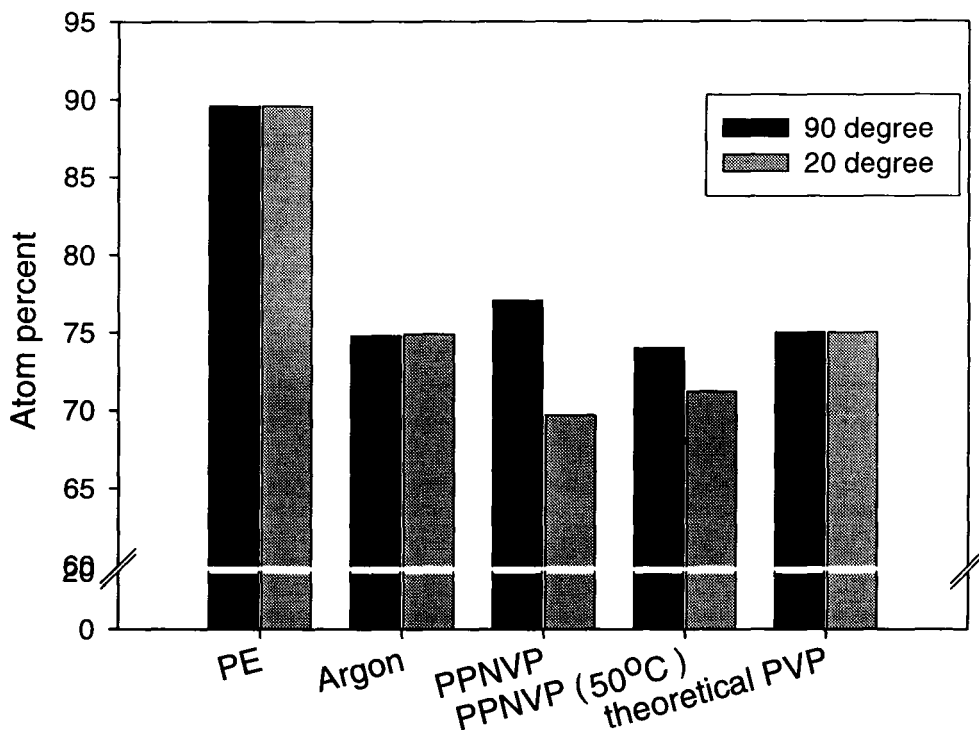


**Figure 4.2.1 C1s Low resolution XPS data for PE, argon plasma treated PE, and plasma polymerized NVP at room temperature and 50°C. The theoretical atomic composition of PVP is shown for comparison. Data are n=2, precision <5%**

Following the plasma polymerization of NVP, particularly with the monomer at room temperature, the surfaces showed a very high level of oxygen. These surfaces were expected to have lower oxygen and higher nitrogen content compared to the argon-treated surfaces. While the measured oxygen contents are consistent with those reported in the literature for similar surfaces (Marchant et al., 1989; Marchant et al., 1990; Kamath et al., 1996, Han and Timmons, 1998), it is likely that contributions from sources other than plasma polymerized NVP are significant. Contributing factors to the O1s signal on these surfaces are: fragmentation of the monomer during the plasma polymerization process, adventitious oxygen or water present in the plasma reactor and most importantly

post-plasma oxidation (Gengenbach and Griesser, 1999; Ko and Cooper, 1993; Yasuda, 1990). These factors may explain the higher values noted on these surfaces compared with those expected for a conventional PVP polymer. Others (Gengenbach and Griesser., 1999; Ko and Cooper, 1993; Marchant et al, 1989; Han and Timmons, 1998) have noted that post-plasma oxidation occurs, particularly on amine plasma polymerized surfaces. Continuing the flow of the monomer after the plasma has been extinguished (Beck et al., 2001) or lowering the power may reduce oxidation (Beck et al., 2001; van Os et al., 2001).

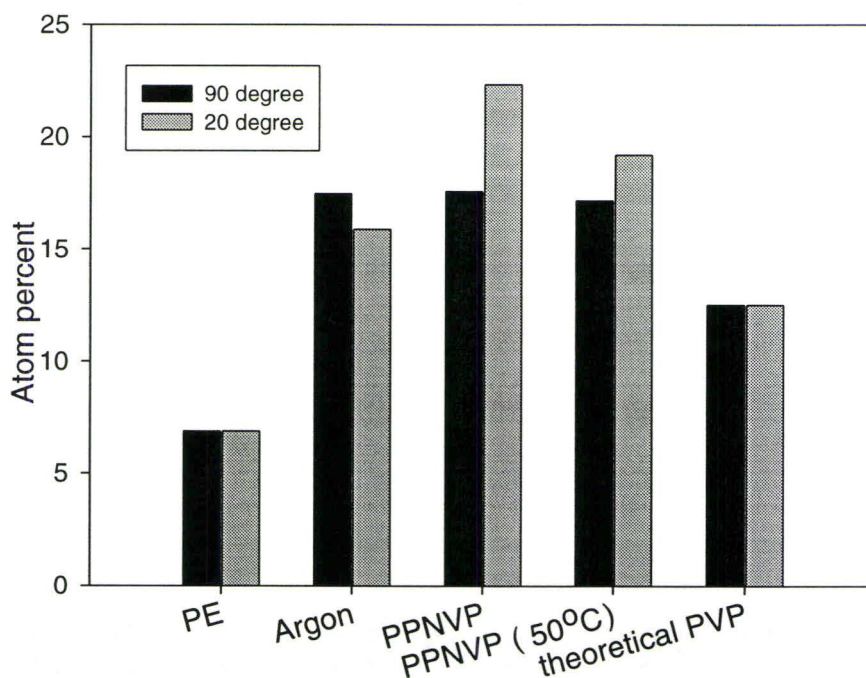


**Figure 4.2.2: O1s low resolution XPS results for PE, argon plasma treated PE and plasma polymerized NVP at room temperature and 50°C. The theoretical atomic composition of PVP is shown for comparison. Note the increase in oxygen content following argon plasma treatment and plasma polymerization of the NVP monomer. Data are n=2, precision <5%**

The low nitrogen content seen on the PPNVP samples in the range of 2 to 6% (Figure 4.2.3) was particularly unexpected, given that PVP has a nitrogen content of approximately 12%. Nitrogen contents between 10-14% have been reported for PPNVP (Marchant et al., 1989, Marchant et al., 1990; Johnson et al., 1992; Han and Timmons 1998; Matteo and Ratner, 1989). For the plasma polymerization of the unheated monomer, nitrogen contents as high as 6% were noted on some samples. However this result was not reproducible and values of about 1.5% were more typical (Figure 4.2.3). While heating the monomer to 50°C resulted in surfaces with a consistently higher nitrogen content, the values obtained are still considerably lower than expected.

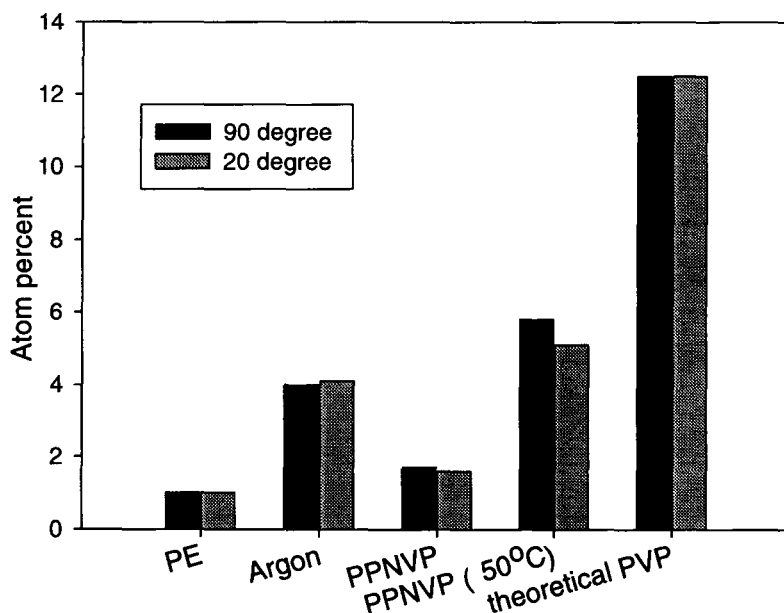


**Figure 4.2.3 N1s low resolution XPS results for PE, argon plasma treated PE and plasma polymerized NVP at room temperature and 50°C. The theoretical atomic composition of PVP is shown for comparison. Nitrogen contents were much lower than expected on both of the PPNVP surfaces. However, there was an increase in the nitrogen content with heating of the monomer. Data are n=2, precision <5%**

## 4.2.2 High Resolution Analysis of Plasma Polymerized NVP Surfaces

High resolution XPS analysis was used to further assess the chemistry of the modified surfaces. Figure 4.2.4 shows the C1s high resolution spectrum of the PPNVP surfaces taken at a 20° take-off angle.

It can be seen that distinct differences exist between the data for the experimental surfaces and those expected for a layer of poly (vinyl pyrrolidone). Of particular note was the absence of a distinct peak at 287.5 eV, assigned to the amide functional group, as indicated in Figure 4.2.4d. While there were differences between the argon-treated surfaces and the PPNVP surfaces, these differences were not as great as expected. The C1s envelope was broader on the argon-treated surface and the C-C components were greater on the plasma polymerized surfaces.

Figure 4.2.5 summarizes the high resolution C1s data. Comparing the data for the PPNVP modified polymers with those for the argon-treated surfaces, it is not clear that the peak attributed to amides (287.5 eV) results from the presence of PVP. The fraction of C1s present as either amide (287.5 eV) or urethane / anhydride (288.8 eV) was actually lower on the PPNVP surfaces than on the argon-treated surfaces. Furthermore, the surface prepared by heating the NVP had a lower content of C-N/C-O (286.4 eV) than the argon-treated surface, and the higher content of C-C (285 eV) of the two plasma modified surfaces. While the ratio of the peak at 287.5 eV to that at 286.4 eV, increased from 0.25 for the unheated monomer to 0.33 for the heated monomer, the ratio was less

than the 0.45 expected for PVP. The increase of this ratio with heating suggested that greater NVP-related deposition occurred in this case.

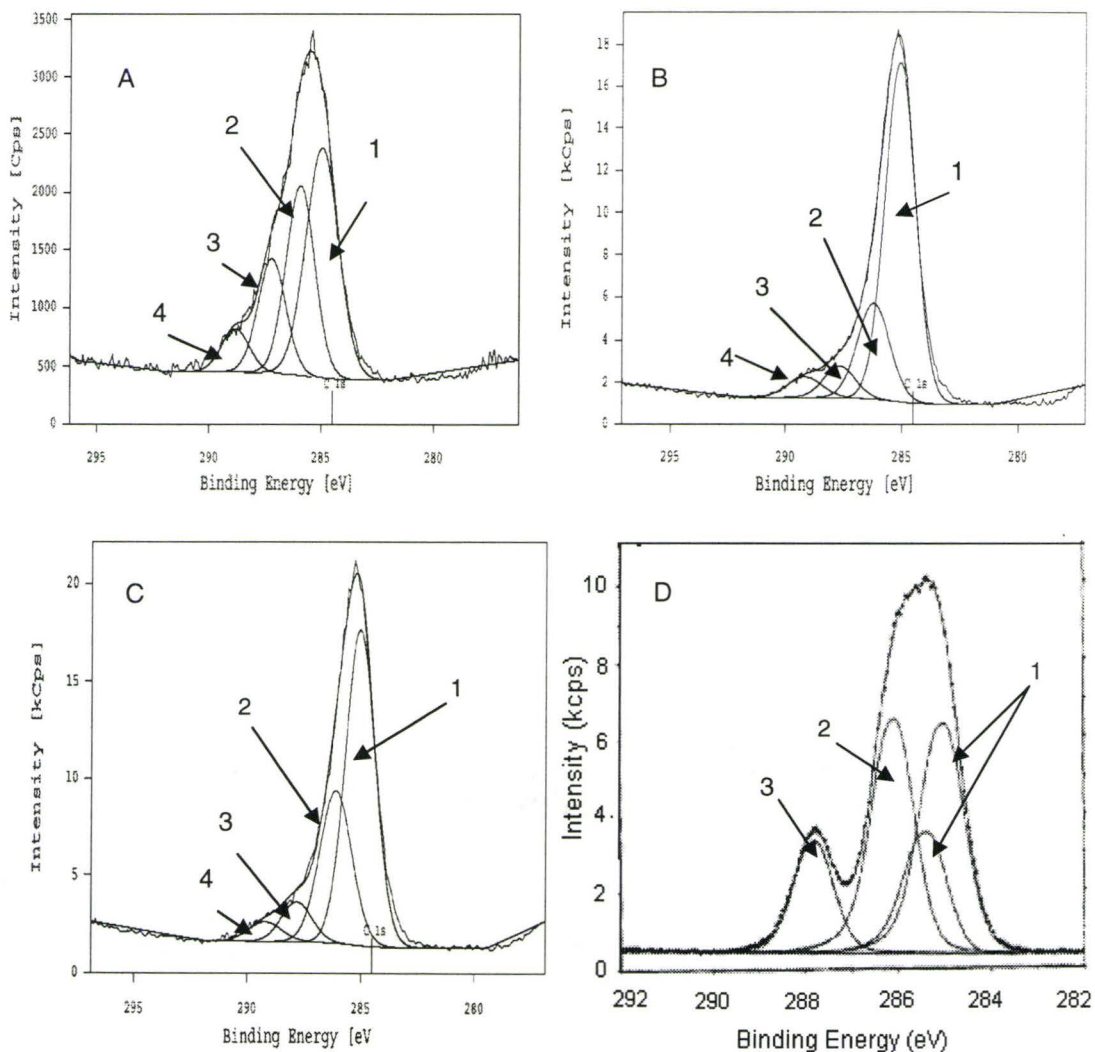


**Figure 4.2.4: C1s High resolution spectra at 20° take-off angle. A) Argon-plasma; B) PPNVP heated to 50°C; C) PPNVP (room temperature); D) theoretical PVP (taken from Beamson and Briggs, 1992). Peaks: 1) 285 eV represents C-C bonds; 2) 286.4 eV represents C-N or C-O bonds; 3) 287.5 eV represents amide bonds; 4) 288.8 eV represents urethane or anhydride bonds.**

In agreement with the low resolution data, which showed very little nitrogen was present on the surfaces, the high resolution carbon spectra



suggested that much of the carbon was bonded to oxygen in carbonyl or hydroxyl functionalities (peaks at 286.2 eV and 287.5 eV in Figure 4.2.5c) and not to nitrogen. It is not surprising that the high resolution XPS data for the PPNVP surfaces do not match the expected values for PVP. It is well known that in the highly reactive plasma environment, the final composition of the plasma polymer is variable and can be quite different from that of the conventional linear polymers (Yasuda, 1990; Marchant et al., 1989). While the low resolution spectra showed that there was more nitrogen present when the monomer was heated, the broad high energy shoulder in the C1s high resolution spectrum may be indicative of the presence of multiple chemical functionalities, (possibly including the amide group of PVP), likely as a result of the highly reactive plasma environment. Similar results were obtained in other work (Marchant et al., 1989, Han and Timmons, 1998).

In order to better understand the chemistry of these plasma polymerized NVP surfaces and particularly the nature of the bonding of the nitrogen atom, high resolution N1s spectra were also obtained for the surfaces prepared with heated monomer. The results are summarized in Figure 4.2.6.

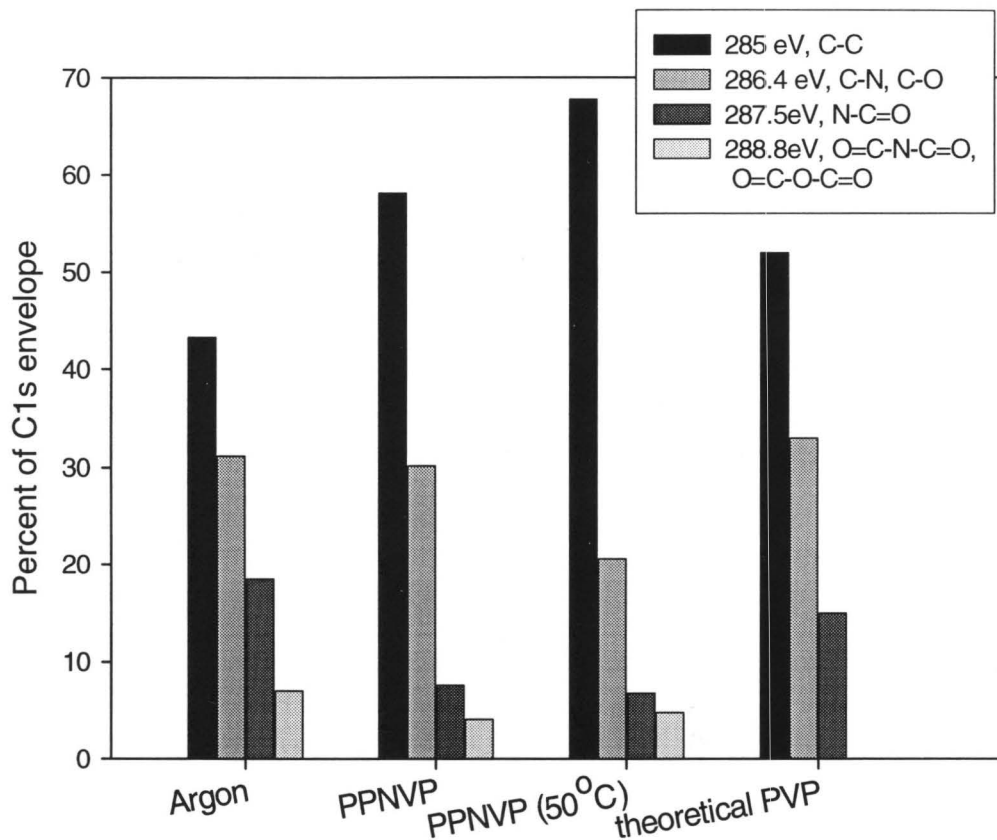
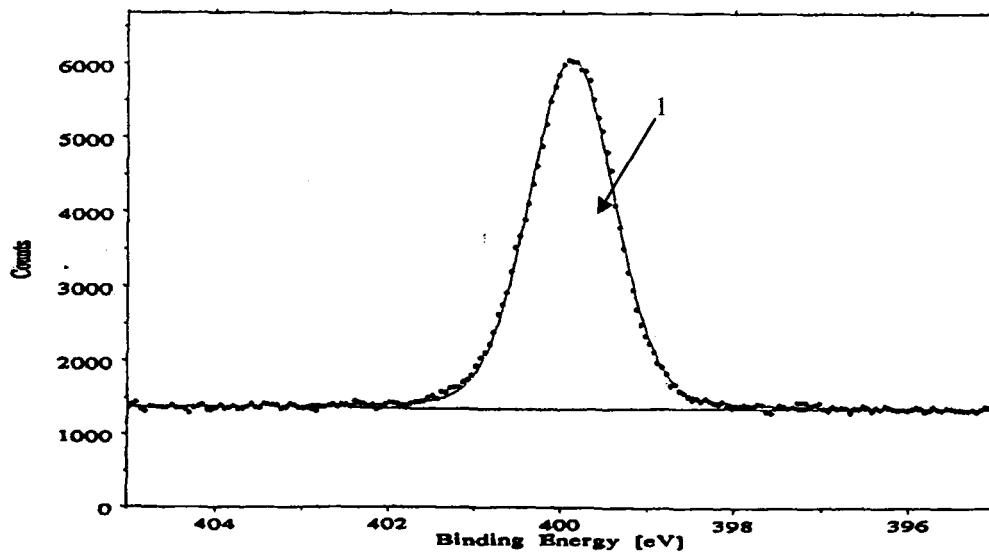
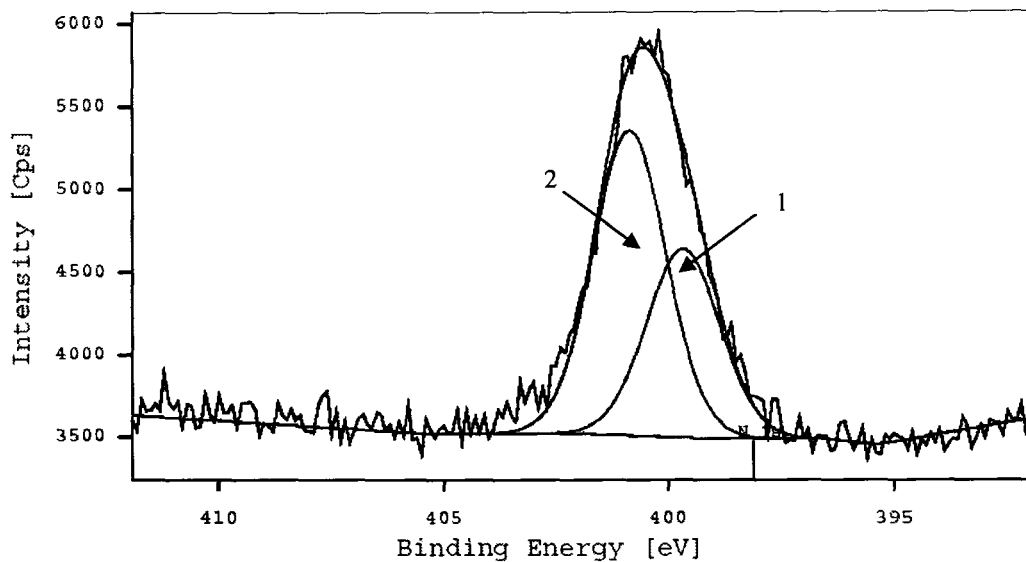


Figure 4.2.5: Composition of the C1s envelope for the argon-treated, and PPNVP surfaces as compared to a “theoretical” PVP surface. The decrease in the peaks >285 eV on PPNVP surfaces compared to the argon-treated surfaces suggested differences in the surface chemistry. However, the values for the PPNVP surfaces did not resemble those expected for a layer of PVP.



**Figure 4.2.6: N1s high resolution spectra of a) PPNVP surface prepared with the monomer at 50°C (taken at 20° take-off angle); and b) linear PVP, with the main peak centered at 399.8 eV (peak 1), (Beamson and Briggs, 1992). The nitrogen in linear PVP is present uniquely as amide groups. The presence of 2 peaks in the PPNVP spectrum indicated that other nitrogen functionalities are present. Peak 2 represents nitrogen in urea or carbonate bonds (400.5 eV).**

The data do not agree with those expected for PVP, which showed a single peak at 399.8 eV attributed to the amide functionality in the side groups of the polymer. The N1s envelope for the plasma modified polymers shows that approximately two thirds of the N1s is present as either urea or carbonate groups, attributed to a peak positioned at 400.5 eV (Beamson and Briggs, 1992). Furthermore, the possible presence of nitriles (399.6 eV) (Beamson and Briggs, 1992) in the plasma polymer surface cannot be disregarded. In addition, the amides may result from post-plasma oxidation (Gengenbach et al. 1996), not from the NVP side groups. As seen in Figure 4.2.6, the N1s peak was broader than the expected N1s peak of polyvinyl pyrrolidone.

The differences noted between the PPNVP surfaces prepared in the present work and those reported in literature (as well as linear PVP) may have resulted from various causes, including plasma etching of the surfaces, fragmentation of the monomers and the power: flow rate ratio used.

Plasma etching or ablation refers to the loss of material as a result of the bombardment of plasma species (Grill, 1994, Ratner et al. 1990). This process competes with the deposition of the plasma polymer. Through etching, the surface may become damaged, and rough. Volatile species may desorb. Air and argon may etch the surface and have been shown to crosslink the upper layers of polyethylene (Grill, 1994, Ratner et al. 1990). Etched surfaces have increased wettability due to the introduction of polar groups and high levels of oxygen incorporated in either carbonyl or ether forms (Grill, 1994, Ratner et al.

1990). The PPNVP surfaces, prepared with the monomer at room temperature, exhibited these properties and may therefore have undergone some degree of etching. Specifically, these surfaces showed an increase in carbon relative to the argon-treated controls at a 90° take-off angle, likely the result of exposure of the underlying PE substrate. The high resolution C1s spectrum for this material, which showed a relatively large C-C component, supports this hypothesis. On the other hand, these PPNVP surfaces had significantly lower contact angles than the argon-treated surfaces. This observation, coupled with the presence of other carbon species in the high resolution C1s spectrum, suggested that these surfaces are highly complex and that many competing processes may be occurring.

Fragmentation occurs throughout the monomer during plasma polymerization and is not limited to opening of the double bond as in conventional polymerization. It may be considered as a form of chemical etching (Yasuda, 1990) somewhat different from the physical etching that occurs with argon treatment. Fragmentation is more likely to occur in monomers with high boiling points, such as NVP, and can result in the loss of functional groups (Yasuda, 1990). Based on the XPS data, it seems reasonable that fragmentation of the NVP monomer could have resulted in opening of the ring and the subsequent loss of nitrogen as well as alteration in the chemical form of the nitrogen present. In the plasma reactor, electron energies are in the range of 1-10 eV, which is sufficient to break covalent bonds in organic compounds

(Krishnamurthy et al., 1989). The C-N bond, with a bond dissociation energy around 3.12 eV, would be more prone to breaking than the C=O bond with a bond energy of 7.69 eV (Marchant et al., 1989; Yasuda, 1990) or the C-O bond with a dissociation energy of 3.74 eV. These fragments may then combine to form other species, including amines, hydroxyls, and nitriles, among other groups. Amines and hydroxyls, with bond dissociation energies of 4.04 eV and 4.83 eV respectively (Yasuda, 1990), may be more stable during the deposition phase. Due to post-plasma oxidation, amines may oxidize to ureas or to amides while hydroxyl groups may be converted to carbonyl functionalities (Gengenbach et al., 1996), in agreement with the XPS spectra in the present work.

The energy parameter, (ratio of power input to the product of flow rate and monomer molecular weight, W/FM), is an important factor in plasma polymerization, particularly in terms of controlling the degree of fragmentation. For example, when plasma polymerizing NVP, Marchant et al. (1989) increased this parameter from  $0.5 \times 10^9$  to  $7.2 \times 10^9$  J/kg and found that the nitrogen content decreased from 10.5% to 5%. In the present work, an initial value of W/FM of  $7.2 \times 10^9$  J/kg was used. However, the decreasing flow rate of the monomer during the experiment likely resulted in an increase in this parameter. The W/FM parameters in this work and in the work of Marchant were strictly not comparable due to differences in the plasma source and in the reactor geometry. It seemed clear that this parameter may have significantly affected surface properties, contributing to the low nitrogen contents obtained on the plasma

polymerized surfaces. However, evaluation of the effect of this parameter on the plasma polymerized surfaces, was not possible due to the flow rate instabilities, which occurred even with heating.

### 4.3 Fibrinogen Adsorption on PPNVP Surfaces

The protein-rejecting properties of the plasma polymerized NVP surfaces were assessed by examining the adsorption of fibrinogen from buffer. The response of the various surfaces is shown in Figure 4.3.1.

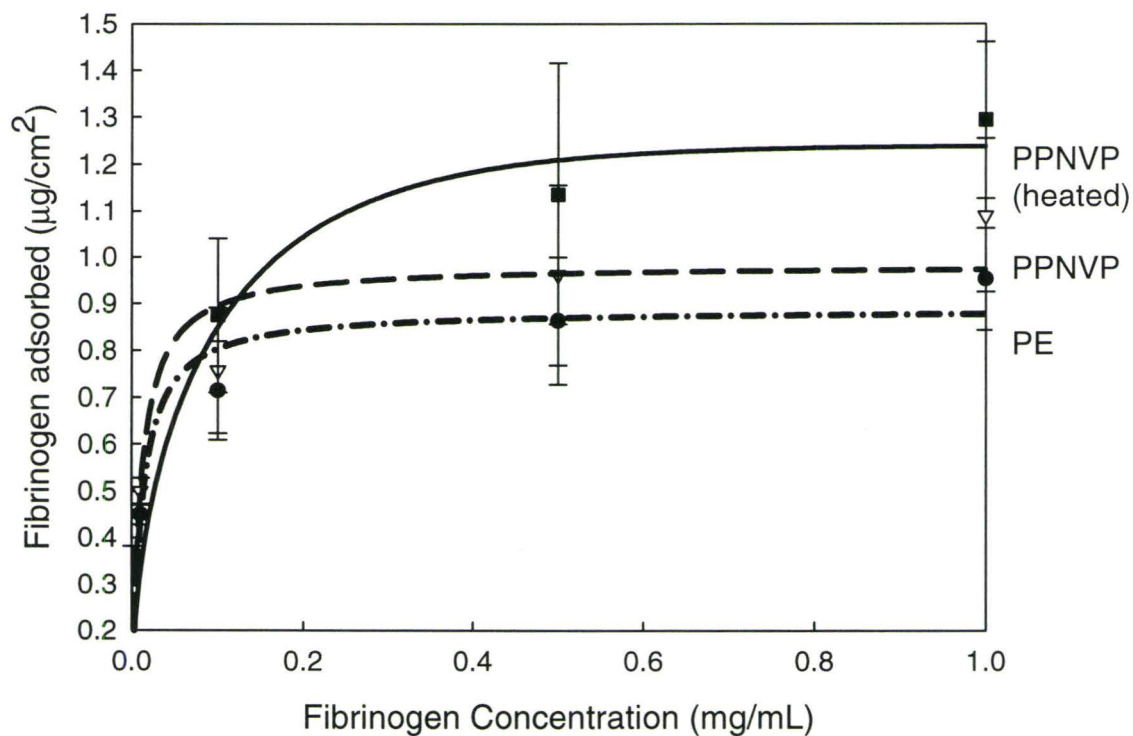


**Figure 4.3.1: Fibrinogen adsorption from PBS (pH 7.4) on PPNVP and PE surfaces. Adsorption time 3h. Data are mean  $\pm$  1 S.D., n=9 (pooled from 3 experiments).**

As can be seen, the PPNVP surfaces with the monomer at room temperature showed an increase in the adsorption of fibrinogen relative to PE by about 14%. Surfaces prepared using heated PPNVP showed even higher levels

of adsorbed fibrinogen of about 30% greater than the unmodified PE. The difference between the PPNVP surfaces is significant at a fibrinogen concentration of 1mg/mL (one way ANOVA,  $\alpha < 0.05$ ).

Numerous studies have suggested that plasma polymerization of NVP may give surfaces that promote endothelialization (Marchant et al., Johnson et al., 1992; Sanborn et al., 2001; Muregesan et al., 2000) and platelet adhesion (Kamath et al., 1996). The mechanism for these effects is unclear. It may be suggested that increases in endothelial cell adhesion may be the result of increases in the adsorption of adhesive plasma proteins. Surfaces where the monomer was heated showed the highest levels of fibrinogen adsorption, perhaps due to incorporation of appropriate functional groups, as suggested by the XPS data.

Plasma polymerization of monomers containing carboxylic acids, amino groups, and hydroxyl groups has been shown to result in wettable surfaces which support cell growth and adhesion (Ko et al., 1993; Lee et al., 1991; Lee et al., 1994; Tseng and Edelman, 1998). Plasma treatment with oxygen resulted in hydrophilic surfaces with contact angles reported to be about 15° by the captive bubble method (Dekker et al., 1991). However, these surfaces also adsorbed increased amounts of albumin and IgG compared to the polytetrafluoroethylene control, thus contradicting the view that hydrophilic surfaces should be protein resistant. Carboxylated surfaces prepared by plasma polymerization have been shown to cause increased platelet adhesion relative to PE (Ko et al., 1993). The



adsorption of fibrinogen can trigger platelet adhesion and other cellular adhesion (Horbett and Brash, 1995; Lamba and Cooper, 2001). Therefore, it is not unexpected that surfaces with carbonyl functionalities that reportedly support cell adhesion may adsorb increased levels of fibrinogen as do those in the present work. Similarly, amine plasma polymers have been shown to adsorb fibrinogen irreversibly (Tang et al., 1998), and showed increased fibrinogen adsorption from plasma relative to a polyethylene control (Lin and Cooper, 1996), despite reduced water contact angles and the presence of a wide variety of functional groups including amides and ureas. Thus, it is perhaps not unexpected that the PPNVP surfaces prepared in this work would adsorb more fibrinogen due to the variety of functional groups that may exist on the surface.

Plasma polymers, especially those synthesized in a continuous plasma reactor, are known to undergo fragmentation, have no clear repeat unit (Yasuda, 1976), and are very different from the polymer obtained using conventional techniques. The PPNVP surfaces in this study were very different from those reported in the literature due to their high oxygen and low nitrogen contents and from linear polyvinyl pyrrolidone. Particular differences were the relatively high oxygen and low nitrogen contents. Since the present PPNVP surfaces were different from those reported on by Marchant et al. (1989), it is difficult to establish whether the high levels of endothelial cell adhesion observed on their surfaces was in fact the result of increased adsorption of adhesive proteins from

the serum-containing medium. Cell adhesion studies with the current polymers may have provided some additional insight.

Due to the high variability of the surfaces prepared and the increases in the levels of fibrinogen adsorption observed with these surfaces, it was clear that they did not have protein resistant properties. Additional protein adsorption studies from plasma may provide insight into the mechanisms by which these surfaces are cell adhesive. SDS PAGE and Western blotting would be desirable to fully characterize the cell adhesive properties of PPNVP surfaces to determine the composition of the adsorbed protein layer and its correlation with cell adhesion.

## 5. Results and Discussion: Grafted PVP and PEO surfaces

In the previous chapter, it was seen that the plasma polymerization of N-vinyl pyrrolidone on polyethylene did not produce structures corresponding to conventional linear polymer (Figure 5.0.1).

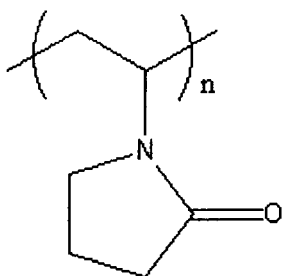


**Figure 5.0.1 The chemical structure of the repeat unit of PVP**

Indeed the surfaces obtained did not show structures that could be easily related to the monomer, and were not protein repellent. In fact, they adsorbed more protein than the unmodified polyethylene.

In this chapter experiments on surfaces prepared by chemically grafting pre-formed PVP to polyethylene surface are discussed. These surfaces are compared to analogous grafted PEO surfaces since PEO is considered to be the “gold-standard” protein repellent material. Polyethylene surfaces were first treated in an allyl amine plasma in an attempt to generate high surface concentrations of amino groups which could serve as reactive sites for grafting of the polymers. Two different catalysts were used in the coupling reactions: 1-[3-(dimethylamino) propyl], 3-ethylcarbodiimide in conjunction with N-hydroxysuccinimide (EDC/NHS):

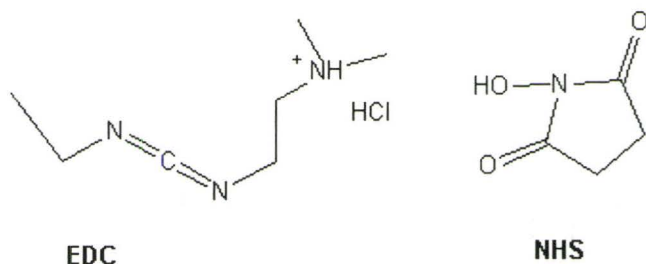


**Figure 5.0.2: Structures of EDC and NHS and N,N-disuccinimidyl carbonate (DSC):**

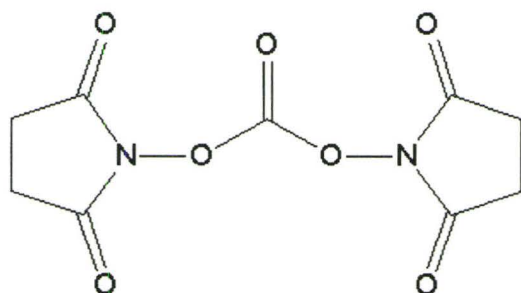


**Figure 5.0.3: Structure of DSC**

The EDC/NHS coupling system activates carboxylic acid groups for reaction with amino groups and is commonly used to modify peptides and proteins. However, since the polymers, as received from the supplier, were hydroxy-terminated, it was necessary to react them with succinic anhydride to generate the required carboxyl end group. The other activator, DSC, reacts directly with hydroxyl groups and promotes their reaction with amino groups. The surfaces prepared

by these grafting reactions were characterized by water contact angle and XPS. Their ability to repel proteins was evaluated by studying the adsorption of fibrinogen from buffer.

### **5.1 Allyl Amine Plasma Treated Surfaces**

While plasma polymerization is in general an excellent technique for surface modification, there are a number of limitations associated with it. It has been shown that in many cases protein adsorption on plasma polymer surfaces is not reproducible due to the lack of stability of the plasma polymer (van Os et al., 2001). In this regard, storage time and storage conditions (e.g. the storage medium) may play a role. Thus, Griesser et al (1994) stated that the age of the plasma polymer should be taken into consideration when designing experiments or evaluating results. Therefore in the present work, the PVP and PEO coupling reactions were performed immediately following the allyl amine plasma polymerization.

As indicated, the continuous plasma polymerization of allyl amine does not produce linear poly(allyl amine); rather a “polymer” with an unknown structure is produced. Imines, nitriles and carboxyls are among the functional groups found in plasma polymerized allyl amine (PPAA) surfaces (Krishnamurthy et al., 1989; Gengenbach and Griesser, 1999). Over time, any amino groups formed can oxidize to amides (Kingshott et al., 2002, Gengenbach and Griesser, 1999, Chatelier et al., 1995a, Gengenbach et al., 1996). Also, plasma polymers

containing amino groups deposited on inorganic substrates (Fally et al, 1995; van Os et al., 2001), and those formed by treatment in an ammonia plasma (Griesser et al., 1994) can be subject to partial or complete loss of the plasma polymer film, especially when immersed in water. Therefore the stability of the plasma polymerized allyl amine surfaces and its dependence on various parameters were examined. These included the position of the polyethylene sample in relation to the glow-discharge region in the reactor, treatment time, immersion in buffer following plasma polymerization, and aging of the samples in air. While the energy input parameter, the ratio of power to flow rate (W/F), is very important for the properties of the film, this was not examined in the present work. The conditions used were established previously (Wickson and Brash, 1999).

### **5.1.1 Water Contact Angles of Allyl Amine Plasma Polymerized Surfaces**

Advancing and receding water contact angles were determined for the surfaces prepared under the various reaction conditions. The data are shown in Figure 5.1.1.

The allyl amine plasma treatment of PE causes a significant decrease in water contact angles for all conditions used. The surface that was treated for 10 min and placed 6 cm from the glow discharge region (the “standard” position) showed contact angles of  $16.2 \pm 4.7^\circ$  (advancing) and  $11.9 \pm 3.9^\circ$  (receding). An increase in the time of plasma treatment to 30 min did not change either the

advancing or receding angle ( $\alpha < 0.05$ , one-way ANOVA). Since it is expected, however, that the thickness of the plasma layer increases as a function time, it can be concluded that a 10-min treatment may be adequate for maximum coverage.

Placement of the samples 2 cm closer to the glow discharge region did not result in contact angles significantly different from those for the samples in the standard position. The possibility that positions closer to the discharge region might give more extensive surface modification due to the increased energy of the plasma and resulting increase in the concentration of active species, was not borne out. It may be that the maximum modification is already achieved at the more distant (standard) position.

From Figure 5.1.1 it is seen that immersion of the 10-min samples in buffer immediately following plasma polymerization caused a significant increase in contact angles: from  $16.2 \pm 4.7$  to  $45.6 \pm 9.2$  degrees for the advancing angle and from  $11.9 \pm 3.9$  to  $39 \pm 9.2$  degrees for the receding angle. A similar increase occurred when the 30-min samples were exposed to buffer. These changes may be due to the persistence of reactive species in the surface immediately following treatment, and the reaction of these species with buffer components, most likely water. It is also possible that immersion in buffer causes surface functional group reorientation, or that the plasma layer is partly removed. The latter does

not seem likely since the contact angles remain significantly below those of the unmodified polyethylene.

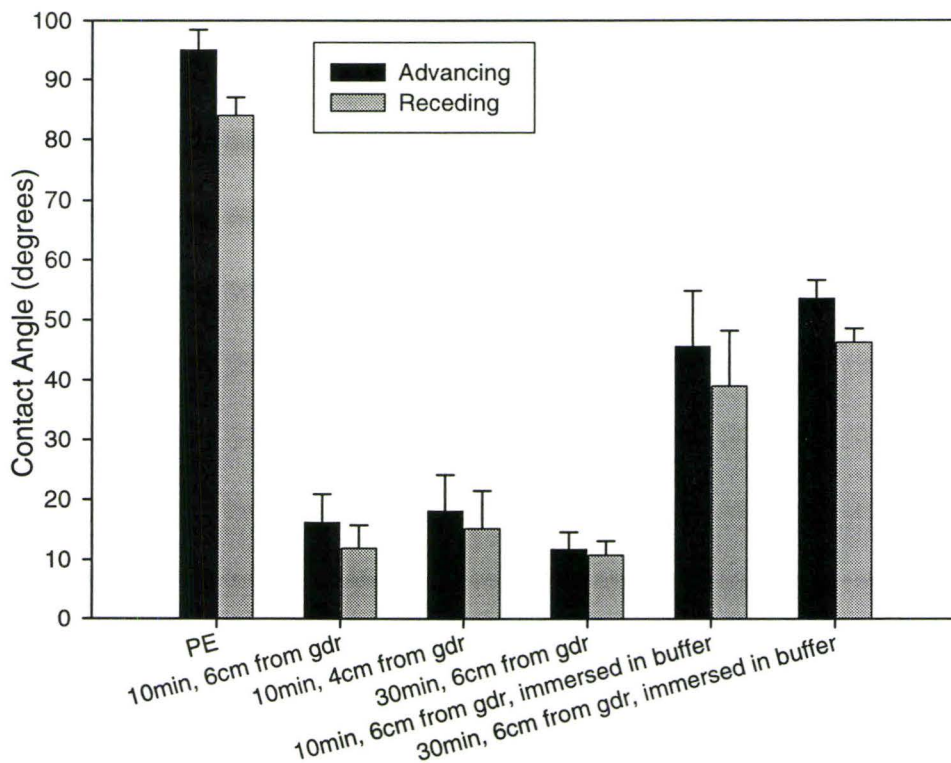


**Figure 5.1.1: Water contact angles of allyl amine plasma polymerized surfaces formed under different conditions. Data are mean  $\pm$ 1 SD,  $n > 6$ . The buffer immersion time was overnight (16 hours) (gdr is glow discharge region). Plasma modified surfaces showed a decrease in contact angles, however, immersing samples in buffer significantly increased contact angles from dry surfaces.**

### 5.1.2. X-ray Photoelectron Spectroscopy Analysis of Allyl Amine Surfaces

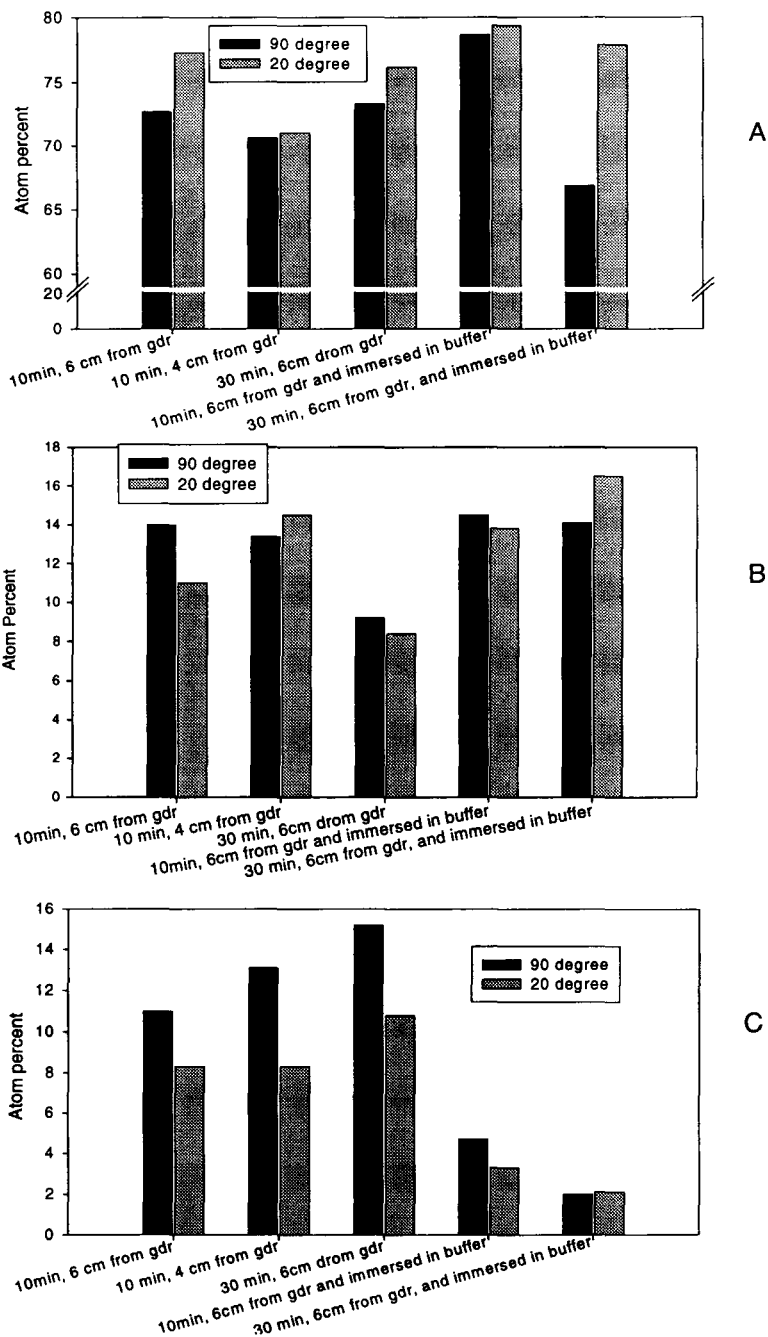
The elemental compositions of the allyl amine plasma treated surfaces were examined using XPS. The results of these evaluations are summarized in



Figure 5.1.2, which shows the carbon (C1s), oxygen (O1s) and nitrogen (N1s) contents. Data are shown for both 90 and 20° take-off angles.

It can be seen that moving the sample closer to the glow discharge region of the reactor increased the nitrogen content slightly at the 90° take-off angle. However, at the more surface sensitive 20° take-off angle no change was observed. The carbon content at both take-off angles was lower for the samples closer to the discharge. The oxygen content was unchanged at 90° and slightly higher at the 20°-take-off angle. Increasing the plasma treatment time to 30 min produced surfaces with a lower oxygen content (9%) and higher nitrogen content (15%) at a take-off angle of 90°. At the 20°-take-off angle, the oxygen content (8.4%) was reduced and the nitrogen content (10.8%) was increased compared to the samples treated for 10 min. The carbon content is not expected to change significantly, and only a slight increase at the 90° take-off angle and a slight decrease at the 20° take-off angle were observed.

Immersion in buffer following plasma treatment caused significant changes in the elemental composition. For the 10-min samples, the nitrogen content dropped to 4%, i.e. a decrease of about 70%. The oxygen content increased slightly and the carbon content increased considerably. Similar changes were seen for the 30-min allyl amine treated surfaces that were exposed to buffer.



**Figure 5.1.2: Elemental composition of the allyl amine plasma surfaces. A)C1s, B) O1s, C)N1s. Lengthening the treatment time lowers oxygen content. Immersing in buffer results in a loss of nitrogen. (gdr is glow discharge region; precision is ~±5%)**

### 5.1.3 General Discussion

Various parameters in the plasma polymerization of allyl amine have been investigated to determine optimal conditions for various objectives (Fally et al., 1995; Beck et al., 2001; van Os et al., 2001). In the present work, maximizing the content of nitrogen in the form of primary amines while minimizing the oxygen content would be desirable. Operating parameters, such as sample position relative to the discharge region and treatment time, are important in controlling film properties.

Sample position relative to the glow discharge zone has been investigated by Yasuda (1990) and Fally et al. (1995). Nitrogen-containing fragments, among other species, may be stable in the glow discharge region where the monomer is fragmented, but may not form a polymer film. Samples placed within the glow-discharge region may produce a plasma polymer having a chemical structure less well defined than in the post-discharge region due to the extent of fragmentation. Although a more extensive reaction may occur in the region downstream of the discharge region, if the location of the sample is too far from the discharge region, the radicals and other active species may terminate or deposit on the reactor walls before reaching the sample (Yasuda, 1990). Placing samples closer to the glow discharge region from the present position (6 cm away from the discharge region) may maximize interactions between the substrate and the active species, and thus improve film formation (i.e.

incorporate more nitrogen). It is also possible that closer to the glow discharge more of the active species (e.g. free radicals) will become trapped within the plasma film and not be available for reaction with the monomer. These species could react with oxygen upon removal from the reactor (Fally et al., 1995). Such reactions can change the properties of the treated surface (Kurosawa et al., 1999). In addition, samples closer to the discharge may incorporate low molecular weight components (Yasuda, 1990).

In the present work, moving the samples closer to the glow discharge region did not seem to improve the film properties. The oxygen content of surfaces closer to the discharge increased ( $20^\circ$  take-off angle) compared to those further away, indicating that the “closer” samples may have a relatively high concentration of trapped radicals. Similar to the allyl amine control surface at a distance of 6 cm from the glow discharge region, these “closer” surfaces may be subject to further oxidation over time. The contact angles of samples plasma polymerized 4 cm from the glow discharge region do not decrease compared to the 10-min sample at 6 cm from the glow discharge region. Furthermore, the nitrogen content at the surface ( $20^\circ$  take-off angle) remained the same for the allyl amine surface at both positions in the reactor. Therefore, placing the samples 2 cm closer to the glow discharge does not seem significantly different from those further away.

Treatment time is clearly also an important variable. In general, it is expected that the thickness of the plasma polymer layer should increase with time. Also, structural changes including crosslinking may occur (van Os et al, 2001). In the XPS experiments, the substrate may be masked under the thicker layers expected at longer treatment times especially at the 20° take-off angle. For the 10-min samples examined at the 90° take-off angle, it is likely that the underlying polyethylene substrate makes a significant contribution. Increases in carbon and nitrogen for the 30min compared the 10-min samples are not unexpected, assuming that the thickness of the plasma layer increases as a function of reaction time. The data show that the nitrogen: carbon ratio is slightly higher for the 30 min than for the 10 min treatment time, indicating perhaps a greater incorporation of nitrogen in the 30-min sample. At longer treatment time, more radicals in the plasma layers will terminate as new material accumulates (Yasuda, 1990; Grill, 1994). With lower radical concentrations, reaction with oxygen will be less extensive. Thus, a decrease in oxygen at both 90 and 20° take-off angles is not unexpected. These surfaces, in view of the contact angle data and lower oxygen content, may also be more resistant to aging effects than the surfaces prepared using the 10-min treatment time. Increased resistance to aging is highly desirable.

Oxygen is present in all of the plasma treated surfaces. Clearly this is not related to the allyl amine monomer, which does not contain oxygen. Presumably

oxygen is incorporated by post-plasma oxidation (Gengenbach and Griesser 1999; Beck et al 2001; van Os et al, 2001; Fally et al 1995), a process that begins instantaneously upon exposure to the atmosphere. Significant amounts of oxygen were found on diaminopropane plasma surfaces by Gengenbach and Griesser (1999) after 4 h in air. It is also possible that oxygen is incorporated due either to the presence of trace amounts of oxygen in the reactor (Li and Netravali, 1992) or to water adsorbed on the walls of the reactor (Yasuda, 1990; Mas et al., 1997), although precautions are generally taken to ensure that these sources of oxygen are minimized.

The majority of post-plasma oxidation is believed to occur by reaction of persistent free radicals or other active species present when samples are removed from the reactor, with oxygen in the air (Gengenbach and Griesser, 1999). It has been shown that oxygen rapidly diffuses into the plasma polymer layer and reacts with radicals to form peroxides that decay into various products or form secondary radicals (Gengenbach and Griesser, 1999; Gengenbach et al., 1996; Chatelier et al. 1995a). It is believed that continuation of the allyl amine flow for a significant period of time (several minutes) after the plasma is extinguished may reduce oxygen incorporation. In one study, a 10 min post reaction flow of allyl amine gave an oxygen content of 4% on aluminum substrates when the plasma was operated at low power input (Beck et al., 2001). On the other hand, Mas et al. (1997) reported that the oxygen content was as

high as 18% after a similar treatment when polymerizing on poly(vinylidene fluoride) at high power input.

Operation of the reactor at low power or at a low power/flow ratio may also help to reduce the incorporation of oxygen (Beck et al., 2001). Reactors operated at low power have been found to yield plasma polymers of allyl amine that have a relatively low content of oxygen, and a relatively high content of amino groups (Beck et al., 2000, van Os et al., 2001). In continuous mode, powers of 15 W and less have been shown to give secondary and tertiary amines in significant amounts (Beck et al., 2001). At higher powers (30-50 W) imines and nitriles were favoured (Krishnamurthy et al., 1989). As well, it has been shown that allyl amine fragments are formed at high power (Krishnamurthy et al., 1989) but not at low power in the range of 0.2-15 W (Beck et al., 2001, Fally et al., 1995). In the present work the power level selected was 20 W.

Plasma polymers formed by pulsing the plasma on and off have been found to give structures that more closely resemble linear poly(allyl amine) with a high content of amino groups (Rinsch et al., 1995). In pulsed mode the power input is lower than in continuous mode over the same time.

It is probable that optimization of the power level and flow rate of allyl amine would lead to more stable surfaces having lower oxygen content.

## **5.2 Aging of Plasma Polymerized Allyl Amine Surfaces**

It has been shown in many studies that the elapsed time following plasma treatment affects the chemistry of carbon-based amino-containing surfaces (Griesser et al., 1994; Gengenbach and Griesser, 1999; Whittle et al., 2000). In particular, aging seems to affect the integrity of allyl amine derived plasma deposits. Therefore, experiments were performed to determine whether this phenomenon was important in the present work.

### **5.2.1 Surface Analysis of Aged Allyl Amine Surfaces**

The XPS data shown in Figure 5.2.1 suggest that there are differences in the elemental composition of allyl amine plasma surfaces (10-min treatment, 6 cm from the glow discharge region) aged respectively for 3 and 11 days.

Most importantly, there is a decrease in the N1s signal at the 90° take-off angle, although at the 20° angle there is no change. The oxygen content is slightly lower at the 90° take-off angle, but higher at 20°. This result is consistent with two previous studies (Mas et al., 1997; Jaaba et al., 1997) where the substrate was poly(hydroxybutyric acid)-co-(3-hydroxyvaleric acid) (polyHBA-co-HVA). Other studies (Jama et al, 1996; Gengenbach et al., 1996; Gengenbach et al., 1999; Whittle et al., 2000) showed that the nitrogen/carbon ratio, as determined by XPS, continued to change for many weeks following plasma polymerization.



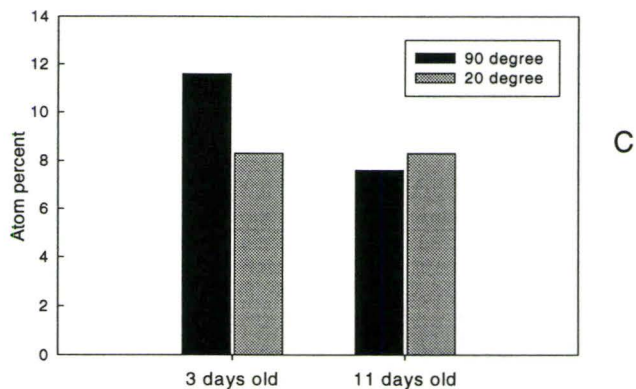
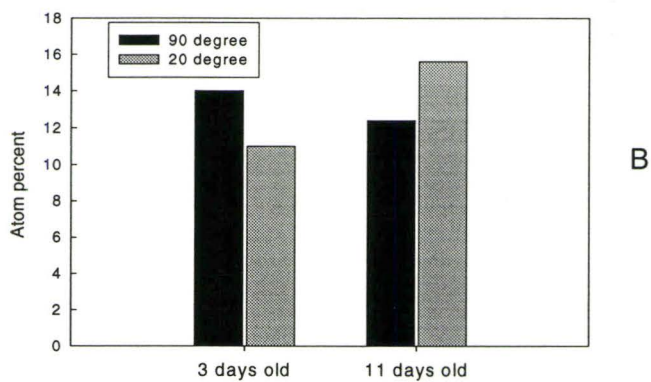
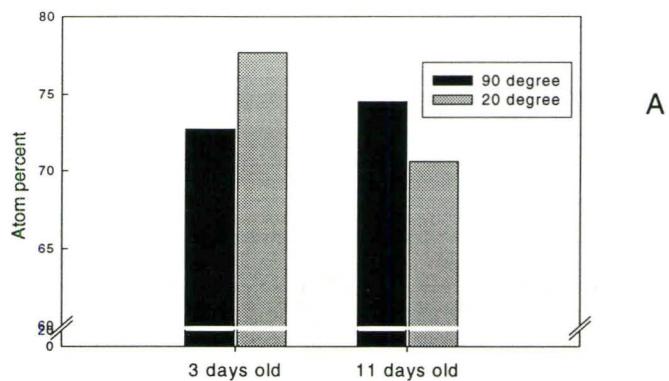


**Figure 5.2.1: Surface composition of plasma polymerized allyl amine surfaces (10 min treatment) aged for 3 and 11 days. A) C1s, B) O1s, and C) N1s. Data precision is  $\sim\pm 5\%$ . At the  $20^\circ$ , there is an increase in oxygen, decrease in carbon and similar nitrogen content.**

Surface hydrophilicity, as determined by water contact angles, was examined over a longer aging period. Figure 5.2.2 shows the change of contact angles over 30 days for surfaces prepared using 10- and 30-minute treatments. The data for the aging of the 10-minute surfaces is consistent with those reported in the literature for surfaces (fluorinated ethylene propylene copolymer [FEP] and poly[HBA-co-HVA]) formed in an ammonia plasma (Griesser et al., 1994; Gengenbach et al., 1996; Chatelier et al., 1995a; Jama et al., 1996) and on glass in an allyl amine plasma (Kurosawa et al., 1999). Similar to the results of Jama et al. (1996) and Kurosawa et al (1999), the contact angle increased over the first 2-5 days in air and then remained constant. The main process responsible for this change may be the continued oxidation of the surfaces facilitated by the inward diffusion of oxygen and subsequent reactions with trapped radicals in the surface, or migration of polar functionalities to the surface (Gengenbach and Griesser, 1999; Gengenbach et al., 1996; Chatelier et al., 1995a).

As seen in Figure 5.2.2, surfaces treated for 30 min showed a slower and less extensive increase in hydrophobicity. This may be due to the lower oxygen content of these surfaces as seen in Figure 5.1.2b, which may in turn be due to a lower radical concentration in the plasma polymer. Furthermore, a longer treatment time may also increase crosslinking of the plasma polymer that may hinder surface rearrangement. Based on refractive index measurements on plasma polymers of allyl amine, van Os et al (2001) has suggested that when the

material is exposed to the plasma for longer times, the deeper layers may undergo more extensive crosslinking than the surface. However, Chatelier et al. (1995a) showed that in radio-frequency ammonia plasmas the mobility of surface amino groups increases with treatment time, suggesting that longer plasma exposure may enhance degradation rather than crosslinking reactions. In the present work, the plasma source, reactor geometry and monomer are different than in Chatelier's work (1995a) and it is possible that crosslinking may be favoured over degradation as found by van Os et al (2001).

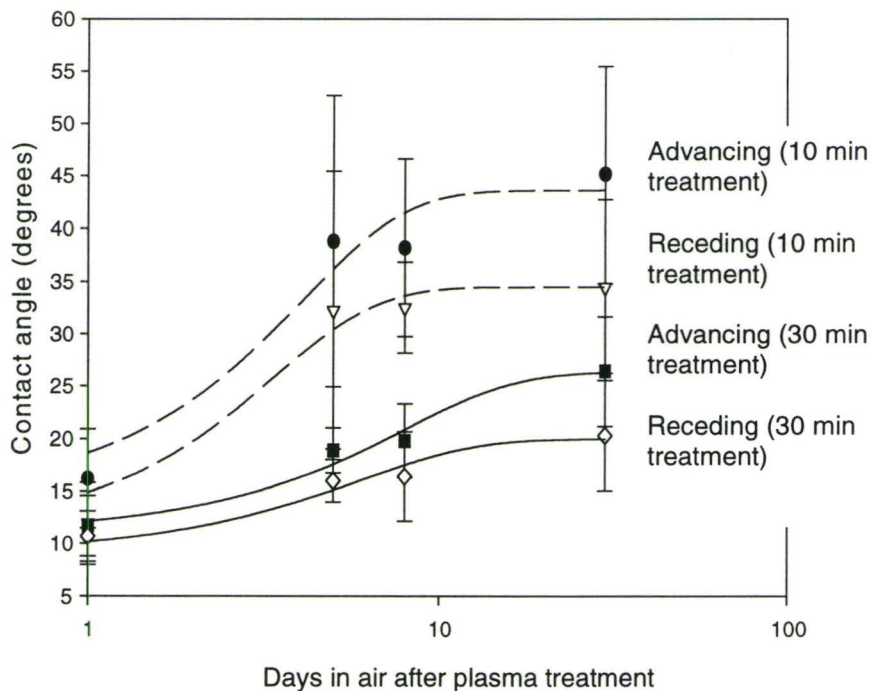


**Figure 5.2.2: Water contact angles of plasma polymerized allyl amine surfaces versus time elapsed after plasma treatment. Data are mean  $\pm$  1 S.D.,  $n > 6$ . 30-min showed a slower increase in contact angles, which may indicate more resistance to aging.**

### **5.2.2 Discussion of Changes in Surface Physical and Chemical Properties with Time in Air after Plasma Treatment.**

It is of interest to consider the phenomena that may be occurring to cause these changes in the surface properties over time. Diffusion in the material surface regions may occur if the presence of the migrating component at the air-material interface lowers the surface tension. Hydrophilic components will tend to migrate away from the hydrophobic air-material interface toward the bulk (Griesser et al., 1994; Gengenbach and Griesser, 1999; Gengenbach et al., 1996; Chatelier et al., 1995a; Wittenbeck and Wokaun, 1993).

Previous aging studies have focused on plasma polymers of saturated monomers such as diaminopropane (Gengenbach and Griesser, 1999), and on plasma polymerized allyl amine deposited on aluminum (Whittle et al., 2000). Whittle et al (2000) showed a slow decrease in the N/C ratio from 0.22 to 0.17 over a period of 30 days. The oxygen/carbon ratio changed from 0.03 to 0.11 over 50 days. Gengenbach et al (1996) showed that in plasma polymers of ethylene diamine on fluorinated ethylene propylene copolymer the N1s and O1s XPS peaks broadened over time, reflecting the occurrence of oxidation processes. However, nitro, nitroso and nitrate groups were not formed. Rather, nitrogen was present as amide and urea functionalities. After 4 months, the amino groups were completely converted to amide groups. As indicated previously, this is probably due to the diffusion of oxygen into the substrate and

its subsequent reaction with long-lived radicals after the material is removed from the reactor and exposed to the atmosphere (Yasuda, 1990, Mas et al., 1997, Gengenbach and Griesser, 1999, Gengenbach et al., 1996, Chatelier et al., 1995a).

Jaaba et al. (1997) and Mas et al (1997) reported that on a poly(hydroxybutyric acid)-co-(3-hydroxyvaleric acid) surface treated with allyl amine plasma, the surface nitrogen content remained constant over 10 days, but the oxygen content increased. These authors concluded that the inward diffusion of oxygen caused the increase.

In light of this previous work, it is expected that in aged samples, the C1s XPS peak will show evidence of oxidized states. However, higher oxidized states of carbon, especially in the form of amides and urethanes, were found to be in lower abundance in the 11 day aged allyl amine surface as shown in Figure 5.2.3. As can be seen, the 285 eV component (C-C bonds) is greater in the 11-day old than in the 3-day old surface. Thus there is a discrepancy between the high resolution data and the low resolution data at 20°. From the low resolution data, an increase in oxygen, a decrease in carbon, and a relatively constant nitrogen content over time suggest that oxidation is occurring. Since the high resolution is based on curve fitting, including an initial guess, it may be considered less reliable than the low resolution data.

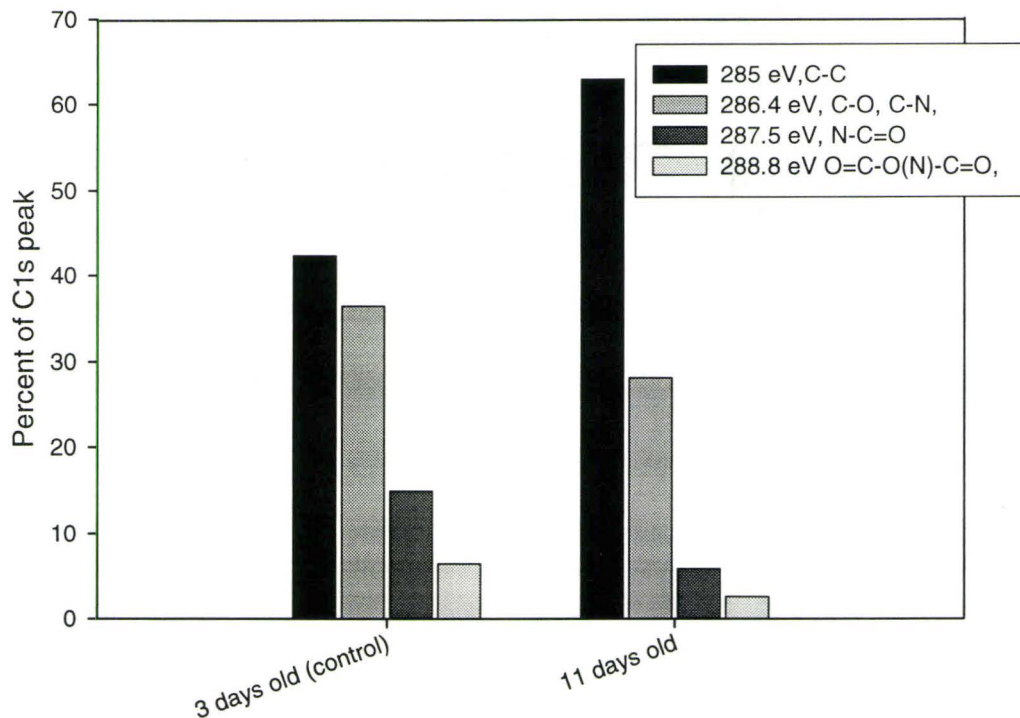


**Figure 5.2.3: Composition of the C1s envelope for aged allyl amine plasma polymers. Surfaces were treated for 10 minutes. High resolution data taken at a 20° take-off angle.**

Several strategies have been suggested to prevent aging. Placing the samples in vacuum, a hydrophobic environment, did not prevent changes in contact angles on plasma polymerized allyl amine deposited on glass (Kurosawa et al., 1999; Krishnamurthy et al., 1989). Another approach is to minimize residual free radicals in the surface. In this regard, the same processes that reduce post-plasma oxidation may reduce aging. Some studies (Beck et al., 2001, van Os et al., 2001) reported low oxygen content when operating at low power (<15 W) where fragmentation of the precursor is expected to be reduced since the concentration of highly energetic species in the plasma will be lower.

Increasing the plasma treatment time in the present work resulted in surfaces of lower oxygen content and which showed smaller changes in contact angles over time. Under these conditions, increased crosslinking may occur, thus giving surfaces that are more resistant to aging. It is unknown if the content of amino groups changes as the treatment time increases. High resolution N1s spectra and derivatization with species known to react with amino groups could be used to estimate the amino group content.

### **5.3 Discussion of Changes in Surface Physical and Chemical Properties on Exposure of Plasma Polymerized Surfaces to Buffer.**

The possible interactions of plasma polymerized allyl amine surfaces with buffers and other aqueous fluids are also important, since as biomaterials the surfaces are exposed to aqueous media in subsequent utilization. It has been shown that the plasma layer on ammonia-plasma-modified fluorinated ethylene propylene copolymer can be removed by immersion in water (Griesser et al., 1994). Hence, organic monomers such as allyl amine were later used to provide a strongly-adhering carbon-carbon network to prevent the loss of the layer and hence the amino groups (Krishnamurthy et al., 1989; Griesser et al., 1994). Loss of the allyl amine plasma layer was observed upon immersion in ethanol when the substrate was titanium (van Os et al, 2001), or upon immersion in water when the substrate was gold-coated silicon wafer (Fally et al, 1995).

In the present work, it was demonstrated that the chemistry of plasma polymerized allyl amine surfaces was altered by exposure to buffer for 16 hours and the changes were independent of plasma treatment time. Specifically, the nitrogen content decreased to less than half of that present immediately following plasma polymerization (both 90 and 20° take-off angle, Figure 5.1.2c). A slight increase in oxygen content also occurred (Figure 5.1.2b at the 20° angle). These changes are unexpected since the plasma polymer was deposited on an organic substrate (polyethylene) with which the allyl amine is expected to form covalent carbon-carbon bonds. A loss of nitrogen was also seen by Tang et al. (1998) when aminated polyethylene terephthalate disks were immersed in buffer for two weeks.

The hydrophobicity of the plasma polymerized surfaces in this work increased on exposure to buffer (in Figure 5.1.1) and the XPS data showed increased carbon content especially at the 90° take-off angle. The high resolution C1s envelope also showed an increase in the -C-C- component (Figure 5.3.1) and a decrease in all oxidized forms of carbon compared to the dry allyl amine plasma surfaces. These data may indicate that part of the plasma polymer layer was removed, thereby exposing the PE substrate. The changes in elemental composition and the increase in contact angles occurred for both treatment times, i.e. 10 and 30 minutes, suggesting that loss of plasma polymer occurred over the first 10 minutes.



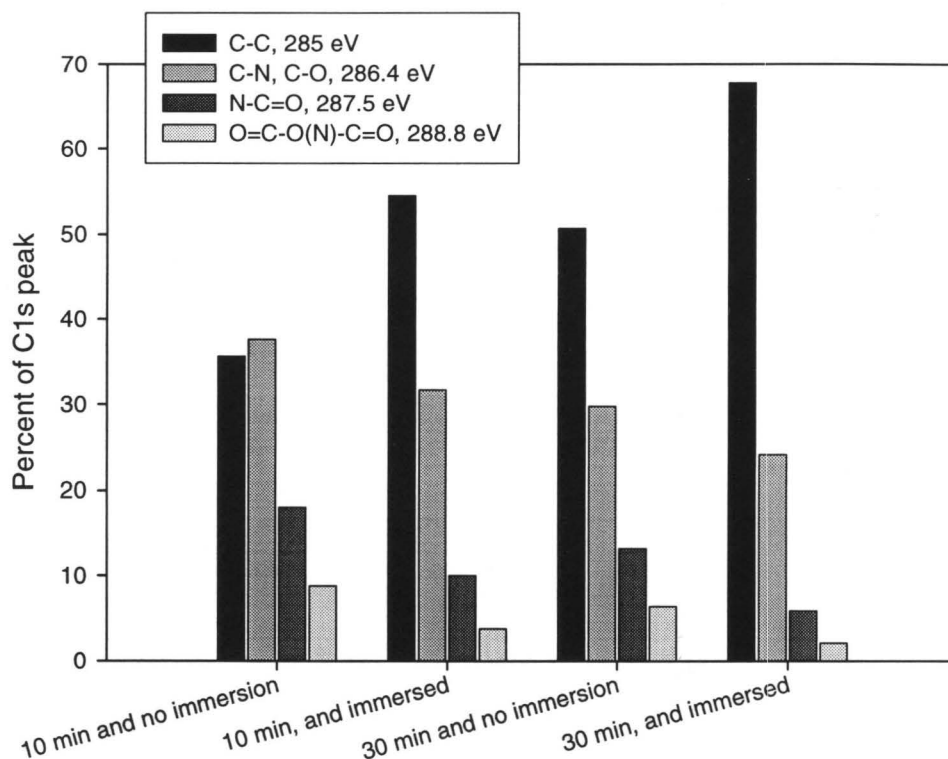
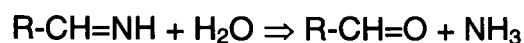


**Figure 5.3.1: Composition of C1s peak of allyl amine plasma polymers: effects of immersion in buffer. Spectra were taken at 90° take-off angle.**

There are two possible reasons for the decrease in nitrogen on exposure to buffer: surface rearrangement or loss of the plasma layer. As discussed in the section on aging (5.2), polar functionalities may migrate towards the bulk in a hydrophobic environment (such as air or a vacuum). Surface rearrangement does not seem likely in this case since PBS buffer is a polar solvent. In addition, the surfaces treated for 30 minutes, which may be more extensively crosslinked and would be expected to exhibit a slower migration process (as seen in Figure 5.2.2), also show the loss of nitrogen. The literature provides support for simple

loss of the plasma polymer layer when placed in a polar solvent. Water present in the plasma polymer may cause hydrolysis and degradation, and when placed in solution, low molecular weight compounds may dissolve out (van Os et al., 2001; Yasuda, 1990; d'Agostino, 1994). Loss of the deposit may occur because of changes in surface chemistry that result in loss of functional groups. These changes may depend on the functional groups present. For allyl amine, amides, imines and nitriles may be present as well as amino groups (Gengenbach and Griesser, 1999; Krishnamurthy et al., 1989). Hydroxyl and carbonyl groups may also be present (Gengenbach and Griesser, 1999). Hydrolysis of certain functionalities may lead to the incorporation of oxygen and the loss of nitrogen in the allyl amine plasma polymer when exposed to buffer. Gengenbach and Griesser (1999) proposed that when imines react with water, oxygen may be incorporated as carbonyl and nitrogen may be eliminated as ammonia:



Gaseous ammonia could escape during or after treatment (Gengenbach and Griesser, 1999) as a result of exposure to water. Nitriles may also be subject to hydrolysis forming amides (Gengenbach et al., 1999). The relatively small increase in oxygen for the 10-min sample that was immersed in buffer (Figure 5.1.2B) suggested that these reactions cannot account for all of the nitrogen loss. The increase in oxygen could explain the loss of nitrogen in the 30-min sample; however it is expected that the loss of nitrogen occurs by the same mechanism

for both treatment times. Water penetration through the plasma polymer with dissolution of low molecular weight polymer chains may be more important (van Os et al., 2001).

Delamination of the plasma-deposited layer may be dependent on other conditions in the reactor. The degree of polymerization has been found to contribute to the level of delamination (van Os et al., 2001). It was seen in the present work that increasing the treatment time, expected to increase the degree of polymerization, did not prevent delamination. Chatelier et al. (1995b) varied the power:flow rate ratio (W/F) in an attempt to produce a plasma polymer of heptylamine that would not delaminate from muscovite mica in water. However, if the energy parameter, W/F, is too low, the plasma polymer may fall into the "powder" regime and subsequently delaminate (d'Agostino, 1994, Yasuda, 1990, Beamson et al, 1985). Highly crosslinked plasma polymers formed from allyl amine at higher power input were insoluble in chloroform, water at room temperature and boiling water (Krishnamurthy et al., 1989).

The significance of buffer effects for the present work is the possibility that the changes that occur may affect subsequent conjugation reactions and interactions with proteins. In light of the XPS and contact angle data, it is unclear whether the proteins in contact with these surfaces will respond to the surfaces as removed from the plasma reactor, or as altered by contact with the buffer. As will be seen below, the time of immersion in buffer between 1 and 2 days does

not appear to affect the interactions between the plasma polymerized allyl amine surface and fibrinogen (Figure 5.6.1).

The choice of solvent in the polymer grafting reactions is important for the yield of these reactions. From the XPS data, it is seen that the nitrogen content decreased upon immersion in buffer. Therefore, the amino group content (the functional groups required for grafting) may also decrease, resulting in fewer sites for grafting of the PEO and PVP polymer chains.

Since the concentration of free amino groups is important for the grafting reactions, quantification of these groups is desirable. High resolution N1s XPS data have the potential to yield functional group information; although the spectral resolution may be marginal for this purpose (e.g. amines versus amides [Griesser et al., 1994]). Derivatization reactions can also be used to quantify specific functions. Common derivatization reagents are pentafluoroaldehyde (Sodhi et al., 2001; Gengenbach and Griesser, 1999) and trifluoroacetic acid (Rinsch et al, 1995), which have been used to determine free amino groups via the XPS fluorine signal. However, incomplete reactions, nonspecific desorption of the reagent, and dissolution of the plasma polymer in the reaction solvent are some of the difficulties associated with these techniques (Fally et al, 1995).

#### **5.4 Chemical Modification of the Polymer Chain Ends of PEO and PVP for Grafting**

PVP and PEO surfaces were prepared by grafting the preformed polymers to polyethylene via chain-end attachment. The polyethylene surfaces were first

modified by the plasma polymerization of allyl amine to provide amino groups for reaction with appropriate functions at the polymer chain ends, e.g.-COOH to form an amide linkage. In this work, two reagents were studied: 1) 1-[3-(dimethylamino) propyl]-3-ethylcarbodiimide and N-hydroxysuccinimide (EDC/NHS), and 2) N-N-disuccinimidyl carbonate (DSC).

#### **5.4.1 Chemical Modification of Hydroxy-PVP and -PEO with EDC and NHS**

The EDC/NHS coupling system activates carboxylic acid groups for reaction with amine groups to form an amide bond. Since the polymers as purchased were hydroxyl-terminated, it was necessary to react them with succinic anhydride to generate the desired carboxyl end group before reacting with EDC/NHS. A schematic illustrating the polymer activation reaction is shown in Figure 3.4.1. Figures 5.4.1 and 5.4.2 show, respectively, the NMR spectra for the products of the reaction of PEO and PVP 2500 with succinic anhydride.

In Figure 5.4.1, the dominant peak at 3.5 ppm (b) can be assigned to the ethylene oxide mer of PEO. The sharp peak at 3.3 ppm (a) represents the methoxy end group protons. The peak at about 4.3 ppm (d) is assigned to the linkage of the PEO and succinic acid moieties, and the new protons from the succinic acid moiety are represented by the peak at 2.62 ppm (e) (Du, 2001). Peak integration shows that the conversion is >70% (ratio of peaks d to a, divided by the expected ratio of 0.66).

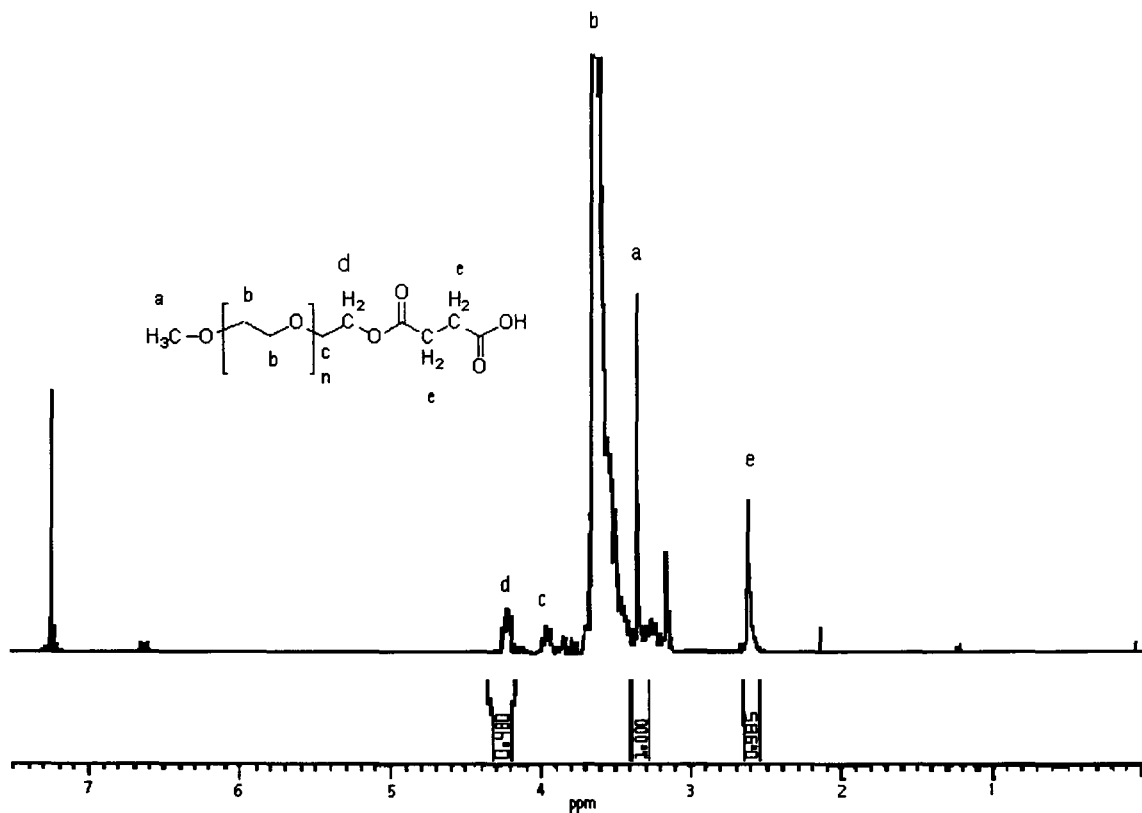


**Figure 5.4.1:** Proton NMR spectrum of PEO following reaction with succinic anhydride. Solvent is CDCl<sub>3</sub> with peak at 7.24 ppm. The expected product is shown in the inset. Note formation of bond at peak d (4.3 ppm).

Figure 5.4.2 shows the NMR spectrum of the product when PVP 2500 reacts with succinic anhydride. The PVP spectrum is more complex. N-vinyl pyrrolidone is generally polymerized in isopropanol, thus leading to an isopropyl residue at one end (Haaf et al., 1985). The other end group is reported to be

methyl. The isopropyl and methyl group protons have similar chemical environments and the peak in the vicinity of 1.2 ppm is assigned to them. The broad peaks represent the protons from the polymer. The backbone protons, methine and methylene, are assigned to peaks b and c. The peaks d, e, and f are assigned to the protons from the lactam group (Haaf et al., 1985). Peaks at 2.92 (g) and 2.81 (h) ppm are assigned to the protons of the succinic acid moiety (Du, 2001). However, the protons assigned to unreacted succinic anhydride (i) and the by-product, succinic acid (j), appear in the spectrum at 2.97 ppm and 2.5 ppm respectively. The products of the reaction of succinic anhydride with PVP 2500 and PVP 10,000 showed similar spectra. The large polydispersity of the PVP samples leads to unreliable peak integration and estimates of conversion, typically of the order of 50%, are only approximate.

The next step in chain end modification was the reaction of the carboxyl group with EDC and NHS. Effectively NHS is substituted for the carboxylic end group: it is a much more effective leaving group in the subsequent polymer coupling reaction. The NMR spectra of carboxylated PVP and PEO after reacting with EDC/NHS are shown in Figures 5.4.3 and 5.4.4 respectively.

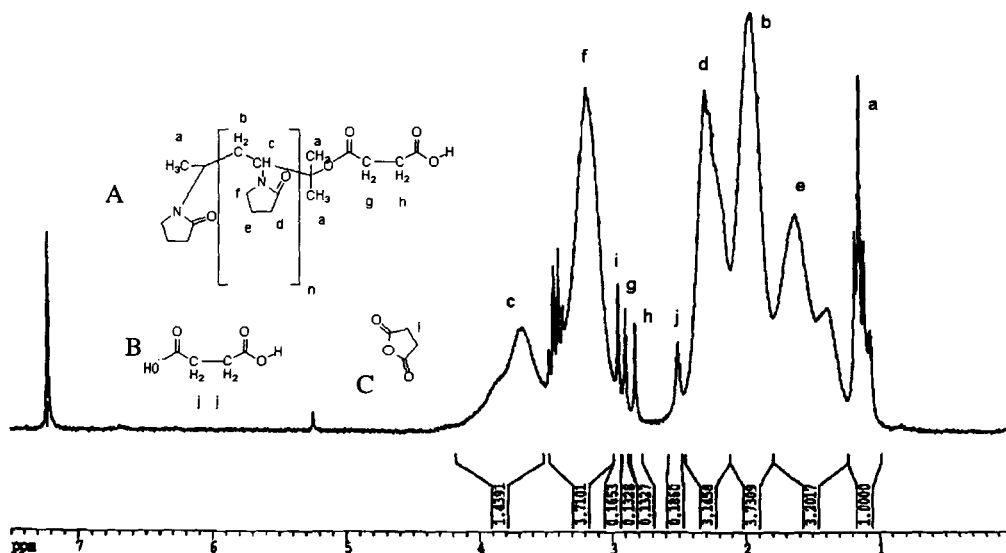


**Figure 5.4.2: Proton NMR spectrum of PVP 2500 following reaction of hydroxy terminated polymer with succinic anhydride. Structures of A) expected PVP product, B) succinic acid, C) succinic anhydride are shown in insets. Solvent is  $\text{CDCl}_3$  with peak at 7.24 ppm. Peak g and h suggested the presence of the protons from the succinic acid moiety.**

As seen in the Figure 5.4.3, the link between the PEO and the succinic anhydride moiety remains intact (peak c at 4.3 ppm). The peak at 2.6 ppm in Figure 5.4.3a should split into two triplets centred at 2.78 and 2.92 ppm (Du, 2001). One triplet appears at 2.92 ppm, while the peak at 2.78 overlaps the proton signal from the N-hydroxy succinimide and the peak splitting is unclear. The peak at 2.83 ppm is assigned to the protons from the N-hydroxy succinimide



moiety (Du, 2001). The conversion for this reaction is estimated to be about 30% (ratio of peak f to peak a). The overall conversion for both steps is estimated to be about 25%.

Figure 5.4.4 shows NMR spectrum of the product after carboxylated-PVP 2500 reacts with EDC/NHS. Since the protons from the N-hydroxy succinimide (peak i) appear in the vicinity of 2.80 ppm, the peak for these protons may overlap the peaks for the succinic acid end group (peak h). The peak (g) at 2.92 ppm is visible, indicating that the succinic acid end group may remain intact. The yield is estimated to be 15% (ratio of peak i to peak g). The overall yield for PVP is about 10%, although it can be as high as 25% for the two-step activation process.

Purification of the intermediates was not as successful for PVP as it was for PEO (Figure 5.4.2), which may affect the yield of subsequent reactions. Free succinic acid may compete with PVP for reaction with EDC and NHS. The NMR spectrum will likely not differentiate between the protons of the N-hydroxy succinimide moiety bonded to succinic acid and those of N-hydroxy succinimide bonded to carboxylated-PVP. The PVP moiety is more than 10 bonds away from the N-hydroxy succinimide, and thus the N-hydroxy succinimide moiety on either carboxylated-PVP or succinic acid will appear at similar positions. The succinic acid also may not be completely removed in the purification steps after the reaction with EDC and NHS. Succinic acid complexed to NHS may react with

amino groups in the surface, thus lowering the grafting yield of PVP to the aminated surfaces.

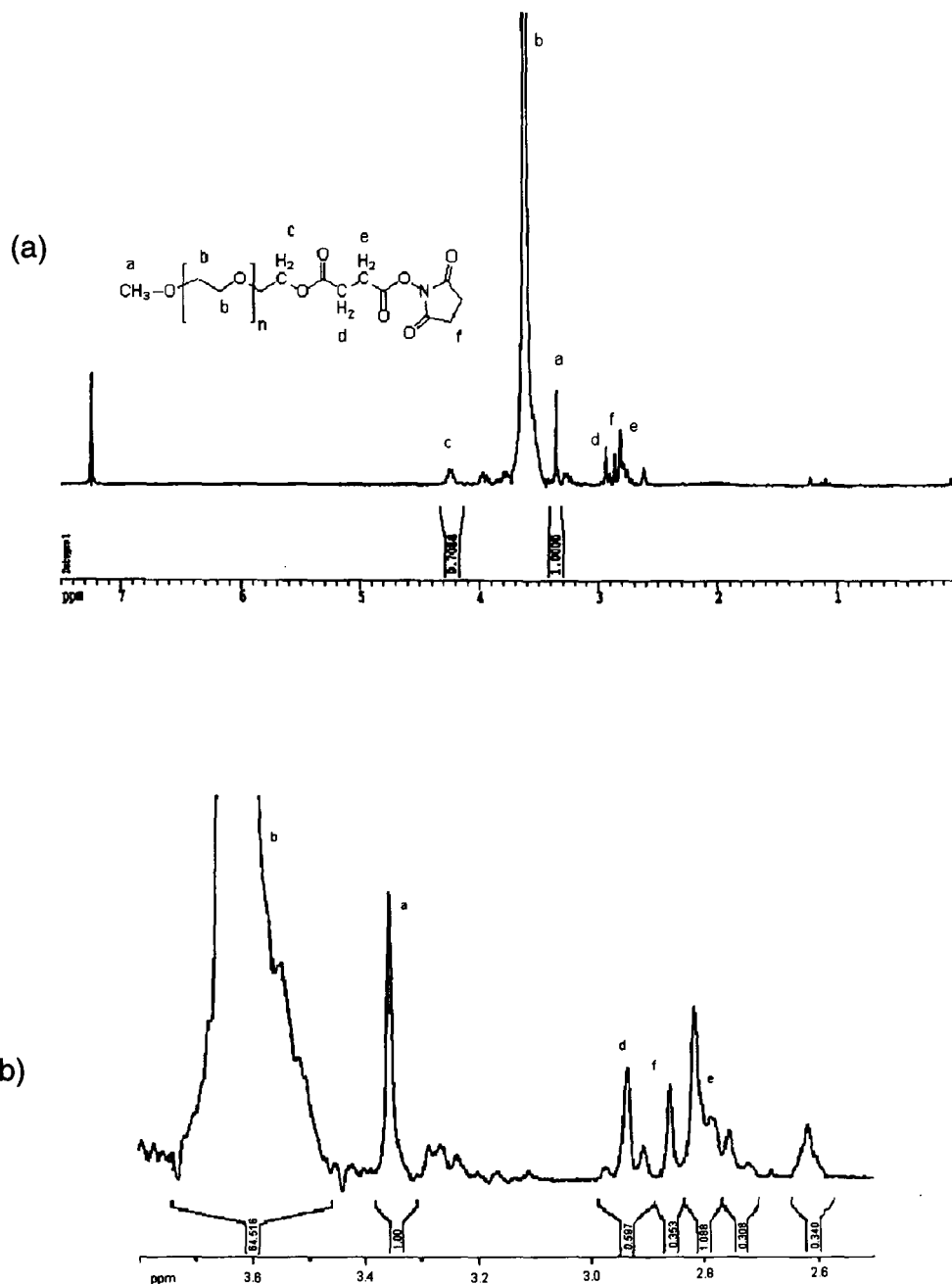


**Figure 5.4.3: Proton NMR spectrum of the carboxylated-PEO after reaction with EDC/NHS. Solvent is CDCl<sub>3</sub> with peak at 7.24 ppm, shown in (a). (a) 0-7.5 ppm (b) 2.6-3.8 ppm. Expected product shown in inset of (a). A triplet at peak d, and the larger integration at f and e may have indicated that NHS has reacted.**

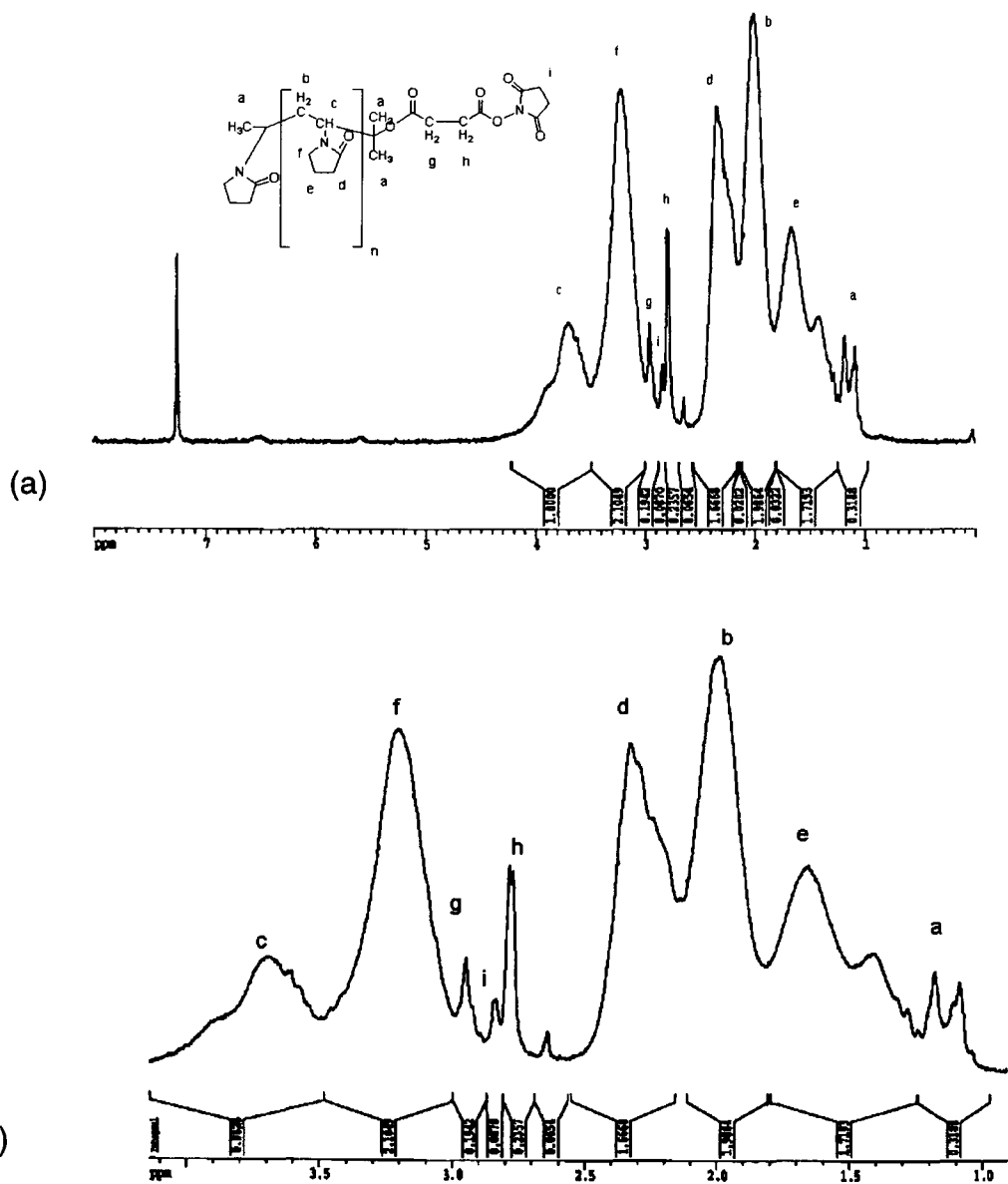


**Figure 5.4.4: Proton NMR spectrum of carboxylated-PVP after reaction with EDC and NHS. Solvent is CDCl<sub>3</sub> with peak at 7.24 ppm; a) 0-8.0 ppm b) 1.0-4.0 ppm. Expected product is shown in inset of (a). Peak i indicated that NHS has reacted.**

#### 5.4.2 Chemical Modification of Hydroxy-PVP and -PEO with DSC

An alternative chain-end activation procedure using N,N-disuccinimidyl carbonate (DSC) was investigated. It was hoped that a higher yield would be obtained since DSC activation is a simpler, one-step process. Disuccinimidyl carbonate has been used to conjugate protected xylofuranose to L-ephedrine (Ghosh et al., 1992) or diacryl-glycerophosphatidylethanolamine to bis- $\omega$ -hydroxypolyethylenoxy disulphide as an anchor for gold surfaces (Boden et al., 1998), and offers a simpler approach by reacting directly with hydroxyl groups. The reaction yield can sometimes be improved by the use of a catalyst, a common one being triethyl amine (Ghosh et al., 1992). The carbonate compound can react subsequently with amino groups to form a carbamate bond (Figure 3.5.2). The leaving group is very similar to that in the succinic anhydride, EDC/NHS 2-step coupling system. The possibility exists that the byproduct NHS could remain if the purification were not complete. However, it was not expected that NHS would compete with the modified PVP for amino groups in the surface.

The NMR spectra for the products of this reaction using the triethyl amine catalyst are shown in Figures 5.4.5 and 5.4.6.

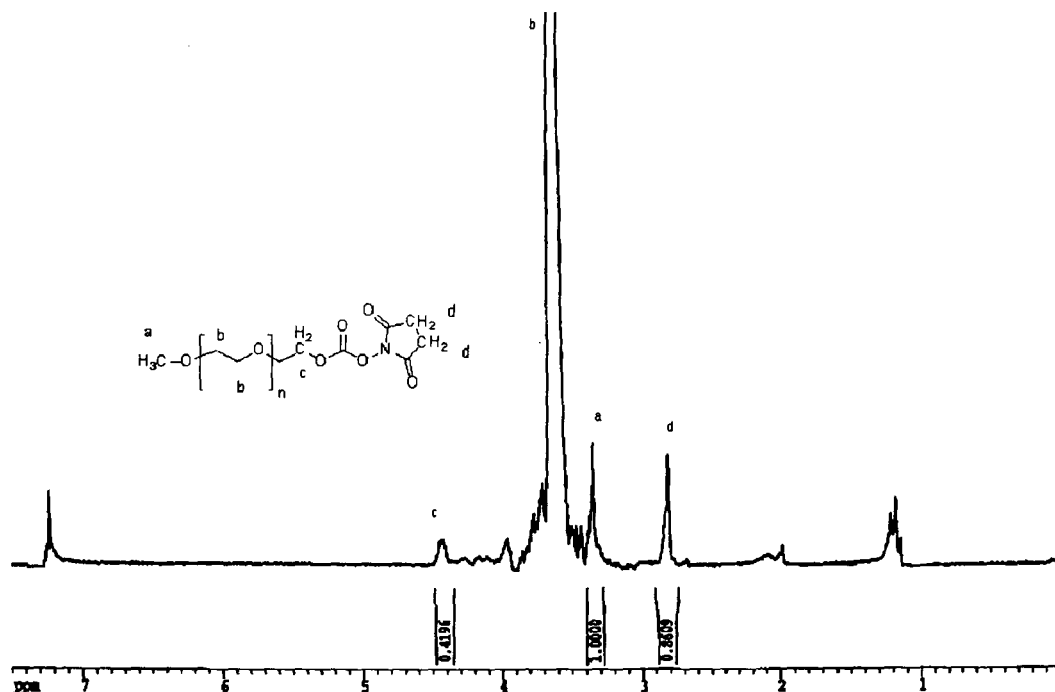


**Figure 5.4.5: Proton NMR spectrum of PEO after reaction with DSC. Solvent is  $\text{CDCl}_3$  with peak at 7.24 ppm. Expected structure is shown in inset. Peak c indicated that a new bond has formed in PEO.**

As seen in Figure 5.4.5, the peak at 4.45 ppm (peak c) showed that a new bond has formed between PEO and DSC, while the protons of the N-hydroxysuccinimide residue appeared at 2.80 ppm (peak d). From peak integration (ratio c:a, divided by the expected ratio of 0.66), the conversion is estimated to be about 70%. Without the catalyst, the conversion for PEO was typically 15%.

Figure 5.4.6 shows the NMR spectrum of the product of the reaction between PVP 2500 and DSC.

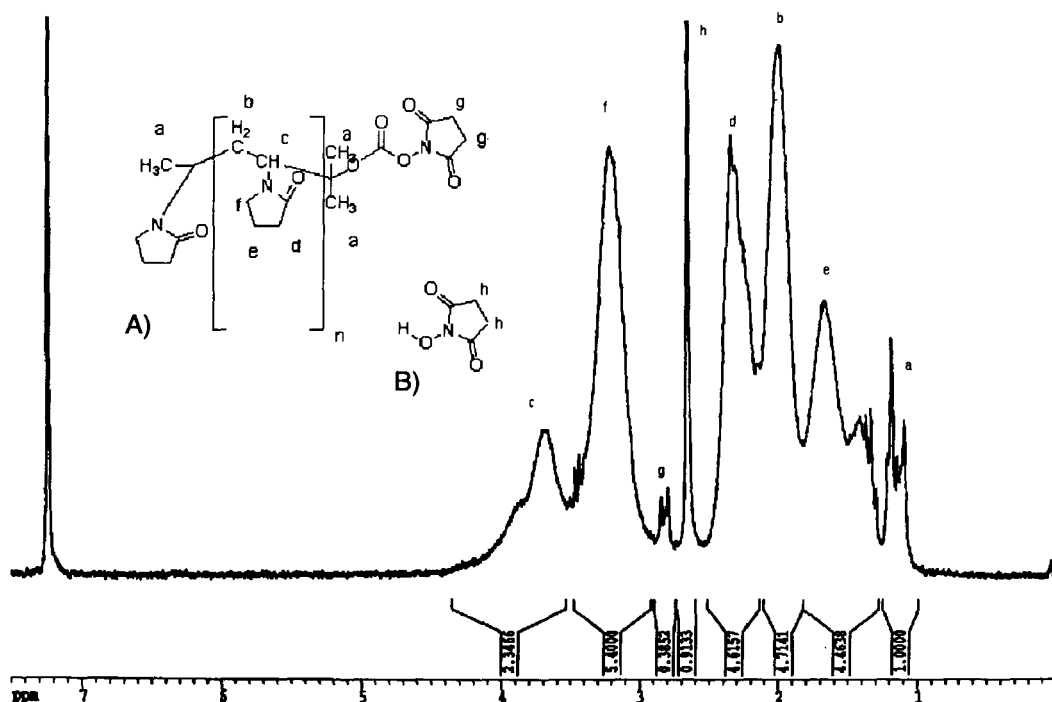


**Figure 5.4.6: Proton NMR spectrum of PVP 2500 after reaction with DSC. Solvent is  $\text{CDCl}_3$ , with peak at 7.24 ppm. Expected product (A) and byproduct NHS (B) are shown in inset. Peak g represents the protons from the NHS moiety, while peak h is from NHS byproduct.**

In Figure 5.4.6, the peak at 2.80 ppm (g) was assigned to the protons of the N-hydroxysuccinimide residue on the PVP. The peak at 2.69 ppm (h) represented the protons of the by-product, N-hydroxy succinimide. Because of the complex chemical environment of PVP, the yield was difficult to determine

accurately but was estimated to be about 55% (ratio g:a), although yields are typically 30%. PVP 10,000 gave a yield of about 25% with or without catalyst.

It was seen, with both coupling systems, that the yield was low especially for PVP (both MWs). Thus it appeared that the yield of activated PEO and PVP (especially PVP) was low whether DSC or EDC/NHS is used. To compensate for the low content of chain-end-activated molecules in the polymer samples, a large stoichiometric excess relative to the assumed amino group content of the surface was used in the grafting step. In addition, relatively long reaction times were used to ensure a high extent of reaction for all three polymers and compensate for differences in diffusivity. From these considerations and since the PEO and PVP have similar molecular weights, it may be reasonable to expect that the graft densities of the polymers are similar.

### **5.5 Surface Properties of PVP and PEO Modified PE Surfaces**

PVP and PEO were grafted to plasma polymerized allyl amine surfaces following activation. For both the EDC/NHS and DSC activation systems, the N-hydroxy succinimide moiety is the leaving group. In the EDC/NHS system, the aminated surface forms an amide bond via the succinic acid moiety to PEO and PVP.



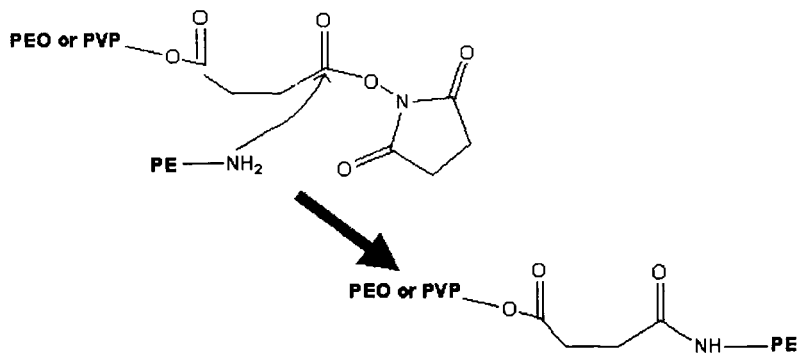


**Figure 5.5.1 Grafting of EDC/NHS activated polymers to allyl amine plasma layer via amide bond formation.**

In the DSC activation system, the aminated surface forms a carbamate bond with PEO and PVP (Figure 5.5.2).

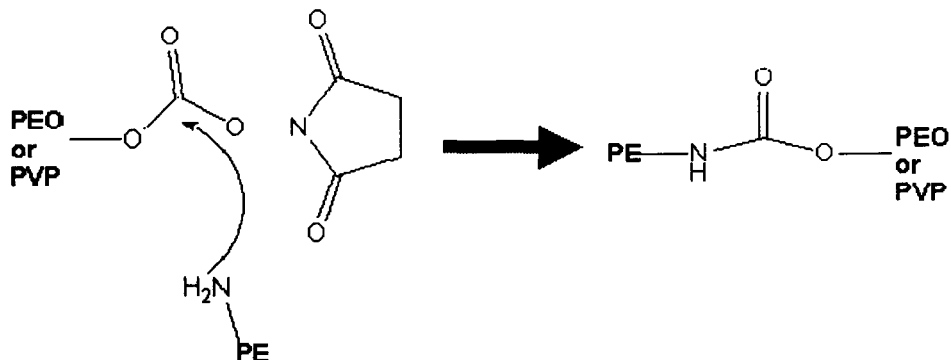


**Figure 5.5.2 Grafting of DSC-activated polymers to allyl amine plasma layer via carbamate bond formation.**

### 5.5.1 Water Contact Angles

Contact angles and XPS were used to characterize the surfaces. Figure 5.5.3 shows the water contact angles obtained for the modified surfaces using the different coupling systems.

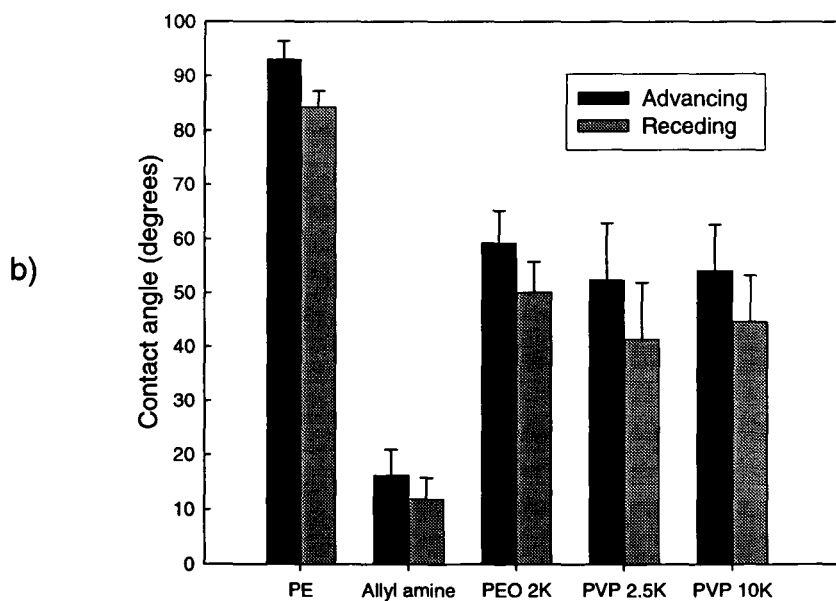
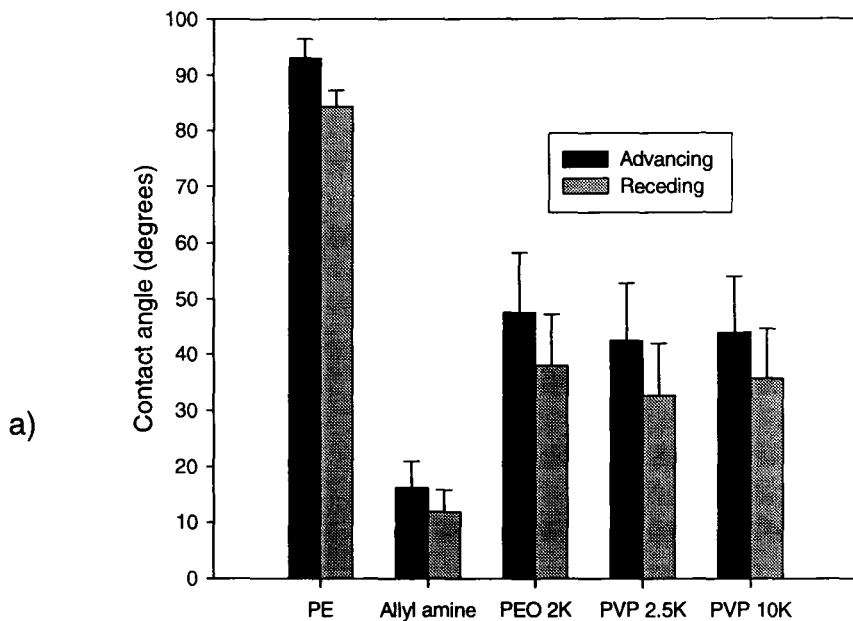


**Figure 5.5.3: Water contact angles of PEO and PVP modified surfaces (a) polymers activated with EDC/NHS; (b) polymers activated with DSC. Data are mean  $\pm$  1 S.D, n>20 (pooled). Contact angles increased on the polymer-modified surfaces, although this increase was higher on surfaces activated with DSC.**

As seen in Figure 5.1.1 and Figure 5.5.3, the plasma polymerization of allyl amine resulted in a large reduction in the water contact angles relative to PE: from 95 to 16° for the advancing, and from 84 to 11° for the receding angles.

Reaction of the allyl amine modified surfaces with the polymers increased the water contact angles in all cases, with the PEO-modified surfaces showing the highest values. PVP and PEO activated with EDC/NHS gave advancing angles between 42 and 47° and receding angles between 32 and 37°. PVP and PEO activated with DSC gave advancing angles between 52 and 59° and receding angles between 41 and 50°. Both PEO and PVP are hydrophilic polymers. Thus coatings of PEO and PVP of various molecular weights on polyethylene terephthalate gave contact angles of 20° (Desai and Hubbell, 1991). Therefore it seems likely that the surface coverage of the polymer-modified surfaces in the present work is less than 100%. It is interesting to note that the polymers activated with the EDC/NHS reagent showed significantly lower contact angles ( $\alpha < 0.05$ , one-way ANOVA) than those activated with DSC. Although the water contact angle measurements do not give information on the chemical composition of the surfaces, the data suggest that more extensive grafting occurred on these surfaces than on those formed with DSC-activated polymers.

### **5.5.3: XPS Analysis of the Grafted Surfaces Using EDC/NHS-activated Polymers.**

XPS was performed on the surfaces obtained using the polymers activated with EDC/NHS at the Institute of Chemical Processing and Environmental Technology (ICPET) in Ottawa. It is important to note that the surfaces had aged anywhere between 11 and 26 days from the time of preparation to the time of analysis. As discussed in section 5.2, aging affects the structure of the allyl amine plasma polymer with significant changes in chemical properties over time.

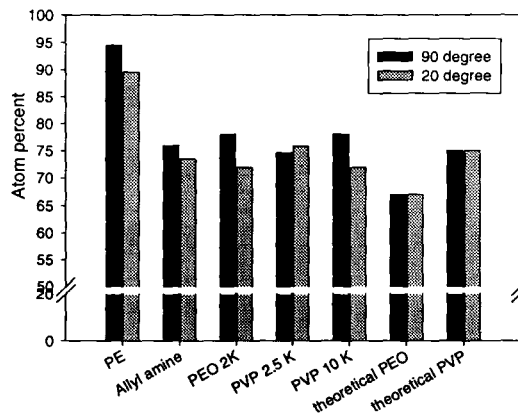
Figure 5.5.4 shows the elemental composition from low resolution data at both 90 and 20 degree take-off angles. For the unmodified PE, the carbon content is of the order of 90 to 95%. Small amounts of nitrogen and oxygen are also present. The latter are presumed to result from surface contamination, and this is supported by the greater values at the more surface sensitive grazing angle. Following plasma polymerization of allyl amine, the XPS spectra show the presence of significant nitrogen as would be expected. The high content of oxygen in this surface is likely the result of reaction of atmospheric oxygen with free radicals present in the plasma polymer following removal of the surfaces from the plasma reactor.

Modification of the plasma polymerized allyl amine surfaces with either PVP or PEO resulted in a slight increase in the C1s signal. The carbon content

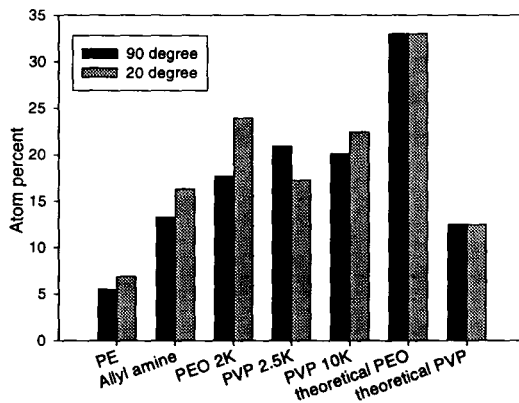
in the PVP surfaces is consistent with theory. The PEO surface has a carbon content higher than the theoretical value at both 90 and 20°, suggesting that the surface coverage is not complete or not thick enough to mask the underlying surface completely.

An increase in the oxygen content was observed on all polymer-modified surfaces compared to the allyl amine precursor, and this increase was slightly greater at both take-off angles on the surfaces modified with PEO than on those modified with PVP. The theoretical XPS oxygen content of PVP is 12.5%, and if the surface coverage is significant, a decrease in oxygen in the PVP-modified surfaces may be expected. The data show in fact that the oxygen content increased, possibly due to the presence of succinic acid residues (as discussed above) or other contaminants. For the PVP 10,000, the oxygen content was greater at 20° than at 90°, possibly due to contaminants. The oxygen content of the PVP 2500 surface was lower at 20° than at 90°, suggesting that more PVP may be incorporated at the lower molecular weight.

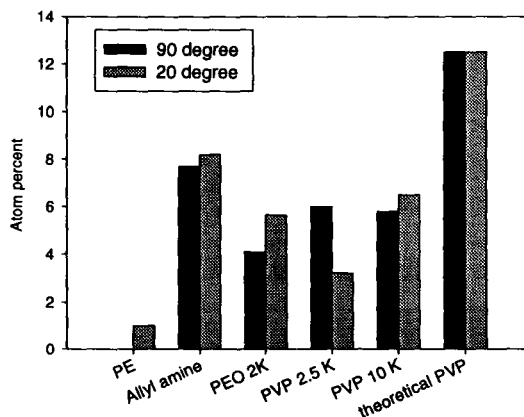
The theoretical oxygen content of PEO is 33% and an increase in surface oxygen was expected after grafting on PE if coverage is significant. The data showed that such an increase, greater at 20° than 90°, was in fact observed.



A)



B)



C)

Figure 5.5.4: XPS elemental analysis of PEO- and PVP-grafted surfaces. Polymers activated with EDC/NHS. A) C1s; B) O1s; C) N1s. Increase in oxygen and decrease in nitrogen seen on all polymer-modified surface, which as expected for PEO. Data precision  $\sim \pm 5\%$

A small decrease in the N1s signal was observed on all polymer-modified surfaces, the decrease being greater on the PEO- than on the PVP-modified surfaces. A decrease for PEO was expected. For PVP since the theoretical nitrogen content was 12.5%, i.e. slightly higher than the observed nitrogen content of the allyl amine layer, an increase in nitrogen was expected if the surface coverage is significant. A decrease was actually observed and, for the moment, this observation was not understood although it may indicate that the allyl amine plasma layer has been partly delaminated from the polyethylene.

High resolution C1s spectra were also obtained to provide information about the chemical bonding states of carbon. These spectra were fitted using a non-linear least squares routine based on the Marquardt-Levenberg method (Sodhi, 2003). An initial guess is made based on the expected chemical environment, taking the line shape into consideration. Parameters such as the full-width at half maximum (FWHM), the peak positions and peak heights are initialized. Typical FWHM are of the order 1.5 - 2 eV, and a Gaussian – Lorentzian (80:20) peak shape is used. When the FWHM is allowed to vary, the algorithm can develop problems. Therefore, the values of FWHM were constrained once a reasonable width was determined. The procedure was continued until a reasonable fit (done by eye) was obtained. It is important to have some independent knowledge of the chemistry of the system and that the final fit is consistent with what is known (Sodhi, 2003). For the high resolution

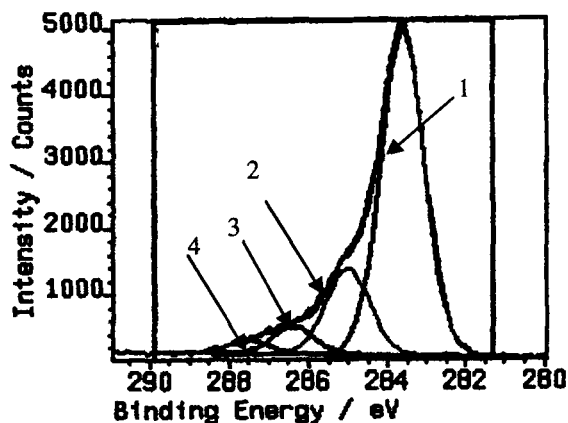
C1s envelope, the standard energies chosen were 285 eV (for C-C), 286.4 eV (for C-O or C-N), 287.5 eV (for N-C=O or C=O), and 288.8 eV (for O=C-N-C=O or O=C-O-C=O) (Beamson and Briggs, 1992).

Figure 5.5.5 shows C1s high resolution spectra for the allyl amine and polymer-modified surfaces. Although the dominant C-C peak is usually fixed at 285 eV, the ICPET data output centred this peak at 283.6 eV (Figures 5.5.5 and 5.5.6).

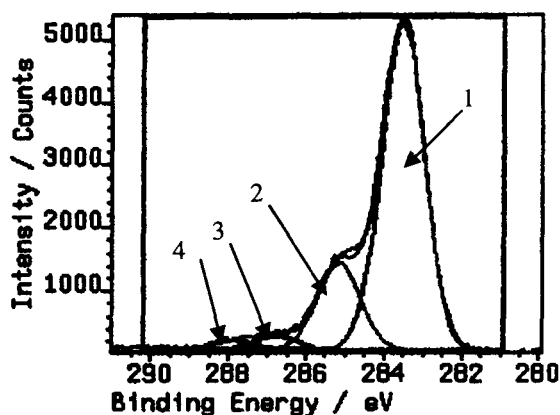
As seen in Figure 5.5.5, the spectrum of the PEO surface was different from that of the allyl amine precursor. The increase in the peak at 285 eV (C-O) suggested the presence of PEO. The spectra of both PVP surfaces are essentially the same as that of the precursor and do not provide any additional evidence of PVP attachment.

Figure 5.5.6 shows the composition of the C1s peaks. Complete surface coverage of PVP with no contribution from the underlying substrate should result in 33% and 15% of the C1s envelope at 285 eV (C-N) and 286.4 eV (N-C=O) respectively (in this case only). However, the C1s envelopes in the PVP surfaces do not show this distribution. The difficulty in comparing PVP to the allyl amine precursor surface is that both surfaces contain essentially the same functions. High resolution C1s spectra may thus not reveal the presence of PVP unless close to complete coverage is achieved.

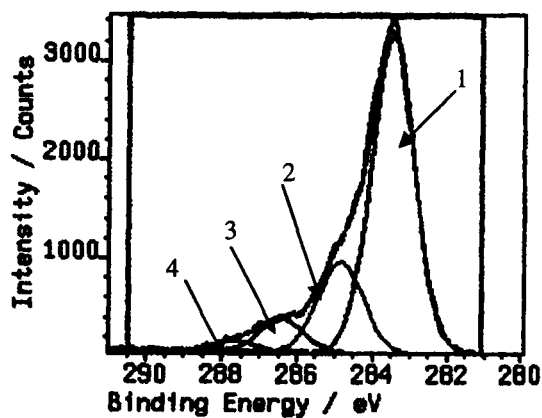




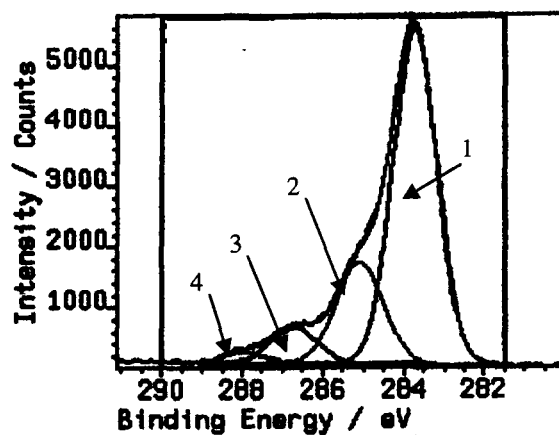
Allyl amine



PEO 2K



PVP 2.5K



PVP 10K

Figure 5.5.5: High Resolution C1s spectra of allyl amine, PEO and PVP (activated by EDC/NHS) surfaces at the 20° take-off angle. ICPET positioned C-C peak at 283.6 eV. The PEO surfaces showed a different shape from the allyl amine surface while PVP surfaces do not show much difference. Peak 1 is assigned to C-C bonds, peak 2 to C-N or C-O, peak 3 to amides and peak 4 to urethane or anhydride functionalities.

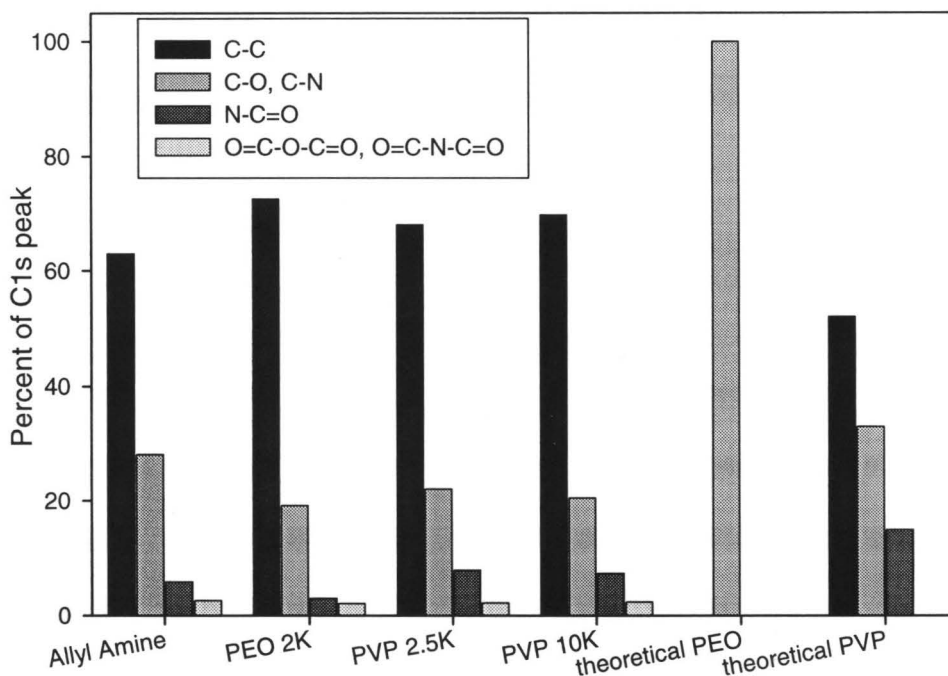


**Figure 5.5.6: Composition of the C1s envelope of the allyl amine, PEO- and PVP-grafted surfaces activated with EDC/NHS at the 20° take-off angle. The PEO surface showed a decrease in amide and urethane functionalities, while PVP surfaces had similar composition to the allyl amine surface.**

### 5.5.3 XPS Analysis of the Grafted Surfaces Using DSC-activated Polymers.

XPS analysis of the DSC-activated polymer surfaces was performed at Surface Interface Ontario (SIO), University of Toronto. In this case, the samples had aged for 3 days prior to analysis. The low-resolution data at take-off angles of 90 and 20° are summarized in Figure 5.5.7.

On all the polymer-modified surfaces, small increases in the C1s signal relative to the allyl amine control are observed. As seen in Figure 5.5.7, a thick layer of PEO would have a lower carbon content than the allyl amine and a layer

of PVP would have about the same carbon content. The interpretation is made difficult by the fact that the XPS most likely “sees” the underlying PE as well as the allyl amine and grafted polymer components. Indeed it would appear that the PE is more evident in the grafted surfaces, especially the PVP, than in the allyl amine.

The PEO surface shows an oxygen content ( $90^\circ$ ) of about 15%, i.e. similar to the allyl amine control, but less than the 33% that would be expected for a thick PEO layer. At  $20^\circ$ , the PEO surface shows slightly higher oxygen content than the allyl amine suggesting that some grafting has occurred. The oxygen content of the PVP surfaces is slightly lower, but not significantly so, than either that of the allyl amine or the theoretical value of 12.5% for PVP. Lower oxygen values support the conclusion that more of the PE substrate is “visible” (XPS) in the PEO than in the precursor allyl amine surface.

For all the polymer-modified surfaces a reduction in the N1s signal relative to the allyl amine control was observed. A decrease in nitrogen is expected for the PEO but not for the PVP. Complete coverage of the surface by a thick layer of PVP would result in a nitrogen content of 12.5%, i.e. an increase compared to the precursor surface. Again, as for the carbon and oxygen data, these results suggest that the content of PVP is low on these surfaces and that there may be patches where the PE substrate is visible.

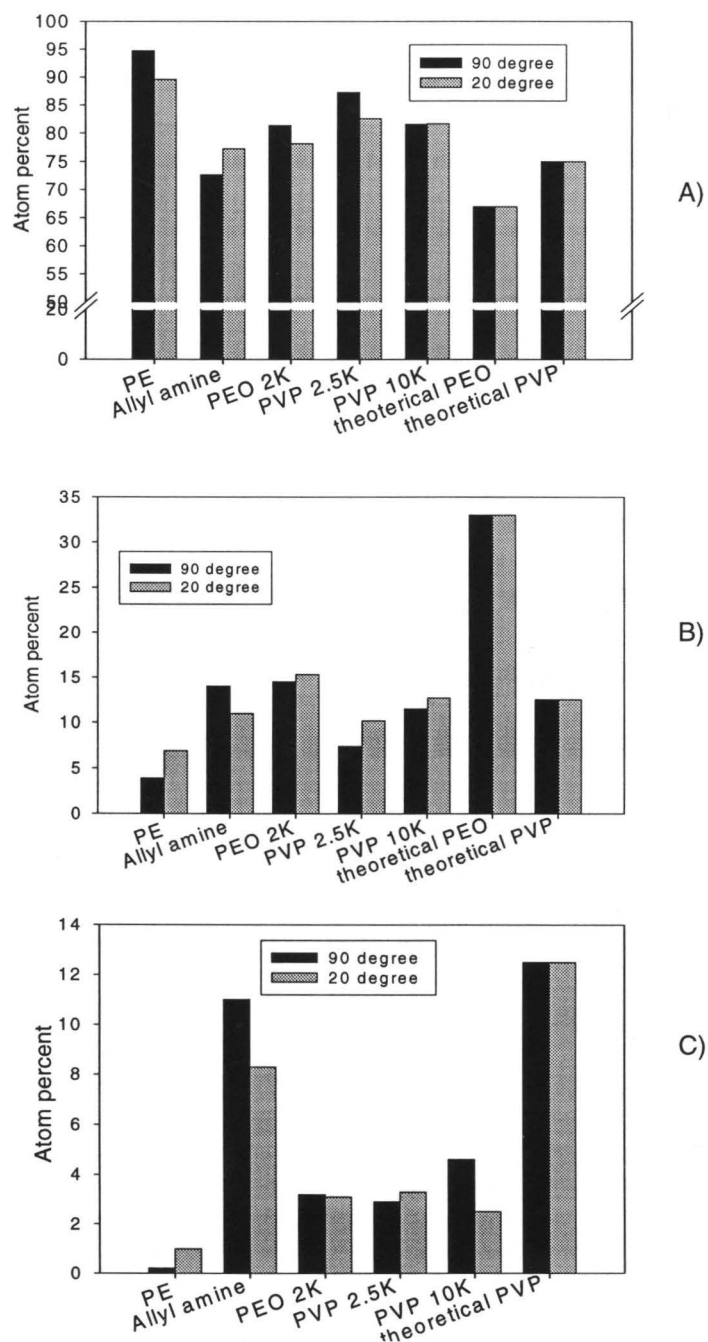
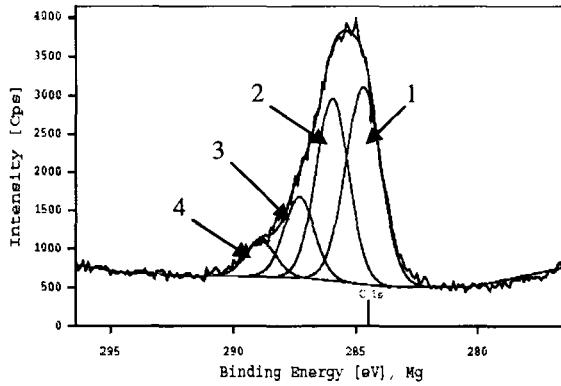


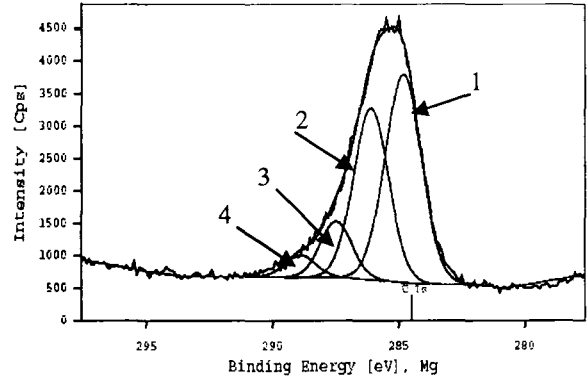
**Figure 5.5.7: XPS elemental analysis of PEO and PVP-grafted surfaces. Polymers activated with DSC. A) C1s; B) O1s; C) N1s. Data precision  $\sim\pm 5\%$ . Decreases in nitrogen for the PVP and a slight increase in oxygen for PEO suggested that there is a low surface coverage for the polymer-modified surfaces.**

The overall conclusion from the low resolution XPS data is that the graft density of the polymers on these surfaces is low.

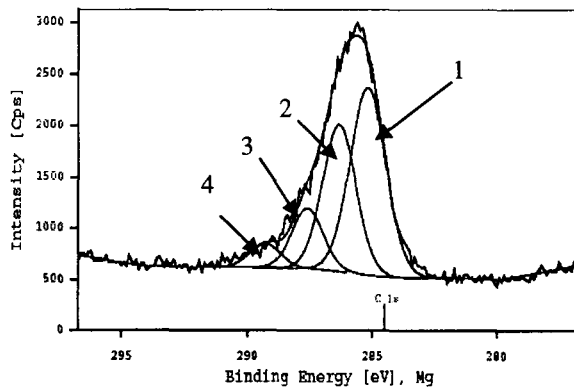
Figure 5.5.8 shows the high resolution C1s spectra for the PEO and PVP modified surfaces. The C1s envelopes for the PEO and PVP surfaces are not qualitatively different from that of the allyl amine. This contrasts with the data for the EDC/NHS activation system. Figure 5.5.9 shows numerical estimates of the peak areas in the C1s envelope. If the surface is completely covered with a thick layer of PEO, the carbon 1s peak should be centred at 286.4 eV, representing C1s in C-O bonds (Beamson and Briggs, 1992). At this energy, there is little difference between the PEO and the allyl amine surfaces. However, there is a decrease in the tail portion of the C1s envelope (greater than 287 eV).



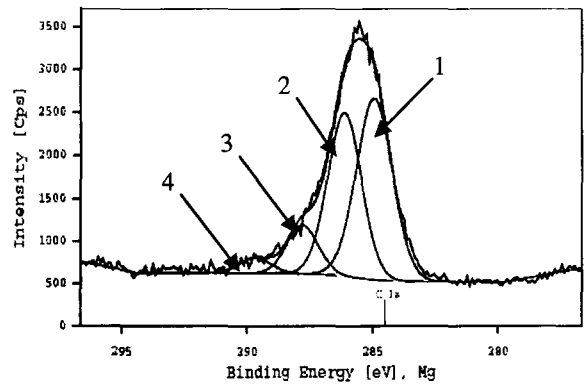
Allyl Amine



PEO 2K



PVP 2.5K



PVP 10K

**Figure 5.5.8: High Resolution C1s spectra at 20° take-off angle of allyl amine, PEO and PVP (DSC activation). Surface Interface Ontario centres C-C bond at 285 eV. Not many differences were seen between allyl amine and the polymer-modified surfaces. Peak 1 represents C-C, peak 2 represents C-O or C-N, peak 3 represents amides, and peak 4 represents urethane or anhydride functionalities.**

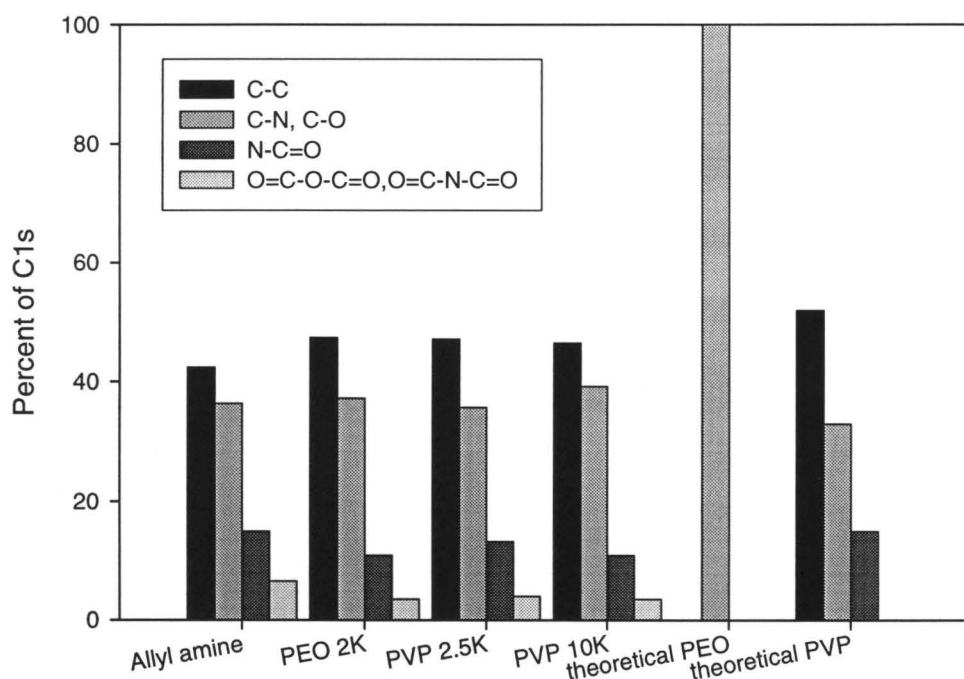


**Figure 5.5.9: Composition of the C1s envelope for DSC-activated polymers and allyl amine. High resolution spectra was taken at 20° and envelope was centred at 285 eV. All modified surfaces showed similar composition, which suggested low surface coverage.**

Similar to the EDC/NHS system, the surfaces grafted with PVP that was activated with DSC are not significantly different from the allyl amine control, although a slight decrease in the tail of the C1s envelope (> 288 eV) is observed. The chemical functionalities of these surfaces are clearly similar and discrimination based on analysis of the C1s peak is not feasible.

The fundamental difficulty in assessing XPS data in this study is that there are no distinct marker elements for PVP or PEO that could distinguish them from the underlying plasma polymerized allyl amine surface. The trends in the low resolution spectra are difficult to assess since an oxidation process occurs in the

allyl amine plasma polymer, resulting in oxygen incorporation. The polymers are expected to be bonded to the surface through an amide bond or a carbamate bond. However, due to post-plasma oxidation and general aging of the allyl amine surfaces, the oxidized species in the C1s envelope of the polymer-modified surfaces cannot be attributed solely to the bonds between the polymer and the surface.

#### **5.5.4 General Discussion of PEO and PVP Grafting**

The comparison of PEO to PVP in the present work is inherently limited by the different properties of the polymers. The PEO used has a narrow molecular weight distribution, with a polydispersity of 1.04. The PVPs have broader molecular weight distribution, with polydispersities of 1.9 and 3.9 for the 2500 and 10,000 molecular weight polymers respectively. In the polymerization of PEO, the anionic mechanism essentially eliminates chain-transfer and termination steps (Harris, 1992) while for PVP, produced by radical polymerization, transfer and termination are important (Robinson et al., 1990).

Polydispersity could significantly affect the reactivity of the polymer chains, the graft density achieved and other properties of the resulting surfaces. For example, it is likely that smaller chains would react preferentially to larger ones.

The approach of grafting preformed polymer chains to surfaces has a number of disadvantages. The relatively high molecular weights of the polymers can result in significant steric inhibition of the grafting reaction and reduce the



achievable surface chain density (Rovira-Bru et al., 2001). Furthermore, the polymer, as it approaches the surface, may not be in the right orientation for the reaction of the chain end with the active site in the surface to occur (Kingshott et al, 2002; Sofia et al, 1998).

Surface grafting may depend on the choice of activation group and grafting reaction conditions. Activating groups play a role in the reaction rate and grafting efficiency of the polymers. Aldehyde-terminated PEO was used to attach the polymer to plasma polymerized allyl amine surface (Kingshott et al, 2002) resulting in a high polymer graft density, as shown by high resolution C1s data. This reaction proceeds through formation of a Schiff base. Activating groups such as tresyl chloride have been used to bond hydroxy-terminated PEO to aminosilane-coated silicon wafers. The density estimated from ellipsometry data was 100 ng/cm<sup>2</sup> for PEO of molecular weight 3400 (Sofia et al., 1998).

In the present work, neither of the chain-end activation reactions gave high conversion despite the fact that a large excess of reagent was used. Clearly this would limit the extent of polymer grafting. Grafting is also dependent on the chemical properties of the underlying plasma polymerized allyl amine. The alteration of this layer by buffer exposure may also contribute to the low graft density of PEO and PVP.

Changing the conditions of the coupling reaction may improve the grafting efficiency and surface coverage. In the present work a pH of 7.4 was used for

the coupling reaction. Although EDC and NHS are effective up to pH 7.5, they are more stable at pH 5 (Hermanson, 1996). Therefore, operating a lower pH may increase the graft density of the polymers on the surface. Varying the concentration of triethyl amine and adding a promoter in the grafting reaction (Boden, 1998) may further improve yields. Other variables that may be important are ionic strength and type of buffer.

In aqueous solution PVP and PEO, exhibit an inverse temperature dependence of solubility (cloud-point) that reflects a phase change due to loss of hydration as temperature increases, resulting in a reduction of interchain distances (Kingshott et al., 2002, Guner, 1996). Salt concentration also affects the cloud point. It is possible that near the cloud point, higher graft density may be achieved. This phenomenon has been clearly demonstrated for thiolated PEO chemisorption to gold-coated surfaces (Unsworth, 2003). However, Kingshott et al. (2002) have cautioned that a minimum density of surface attachment points (e.g. amino groups) is required, even near the cloud-point. In this regard it was shown that the allyl amine plasma surfaces are altered when immersed in buffer, and it is possible that a loss of amino group content occurs.

Graft density is an important factor in resistance to protein adsorption as has been shown for PEO (Szeleifer, 1997; McPherson et al, 1998, Jeon et al., 1991). Knowledge of the graft densities of the polymer chains would allow a more meaningful comparison between PVP and PEO. The XPS data in the

present work do not allow determination of graft density. However, since PVP is a bulkier molecule than PEO, it might be expected to give surfaces of lower graft density that would show lower resistance to protein adsorption.

## **5.6 Fibrinogen Adsorption to the PEO- and PVP-grafted Surfaces**

The interaction of fibrinogen with the different surfaces was examined using radiolabeling methods as described in Chapter 3. It is expected that surfaces with terminally-attached hydrophilic polymer chains at sufficiently high graft density should show reduced protein adsorption (Leckband et al., 1999). PEO has been widely reported to repel proteins. PVP has been shown to be biocompatible, e.g. as a plasma expander, and thus may also be protein repellent (Robinson and Williams, 2002; Rovira-Bru et al., 2001; Francois et al., 1996).

Data on fibrinogen adsorption from buffer to: (a) the surfaces prepared using PEO and PVP activated by EDC/NHS, and (b) the surfaces prepared using PEO and PVP activated by DSC are shown in Figure 5.6.1.

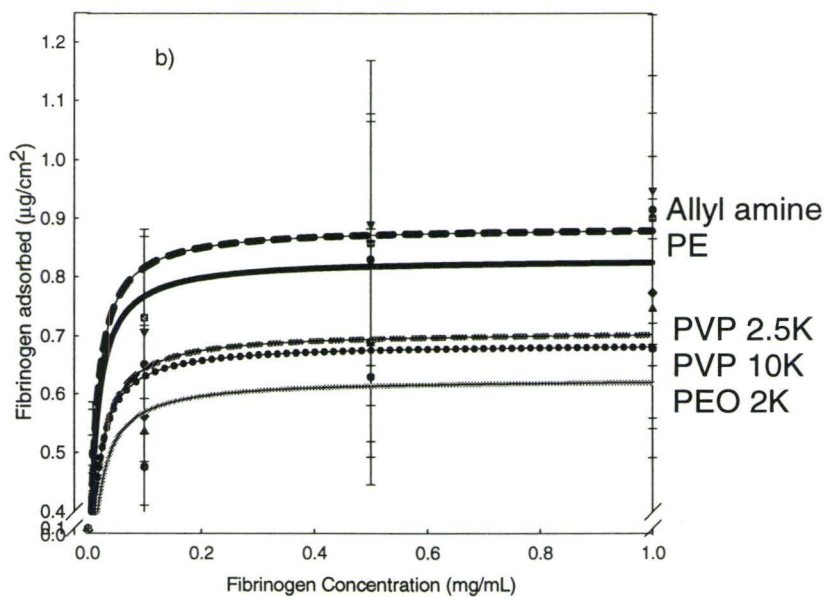
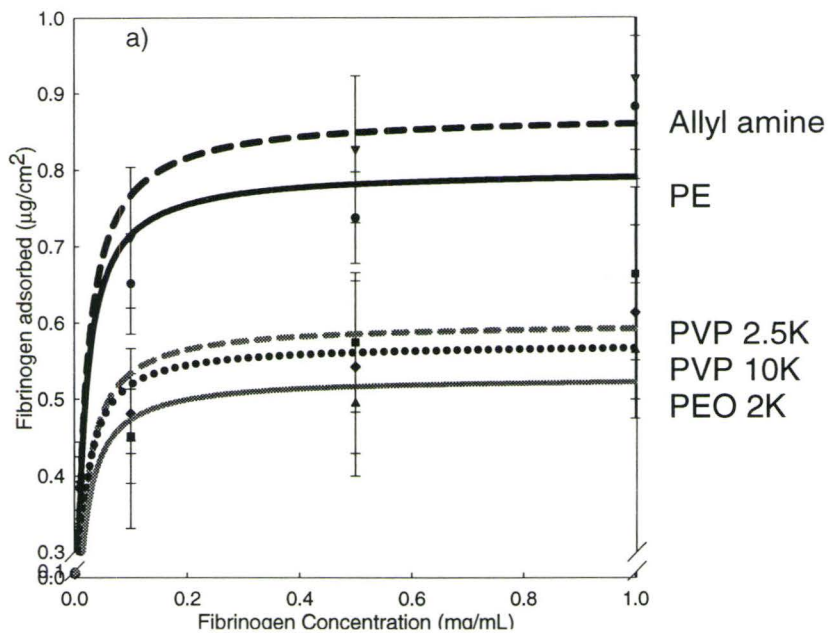


**Figure 5.6.1: Fibrinogen Adsorption to PEO and PVP surfaces a) EDC/NHS activation system b) DSC activation system. Adsorption time 3 h, PBS buffer pH 7.4. Data are mean  $\pm$  1 S.D.,  $n > 9$  (pooled data from 3 experiments). The PEO surface is the most protein repellent surface in both activation systems.**

As seen in this figure, the allyl amine plasma surface adsorbs more fibrinogen than PE. A similar trend has been observed by other investigators (Tang et al., 1998). The time of immersion in buffer prior to adsorption did not affect the data: exposures of 16 or 48 h gave similar adsorption values. From these data, it is clear that hydrophilicity is not the only factor involved in determining the level of protein adsorption to the surfaces, since the water contact angles on the plasma polymerized allyl amine surface were significantly lower than on any of the other surfaces. Plasma polymers of allyl amine seem to contradict the commonly held view that hydrophilic surfaces adsorb less protein than hydrophobic ones (Griesser et al., 1994; Tseng and Edelman, 1998; Tang et al., 1998). The polymer-modified surfaces show reduced protein adsorption in varying degrees. The surface modified with PEO, activated by either EDC/NHS or DSC, adsorbed the smallest amount of fibrinogen. Surfaces based on the EDC/NHS activated polymers show lower fibrinogen adsorption than those based on activation with DSC. This trend correlates with greater hydrophilicity of the surfaces based on activation with EDC/NHS compared to those based on activation with DSC. Figure 5.6.2 shows the reduction in fibrinogen adsorption for the two activation systems compared to PE at a fibrinogen concentration of 1 mg/mL. In spite of the relatively large data scatter, particularly for the DSC-activated system, it is clear that these surfaces are significantly protein repellent, and adsorb less fibrinogen than the precursor polyethylene. The PEO surface shows a reduction in

fibrinogen adsorption of  $36\pm 7\%$  when activated with EDC/NHS, and only  $21\pm 7\%$  when activated with DSC. The PVP surfaces show a reduction of 25-30% when activated with EDC/NHS, but only 10-14% when activated with DSC. From these data, it appears that there are no differences between the PEO and PVP or between the PVP 2500 and PVP 10000 surfaces. The similarity in the fibrinogen-repellent properties between the two PVP molecular weights is perhaps not surprising since the molecular weight distributions overlap. It may be that the molecular weights of the actual grafted chains (favouring the lower molecular weights) are similar in both cases.

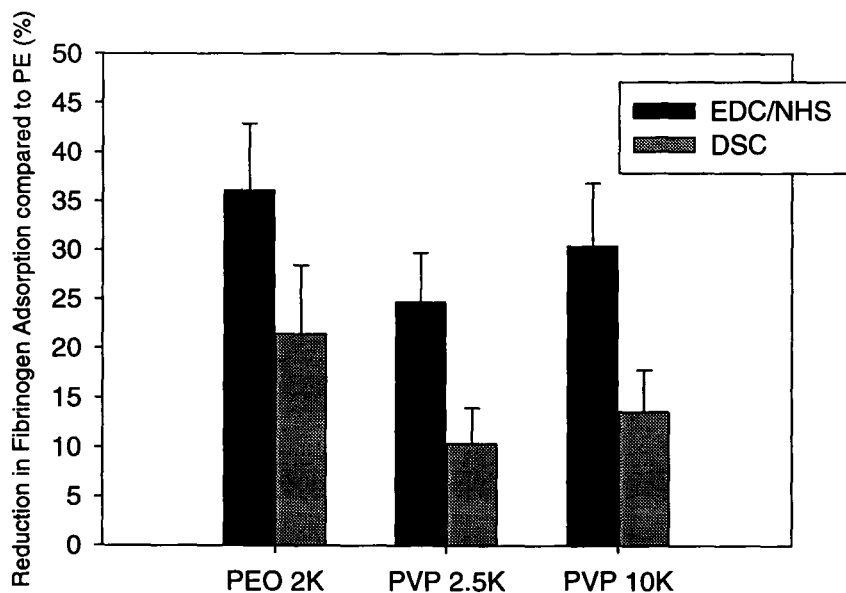


**Figure 5.6.2:** Reduction in fibrinogen adsorption compared to PE for both chemical-activating systems at 1mg/mL fibrinogen concentration of PEO and PVP. Data are mean  $\pm 1$  S.D.,  $n > 9$ .

## **5.7 General Discussion of Protein Resistance**

Although the XPS data suggest that high densities of PEO and PVP were not achieved in this work, the protein adsorption data show that the surfaces are significantly protein repellent. Relative to the data of Kingshott et al (2002) for PEO surfaces prepared in a similar manner, the reduction in fibrinogen adsorption on the surfaces in the present work is lower, and again it is clear that the density of PEO grafts is relatively low. Similarly for the PVP surfaces, the reductions achieved in the present work are lower than those observed by others (e.g. Rovira-Bru et al (2001) showed that PVP graft-polymerized on silica at a high density reduced lysozyme adsorption by 75%).

It is useful to consider the mechanisms generally considered to be responsible for the protein resistance of polymer-grafted surfaces. In particular, comparison of PVP and PEO in the context of these mechanisms with a view to understanding the reasons for the apparent greater effectiveness of PEO is of interest.

### **5.7.1 Steric Exclusion Mechanism of Protein Resistance**

Steric exclusion has frequently been advanced as a mechanism to explain the protein repellent properties of polymer-grafted surfaces, especially PEO surfaces (Leckband et al., 1999; Morra, 2000; Nagaoka et al., 1984). This mechanism was also invoked to explain why PVP-grafted liposomes have longer

lifetimes in the circulation (Torchilin, 2001) because of resistance to protein adsorption (Robinson and Williams, 2002; Rovira-Bru, 2001). The steric exclusion mechanism holds that terminally grafted polymer chains are compressed when a protein approaches the surface. This action generates repulsive entropic and osmotic interactions which overcome attractive van der Waals interactions and thus prevent the protein from adsorbing (Leckband et al., 1999). A surface with a high density of relatively long, hydrophilic polymer chains was suggested to be an effective protein repellent material via steric exclusion (Jeon and Andrade, 1991). The effectiveness of the steric barrier is dependent on excluded volume effects that are related to chain properties such as the radius of gyration, flexibility and solvent-polymer interactions (Szleifer, 1997, Nagaoka et al, 1984). On this basis, PEO and PVP should be effective protein repellent agents.

Protein repulsion is expected to be dependent on polymer size. Radius of gyration and end-to-end distance may be relevant parameters in this regard. It is also clear from the literature (Jeon and Andrade, 1991, Leckband et al., 1999; Szleifer, 1997a) that the graft density of terminally attached chains should be such that the distance between chains is smaller than the protein. One criterion is that  $D$ , the distance between chains, is less than the Flory radius (Leckband et al., 1999; Jeon et al., 1991), which is dependent on monomer size. PEO is reported to have a monomer size of 0.278 nm (Morra, 2000), while for PVP, a



value of 0.4 nm has been estimated (Rovira-Bru, 2001, Tonelli, 1982). Because of PEO's smaller size, it may be expected that a higher density of polymer chains could be achieved.

However, this contradicts data on the size of PEO and PVP in water. Using literature data (Kurata and Tsunashima, 1999), the radius of gyration was estimated for PEO and PVP in water at 25°C. Along with end-to-end distance, the values are presented in Table 5.7.1. From these data, PEO is similar for a given molecular weight, and may achieve a similar graft density of chains on a surface than a surface with PVP chains.

**Table 5.7.1: Root mean square end-to-end distance and radius of gyration of PEO and PVP**

Polymer	Root mean square end-to-end distance (Å)	Root mean square radius of gyration (Å)
PEO 2000	43.7	17.8
PVP 2500	42.8	17.6
PVP 10 000	88.6	36.2

The chain flexibilities of PEO and PVP are undoubtedly different since PEO has a carbon-carbon-oxygen backbone while PVP has a carbon backbone. PEO should be able to adopt a greater number of conformations, and more compact ones, than PVP, either in solution or when terminally-attached to a surface (Szeleifer, 1997a). The planar pyrrolidone side group of PVP will limit the

conformational freedom of the polymer chain (Tonelli, 1982). In fact, Tonelli (1982) predicted only two conformational states of the hydrocarbon backbone using the rotational isomeric state model (RIS).

Kurata and Tsunamshima have introduced theory to account for steric hindrance. In this theory, the parameter  $\sigma$  is the ratio of the unperturbed root mean square end-to-end distance of a polymer in a particular solvent ( $r_o^2$ ) to the root mean square end-to-end distance for the freely jointed chain ( $r_{of}^2$ ) with distances corrected for the types of bonds found in the basic structure.

$$\sigma = \left( \frac{r_o^2}{r_{of}^2} \right)^{1/2} = \left( \frac{\sum n_i l_i^2}{\sum n_i l_i^2 [(1 + \cos \theta_i)/(1 - \cos \theta_i)]} \right)^{1/2} \quad (5.7.1)$$

where  $i$  refers to the type of bond,  $n$  is the number of bonds,  $l$  is the bond length, and  $\theta$  the bond angle. The parameter  $\sigma$  provides a measure of the effects of steric hindrance and is independent of the number of repeat units (Kurata and Tsunashima, 1999).

In water at 25°C, the steric hindrance factor for PEO is estimated as 1.57, compared to 2.48 for PVP (Kurata and Tsunashima, 1999). This hierarchy is as expected since PEO has no substituents on the main backbone, and rotates more freely around the carbon-oxygen bonds. PVP, with its side chain lactam rings, is limited by the number of conformations the molecule can adopt. Rapid movements of the grafted polymer chains may also be important in limiting interactions with plasma proteins that would result in adsorption (Nagaoka et al.,

1984). The limited flexibility of PVP may hamper its ability to compress and repel proteins.

### **5.7.2 Water Barrier Theory**

The water barrier mechanism has been advanced more recently (Morra, 2000; Vogler, 1998) and it proposes that water bound to the grafted polymer plays a key role in protein resistance. Under this mechanism bound water generates repulsive hydration forces when a protein approaches the surface. The important properties of an agent operating under this mechanism are the structure of bound water and its interactions with the agent and the surrounding environment (Vogler, 1998; Morra, 2000).

In the steric exclusion mechanism any involvement of water is essentially ignored (Morra, 2000), and protein resistance is predicted to be related to chain length, with longer chains giving surfaces of greater resistance. However, in recent studies, self-assembled monolayers of oligoethylene glycols (Harder et al., 1998), and plasma layers of short chain PEO species such as tetraglyme (Wu et al., 2000; Beyer et al., 1997; Lopez et al., 1992) have been shown to have protein resistant properties. Harder et al (1998) proposed that at high density, short PEO chains chemisorbed on gold form a tightly bound hydration shell which prevents protein-surface interactions. The effectiveness of these surfaces depends on the conformation of the PEO chains. It was proposed that the helical conformation of the oligo EO chains allows tight water binding leading to high

protein resistance, whereas in the extended chain conformation water is bound more weakly and does not provide an effective water barrier (Harder et al, 1998).

PVP, like PEO, is highly water-soluble and forms aggregates in solution dependent on the structure of bound water (Sun and King, 1996; Guven and Eltaman, 1981). Whereas PEO interacts with water through the oxygen atom, which acts as a Lewis base, the relevant feature of PVP is the strongly electronegative carbonyl oxygen adjacent to the nitrogen atom. When PVP is adsorbed to polystyrene or silica surfaces in contact with aqueous fluids (Smith et al., 1996, Robinson and Williams, 2002), the lactam group is oriented towards the solution. The carbonyl group forms hydrogen bonds with water, while the hydrophobic carbon backbone interacts preferentially with the surface (Smith et al., 1996).

Figure 5.7.1 shows space filling models of PEO and PVP chains

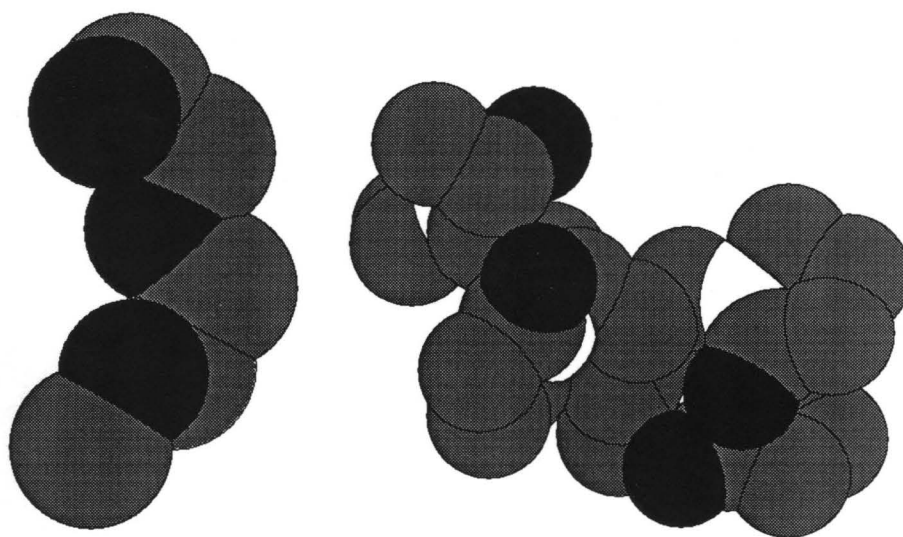


**Figure 5.7.1:** Space filling structures of: left) PEO, right) PVP; grey is carbon, black is oxygen, white is nitrogen. Hydrogen atoms are left out. Drawn with CS Chem 3D Ultra software (Cambridgesoft.com, Cambridge MA, USA). Increased flexibility can be seen with the PEO molecule.

From these diagrams, it is clear that PEO is a more flexible chain than PVP and that its oxygen atoms are more accessible to hydrogen bond with water. In PVP, the nitrogen atoms are located close to the carbon backbone, and the oxygen atoms point outward (Smith et al., 1996). The oxygen atoms in PVP may be more shielded than those in PEO, and this may limit the freedom of PVP to interact with water.

Inherent water binding capacity may contribute to protein repellency. PEO has been shown to bind to 2 to 3 molecules of water per EO unit (Antonsen and Hoffman, 1992). Antonsen and Hoffman (1992) postulated that at lower PEO molecular weights, these water molecules may be more tightly bound, while at higher molecular weights, a greater number of water molecules may be

associated through trapping in the folded PEO coil. A study by Ping et al. (2001) using differential scanning calorimetry and FTIR concluded that PVP may associate with 4 molecules of water per mer. Others have suggested that the mer of PVP may also bind 1 to 2 molecules of water (Garrett, 2000; Sun and King, 1996; Guven and Eltaman, 1981). PVP may thus be considered to have similar water binding properties to PEO.

Lewis acid-base interactions may contribute to the repulsive hydration forces that cause protein resistance (Morra, 2000). The electron-donor parameter may give some indication of the Lewis-base strength of the polymers, with high values indicating a strong effect on water orientation and a higher repulsive force (Morra, 2000). Morra (2000) estimated values of the electron-donor parameter for a number of hydrophilic polymers. The values for PEO and PVP are 58.5 to 64  $\text{mJ/m}^2$  and 29.7  $\text{mJ/m}^2$  respectively (Morra, 2000), again suggesting that PEO may be a more effective protein repellent agent.

The steric exclusion and the water barrier mechanisms bear on the repulsive interactions between the grafted polymer chains and the protein. Attractive interactions should also be considered, and in this regard differences between PVP and PEO are to be expected. The attractive forces between a protein and a material will depend to a large extent on van der Waals interactions, and refractive index may give an indication of the relative magnitude of these interactions. A lower refractive index may indicate weaker van der

Waals interactions giving lower protein adsorption (Jeon et al., 1991). The refractive indices of PEO and PVP are 1.45 and 1.53 respectively (Seferis, 1999). On this basis, attractive interactions should be of lower magnitude for PEO than PVP.

As discussed above, the conformational freedom and water binding of PEO are thought to be responsible for the protein resistance of surfaces modified with this polymer. PVP also has the ability to bind water through its cyclic amide or lactam side groups (Garrett et al, 2000), but may not have particularly high conformational freedom. Therefore in relation to steric exclusion effects, PEO may be superior due to its greater conformational freedom, and chain flexibility. Conformational freedom may be important for longer chains, such as those used in the present study, but given recent literature showing that short chain oligomers of PEO can repel proteins, it would be interesting to see whether short chains of PVP when attached at high graft densities would be protein repellent. If so it might then be concluded that protein resistance depends principally on the water binding properties of the grafted chains.

## 6. Conclusions

The goals of this work were to investigate poly (N-vinyl pyrrolidone) as a protein repellent surface modifier. The initial approach to the preparation of poly (N-vinyl pyrrolidone)-modified surfaces was to treat polyethylene films directly in an N-vinyl pyrrolidone plasma generated in a microwave frequency plasma reactor. The second approach was to graft pre-formed poly (N-vinyl pyrrolidone) to aminated surfaces that were generated by plasma polymerization of allyl amine on polyethylene. Polyethylene similarly grafted with PEO, a polymer known as a protein repellent surface modifier, was also prepared for comparison.

A number of conclusions can be drawn from this work:

- Plasma polymerization of N-vinyl pyrrolidone (VP) monomer on PE resulted in surfaces with increased wettability. Significant increases in oxygen and nitrogen content were observed following the plasma polymerization process, suggesting attachment of NVP-derived species. The changes were more pronounced at higher temperatures (higher vapour pressure of NVP).
- It is likely that NVP decomposition and fragmentation contributed to the variety of functional groups found on the plasma treated surfaces.



- The adsorption of fibrinogen on the plasma polymerized NVP surfaces was at about 15 % greater than on the PE controls.
- In the plasma polymerization of allyl amine on polyethylene, variation of the sample position relative to the glow discharge region in the plasma reactor had little effect on the surface chemical properties.
- An increase in the plasma polymerization time of allyl amine from 10 to 30 minutes gave surfaces with increased nitrogen and decreased oxygen content.
- Plasma polymerized allyl amine surfaces were found to change over time when stored in air by becoming more hydrophobic. XPS and water contact angle measurements suggest that oxidation of the material may be occurring. In the thicker layers formed at longer treatment time, contact angle changes with time in air were less pronounced.
- Exposure of the allyl amine treated surfaces to aqueous buffer resulted in a reduction in surface nitrogen content. This reduction may be due to loss of the plasma polymer. This effect occurred regardless of the plasma polymerization time, and could probably be minimized by optimization of the plasma reaction conditions.
- PVP and PEO were activated for coupling to amino groups in the allyl amine treated surfaces by reaction with both EDC/NHS and DSC. NMR spectra of the products showed yields of about 25% for the reaction of

PEO and PVP with EDC/NHS. Using triethyl amine as catalyst yields of about 70% were obtained for the reaction of PEO with DSC. The yields for reaction of PVP with DSC, with or without catalyst, were on the order of 35%.

- Surfaces prepared using PEO and PVP activated by EDC/NHS were more hydrophilic than those prepared using DSC for activation.
- XPS data did not provide conclusive evidence of covalent bonding of the polymers to the surface using either activation system. The data suggested low coverage of the polymer chains on the polyethylene surface.
- Nonetheless significant reductions in fibrinogen adsorption were observed on all the modified surfaces. Surfaces grafted with polymers that were activated with EDC/NHS showed a greater reduction in fibrinogen adsorption than surfaces grafted with DSC-activated polymers.
- The PEO-modified surfaces showed somewhat greater reductions in fibrinogen adsorption than the PVP, although the differences in adsorption among the surfaces were not significant.

## 7. Recommendations for Future Studies

- Optimization of the plasma polymerization of allyl amine should be performed with respect to minimizing changes on subsequent exposure to aqueous media. In particular optimization of the power-to-flow rate ratio during the plasma treatment may yield plasma polymer layers more resistant to delamination.
- Operation of the plasma reactor at lower power input should be examined to determine if a higher amino group content and a lower generation of oxygen-containing species are possible.
- Determination (and optimization) of the free amino group content of the allyl amine plasma treated surfaces is important and may be possible using derivatization with fluorine-containing reagents and subsequent XPS analysis.
- Increased yields of the polymer grafting reactions may be achieved by operating closer to the cloud point, i.e. at higher temperatures and higher ionic strength.
- Different types of PVP-grafted surfaces should be investigated. The use of inorganic substrates such as silicon or gold may facilitate surface chemical characterization (e.g. graft density determination) of the polymer grafted surfaces.

## References

- Abbott NL, Blankschtein D and Hatton TA. Protein partitioning in two-phase aqueous polymer systems 3. A neutron scattering investigation of the polymer solution structure and protein-polymer interactions. *Macromolecules* 25: 3932-3941 (1992).
- Antonsen KP and Hoffman AS. Chapter 2: Water structure of PEG solutions by differential scanning calorimetry measurements, in *Poly(ethylene glycol) Chemistry: Biotechnical and Biomedical Applications*, J.M Harris (ed), New York: Plenum Press (1992) p.15-28
- Arora JPS, Arora SK, and Duggal AK. Interactions between surfactants and polyvinyl pyrrolidone. *Surfactants and Biomolecules* 35:24-32 (1998).
- Bakaltcheva, I; Ganong, JP; Holtz, BL; Peat, RA; and Reid, T. Effects of high-molecular-weight cryoprotectants on platelets and the coagulation system. *Cryobiology* 40:283-293 (2000).
- Bailey FA and Koleske JV. *Poly(ethylene oxide)*. New York: Academic Press (1976). p. 6, 29-36.
- Beamson G, Brennan WJ, Clark DT and Howard J. Modification of surfaces and surfaces layers by non-equilibrium processes. *Journal of Physica Scripta* T23: 249 (1985).
- Beamson G and Briggs D. *High Resolution XPS of Organic Polymers*. New York: John Wiley & Sons (1992). p. 84-85, 192-193.
- Beck AJ, Candan S, Short RD, Goodyear A and Braithwaite NSJ. The role of ions in the plasma polymerization of allyl amine. *Journal of Physical Chemistry B* 105:5730-5736 (2001).
- Beyer D, Knoll W, Ringsdorf H, Wang J, Timmons RB, and Sluka P. Reduced protein adsorption on plastics via direct plasma deposition of triethylene glycol monoallyl ether. *Journal of Biomedical Materials Research* 36: 181-189 (1997).
- Boden N, Bushby RJ, Liu Q, Evans SD, Jenkins ATA, Knowles PF, and Miles RE. N,N,-Disuccinimidyl carbonate as a coupling agent in the synthesis of

thiophospholipids used for anchoring biomembranes to gold surfaces. *Tetrahedron* 54:11537-11548 (1998).

Boenig, HV. *Plasma Science and Technology*. Ithaca, NY: Cornell University Press, 1982. p.5-45.

Boffa GA, Lucien N, Faure A and Boffa MC. Polytetrafluoroethylene-N-vinylpyrrolidone graft copolymers: affinity with plasma proteins. *Journal of Biomedical Materials Research* 11:317-337 (1977).

Bohnert J, Horbett TA, Ratner BD, and Royce FH. Adsorption of proteins from artificial tear solutions to contact lens materials. *Investigative Ophthalmology and Visual Science* 29:362-373 (1988).

Brash J. Exploiting the current paradigm of blood-material interactions for the rational design of blood-compatible materials. *Journal of Biomaterial Science, Polymer Edition* 11(11): 1135-1146 (2000).

Bridgett MJ, Davies MC, Denyer SP, and Eldridge PR. In vitro assessment of bacterial adhesion to hydromer ®-coated cerebrospinal fluid shunts. *Biomaterials* 14(3): 184-188 (1993).

Calderon JG, Harsch A, Gross GW, Timmons RB. Stability of plasma-polymerized allyl amine films with sterilization by autoclaving. *Journal of Biomedical Materials Research* 42(4): 597-603 (1998)

Carmeliet P and Collen D. Molecular analysis of blood vessel formation and disease. *American Journal of Physiology* 273:H2091-H2104 (1997)

Chan CM, Ko TM, and Hiraoka H. Polymer surface modification by plasmas and photons. *Surface Science Reports* 24(1-2): 3-54 (1996).

Chatelier RC, Xie X, Gengenbach TR, and Griesser HJ. Effects of plasma modification conditions on surface restructuring. *Langmuir* 11: 2585-2591 (1995a).

Chatelier RC, Drummond CJ, Chan DYC, Vasic ZR, Gengenbach TR, and Griesser HJ. Theory of contact angles and the free energy of formation of ionizable surfaces: application to heptylamine radio-frequency plasma-deposited films. *Langmuir* 11: 4122 (1995b).

- Chen, H and Belfort, G. Surface modification of poly (ether sulfone) ultrafiltration membranes by low-temperature plasma-induced graft polymerization. *Journal of Applied Polymer Science* 72:1699-1711 (1999).
- Chun TI, Choi SK, Täschner C, Leonhardt A, Kaufmann R, Rehwinker C, and Rossbach V. Surface modification of polytetrafluoroethylene with tetraethoxysilane by using remote argon/dinitrogen oxide microwave plasma. *Journal of Applied Polymer Science* 76:1207-1216 (2000).
- Collen D and Lijnen HR. Basic and clinical aspects of fibrinolysis and thrombolysis. *Blood* 78: 3114-3124 (1991)
- Colman RW, Clowes AW, George JN, Hirsh J, and Marder VJ. Chapter 1: Overview of Hemostasis. *Hemostasis and Thrombosis: Basic Principles and Clinical Practice*, 4<sup>th</sup> Edition. (editor R. Colman) Philadelphia: Lippincot Williams and Wilkins, p. 4-10, (2001).
- d'Agostino, R. *Plasma Deposition, Treatment, and Etching of Polymers*. Boston: Academic Press, (1990). p.3-30.
- Dai LM, St John HAW, Bi JJ, Zientek P, Chatelier RC and Griesser HJ. Biomedical coatings by the covalent immobilization of polysaccharides onto gas-plasma-activated polymer surfaces. *Surface and Interface Analysis* 29(1): 46-55 (2000).
- Davie EW, Fujikawa K, and Kisiel, W. The coagulation cascade: initiation, maintenance and regulation. *Biochemistry* 30(43): 10363-10370 (1991).
- Dekker A, Reitsma K, Beugeling T, Bantjes A, Feijen J, and van Aken WG. Adhesion of endothelial cells and adsorption of serum proteins on gas plasma-treated polytetrafluoroethylene. *Biomaterials* 12: 130-138 (1991).
- De Sousa Delgado, A, Leonard M, and Dellacherie E. Surface properties of poly styrene nanoparticles coated with dextrans and dextran-PEO copolymers. Effect of polymer architecture on protein adsorption. *Langmuir* 17:4386-4391 (2001).
- Desai NP and Hubbell JA. Solution technique to incorporate polyethylene oxide and other water-soluble polymers into surfaces of polymeric biomaterials. *Biomaterials* 12: 144-153 (1991).

- Dilsiz N and Akovali G. Plasma polymerization of selected organic compounds. *Polymer* 37:333-342 (1996).
- Du YJ. PEO and PEO-heparin Modified Surfaces for Blood Contacting Applications. Hamilton: McMaster University (2001).
- Epailard F and Brosse JC. Plasma-induced polymerization. *Journal of Applied Polymer Science* 38:887-898 (1989).
- Efremova, NV, Sheth SR and Leckband DE. Protein-induced changes in poly(ethylene glycol) brushes: molecular weight and temperature dependence. *Langmuir* 17:7628-7636 (2001).
- Eliassaf J, Eriksson F and Eirich FR. The interaction of poly(vinyl pyrrolidone) with cosolutes. *Journal of Polymer Science* 47:193-202 (1960).
- Fally F, Doneux C, Riga J and Verbist JJ. Quantification of the functional groups present at the surface of plasma polymers deposited from propylamine, allylamine and propargylamine. *Journal of Applied Polymer Science* 56:597-614 (1995).
- Favia P, d'Agostino R, Palumbo F. Grafting of chemical groups onto polymers by means of RF plasma treatments: a technology for biomedical applications. *Journal de Physique IV (C4)*: 199-208 (1997).
- Fournier C, Leonard M, Dellacherie E, Chikhi M, Hommel H, Legrand AP. EPR analysis of hydrophobically modified dextran-coated polystyrene. *Journal of Colloid and Interface Science* 198:27-33 (1998).
- Francois P, Vandaux P, Nurdin N, Mathieu HJ, Descouts P, and Lew DP. Physical and biological effects of a surface coating procedure on polyurethane catheters. *Biomaterials* 17(7): 667-678 (1996).
- Garrett, Q; Laycock, B; and Garrett, RW. Hydrogel monomer constituents modulate protein sorption. *Investigative Ophthalmology and Visual Science* 41(7): 1687-1695 (2000).

- Gengenbach TR, Chatelier RC and Griesser HJ. Correlation of the nitrogen 1s and oxygen 1s XPS binding energies with compositional changes during oxidation of ethylene diamine plasma polymers. *Surface and Interface Analysis* 24:611-619 (1996)
- Gengenbach TR and Griesser HJ. Aging of 1, 3-diaminopropane plasma-deposited polymer films: mechanisms and reaction pathways. *Journal of Polymer Science Part A: Polymer Chemistry* 37:2191-2206 (1999).
- Ghosh AK, Duong TT, McKee SP, and Thompson WJ. N,N-Disuccinimidyl carbonate: a useful reagent for alkoxycarbonylation of amines. *Tetrahedron Letters*, 33:2781-2784 (1992).
- Griesser HJ, Chatelier RC, Gengenbach TR, Johnson G, and Steele JG. Growth of human cells on plasma polymers: putative role of amine and amide groups. *Journal of Biomaterial Science, Polymer Edition* 5(6): 531-554 (1994).
- Grill, A. *Cold Plasma in Materials Fabrication: from fundamentals to applications*. Piscataway, NJ: IEEE Press, (1994). p.3-50.
- Guner A. Properties of aqueous salt solutions of polyvinyl pyrrolidone. I. viscosity characteristics. *Journal of Applied Polymer Science* 62:785-788 (1996).
- Guner A and Ataman M. Effects of inorganic salts on the properties of aqueous polyvinyl pyrrolidone solutions. *Colloid and Polymer Science* 272:175-180 (1994)
- Guen O and Eltan E. Molecular association in aqueous solutions of high molecular weight poly(N-vinyl-2-pyrrolidone). *Makromolekulare Chemie* 16:3129-3134 (1981).
- Haaf F, Sanner A and Straub F. Polymers of N-vinyl pyrrolidone: synthesis, characterization and uses. *Polymer Journal* 17(1): 143-152 (1985).
- Halperin, A. Polymer brushes that resist adsorption of model proteins: design parameters. *Langmuir* 15:2525-2533 (1999)



- Han, LM and Timmons, RB. Pulsed-plasma polymerization of 1-vinyl-2-pyrrolidone: synthesis of a linear polymer. *Journal of Polymer Science Part A: Polymer Chemistry* 36:3121-3129 (1998).
- Harder P, Grunze M, Dahint R, Whitesides GM and Laibinis PE. Molecular conformation in oligo(ethylene glycol)-terminated self-assembled monolayers on gold and silver surfaces determines their ability to resist protein adsorption. *Journal of Physical Chemistry B* 102:426-436 (1998).
- Harris JM. *Poly(ethylene glycol) Chemistry: Biotechnical and Biomedical Applications*. New York: Plenum Press (1992), p.1-25
- Hermanson GT. *Bioconjugate Techniques*. London: Academic Press (1996) p.169
- Higa, OZ; Rogero, SO; Machado, LDB; Mathor, MB; and Lugao, AB. Biocompatibility study for PVP wound dressing obtained in different conditions. *Radiation Physics and Chemistry* 55:705-707 (1999).
- Higuchi A, Shirano K, Harashima M, Yoon BO, Hara M, Hattori M, and Imamura K. Chemically modified polysulfone hollow fibres with vinylpyrrolidone having improved blood compatibility. *Biomaterials* 23:2659-2666 (2002).
- Hoenich NA, Stamp S. Clinical performance of a new high-flux synthetic membrane. *American Journal of Kidney diseases* 36(2): 345-352 (2000).
- Hollahan JR and Stafford BB. Attachment of amino groups to polymer surfaces by radio-frequency plasmas. *Journal of Applied Polymer Science* 13:807-816 (1969).
- Horbett TA and Brash JL. *Proteins at Interfaces II: Fundamentals and Applications*. San Diego: American Chemical Society (1995). p.3-25.
- Hynes AM, Shenton MJ, and Badyal JPS. Pulsed plasma polymerization of perfluorocyclohexane. *Macromolecules* 29:4220-4225 (1996).
- Jaaba H, Mas A, and Schue F. Modification de surface de poly(hydroxybutyrate-co-hydroxyvalerate) par polymerization par plasma d'allyl amine. *European Polymer Journal* 33:1607 (1997).

- Jama C, Dessaux O, Goudmand P, Mutel B., Gengembre L, Drevillon B, Vallo S and Grimblot J. Surface modifications of polycarbonate (PC) and polyethylene terephthalate (PET) by cold remote nitrogen plasma (CRNP). *Surface Science* 352-354:490-494 (1996).
- Janatova J. Activation and control of complement, inflammation, and infection associated with the use of biomedical polymers. *American Society for Artificial Internal Organs Journal* 46:S53-S62 (2000).
- Jeon SI, Lee JH, Andrade JD, and de Gennes PG. Protein-surface interactions in the presence of polyethylene oxide. I Simplified theory. *Journal of Colloid and Interface Science* 142: 149-158 (1991).
- Jeon SI and Andrade JD. Protein-surface interactions in the presence of polyethylene oxide. II Effect of protein size. *Journal of Colloid and Interface Science* 142: 159-166 (1991).
- Jia, Z. Estimation of the amine content. *Personal Communication* (2001).
- Johnson, SD, Anderson JM, Marchant RE. Biocompatibility studies on plasma-polymerized interface materials encompassing both hydrophobic and hydrophilic surfaces. *Journal of Biomedical Materials Research* 26:915-935 (1992).
- Kamada H, Tsutsumi Y, Tsunoda S, Kihara T, Kaneda Y, Yamamoto Y, Nakagawa S, Horisawa Y and Mayumi T. Molecular design of conjugated tumor necrosis factor  $\alpha$ : synthesis and characteristics of polyvinyl pyrrolidone modified tumor necrosis factor- $\alpha$ . *Biochemical and Biophysical Research Communications* 257: 448-453 (1999).
- Kamath, KR, Danilich MJ, Marchant RE and Park K. Platelet interactions with plasma-polymerized ethylene oxide and N-vinyl-2-pyrrolidone films and linear poly(ethylene oxide) layer. *Journal of Biomaterial Science Polymer Edition* 7(11):977-988 (1996).
- Kao, F; Manivannan, G; and Sawan, SP. UV curable bioadhesives: copolymers of N-vinyl pyrrolidone. *Journal of Biomedical Materials Research* 38:191-196 (1997).

- Keil M, Rastomjee CS, Rajagopal A, Sotobayashi H, Bradshaw AM, Lamont CLA, Gador, D, Buchberger C, Fink R, Umbach E. Argon plasma-induced modifications at the surface of polycarbonate thin films. *Applied Surface Science* 125:273-286 (1998).
- Kingshott P, Thissen H, Griesser HJ. Effects of cloud-point grafting, chain length, and density of PEG layers on competitive adsorption of ocular proteins. *Biomaterials* 3:2043-2056 (2002).
- Klotz IM and Shikama. Nature of urea effects on anion binding by macromolecules. *Archives of Biochemistry and Biophysics* 123:551-557 (1968).
- Ko T, Lin J, Cooper SL. Surface characterization and platelet adhesion studies of plasma-carboxylated polyethylene. *Journal of Colloid and Interface Science* 156:207-217 (1993).
- Ko T and Cooper SL. Surface properties and platelet adhesion characteristics of acrylic acid and allyl amine plasma treated polyethylene. *Journal of Applied Polymer Science* 47:1601-1619 (1993).
- Kottke-Marchant K, Veenstra AA, and Marchant RE. Human endothelial cell growth and coagulant function varies with respect to interfacial properties of polymeric substrates. *Journal of Biomedical Materials Research* 30: 209-220 (1996).
- Krishnamurthy V, Kamel IL and Wei Y. Analysis of plasma polymerization of allylamine by FTIR. *Journal of Polymer Science: Part A: Polymer Chemistry* 27:1211-1224 (1989).
- Kurata M and Tsunashima Y. Chapter 7: Viscosity-molecular weight relationships and unperturbed dimensions of linear chain molecules in *Polymer Handbook 4<sup>th</sup> Edition*, J Brandrup, EH Immergut and EA Grulke (eds), New York: John Wiley and Sons, Inc. (1999). p.1-15
- Kurosawa S, Kobayashi K, Aizawa H, Yoshimi Y and Yoshimoto M. Behaviour of contact angle on glass plates coated with plasma-polymerized styrene, allyl amine, and acrylic acid. *Journal of Photopolymer Science and Technology* 12(1): 63-68 (1999).

- Lamba, N.M.K. and Cooper, S.L. Chapter 38: Interaction of Blood with Artificial Surfaces. *Hemostasis and Thrombosis: Basic Principles and Clinical Practice*, 4<sup>th</sup> Edition. (editor R. Colman) Philadelphia: Lippincot Williams and Wilkins (2001) p. 661-672.
- Leckband D, Sheth S and Halperin A. Grafted poly(ethylene oxide) brushes as nonfouling surface coatings. *Journal of Biomaterial Science Polymer Edition* 10(10): 1125-1147 (1999)
- Lee, JH, Park JW and Lee HB. Cell adhesion and growth on polymer surfaces with hydroxyl groups prepared by water vapour plasma treatment. *Biomaterials* 12:443-448 (1991).
- Lee JH, Jung HW, Kang I and Lee HB. Cell behaviour on polymer surfaces with different functional groups. *Biomaterials* 15(9): 705-711. (1994)
- Li Z and Netravali AN. Surface modification of UHSPE fibers through allylamine plasma deposition. I: Infrared and ESCA study of allylamine plasma formed polymers. *Journal of Applied Polymer Science* 44:319-331 (1992)
- Lin J and Cooper SL. In vitro fibrinogen adsorption from various dilutions of human blood plasma on glow discharge modified polyethylene. *Journal of Colloid and Interface Science* 182:315-325 (1996).
- Lopez GP, Ratner BD, Tidwell CD, Haycox CL, Rapoza RJ, and Horbett TA. Glow discharge plasma deposition of tetraethylene glycol dimethyl ether for fouling-resistant biomaterial surfaces. *Journal of Biomedical Materials Research* 26:415-439 (1992).
- Majhi PR, Moulik SP, Burke SE, Rodgers M, and Palepu R. Physicochemical investigations on the interaction of surfactants and salts with polyvinyl pyrrolidone in aqueous medium. *Journal of Colloid and Interface Science* 235:227-234 (2001).
- Malet TH, Challier B, David N, Bertrand A, George J. Clinical and scintigraphic comparison of silicone and polyvinyl pyrrolidone coated silicone perforated plugs. *British Journal of Ophthalmology* 82:1416-1419 (1998).

- Marchant, RE, Yu, D and Khoo, C. Preparation and characterization of plasma-polymerized N-vinyl-2-pyrrolidone films. *Journal of Polymer Science Part A: Polymer Chemistry*, 27:881-895 (1989).
- Marchant, RE, Johnson, SD, Schneider, BH, Agger, MP and Anderson, JM. A hydrophilic plasma polymerized film composite with potential application as an interface for biomaterials. *Journal of Biomedical Materials Research* 24:1521-1537 (1990).
- Mas, A, Jaaba H, Schue F. XPS analysis of poly[(3-hydroxybutyric acid)-co-(3-hydroxyvaleric acid)] film surfaces exposed to an allylamine low-pressure plasma. *Macromolecule Chemical Physics* 198:3737-3752 (1997).
- Matteo NB and Ratner BD. Relating the surface properties of intraocular lens materials to endothelial cell adhesion damage. *Investigative Ophthalmology and Visual Science* 30:853-860 (1989).
- McPherson T, Kidane A, Szleifer I and Park K. Prevention of protein adsorption by tethered poly(ethylene oxide) layers: experiments and single-chain mean-field analysis. *Langmuir* 14:176-186 (1998).
- McVey, JH. Tissue factor pathway. *Balliere's Clinical Haematology* 12(3): 361-372 (1999).
- Merrett K, Cornelius RM, McClung WG, Unsworth LD and Sheardown H. Surface analysis methods for characterizing polymeric biomaterials. *Journal of Biomaterial Science, Polymer Edition* 13: 593-621 (2002).
- Miyama M, Yang Y, Yasuda T, Okuno T and Yasuda H. Static and dynamic contact angles of water on polymeric surfaces. *Langmuir* 13:5494-5503 (1997).
- Moisan M, and Wertheimer MR. Comparison of microwave and r.f. plasmas: fundamentals and applications. *Surface and Coatings Technology* 59:1-13 (1993).
- Morra. M. On the molecular basis of fouling review. *Journal of Biomaterial Science Polymer Edition* 11: 549-569 (2000).

- Mu, Y., Kamada, H., Kodaira, H, Sato, K., Tsutsumi, Y., Maeda, M., Kawasaki, K., Nomizu, M., Yamada, Y and Mayumi, T. Bioconjugation of laminin-related peptide YIGSR with Polyvinyl Pyrrolidone increases its antimetastatic effect due to a longer plasma half-life. *Biochemical and Biophysical Research Communications* 264:763-767 (1999).
- Murugesan, G, Rani MRS, Ransohoff, RM, Marchant, RE and Kottke-Marchant, K. Endothelial cell expression of monocyte chemotactic protein-1, tissue factor, and thrombomodulin on hydrophilic plasma polymers. *Journal of Biomedical Materials Research* 49:396-408 (2000).
- Nagaoka S, Mori Y, Takiuchi H, Yokota K, Tanzawa H and Nishiumi S. Interaction between blood components and hydrogels with poly(oxyethylene) chains., in *Polymers as Biomaterials*. Shalaby SW, Hoffamn AS, Ratner BD, and Horbett TA (eds). New York: Plenum Press (1984) p.361-374.
- Nesheim M, Wang W, Boffa M, Nagashima M, Morser J, and Bajzar L. Thrombin, thrombomodulin and TAFI in the molecular link between coagulation and fibrinolysis. *Thrombosis and Hemostasis* 78(1): 386-391 (1997)
- O'Toole L, Mayhew CA and Short RD. On the plasma polymerization of allyl alcohol: an investigation of ion-molecule reactions using a selected ion flow tube. *Journal of Chemical Society: Faraday Transactions* 93(10): 1961-1964 (1997).
- O'Toole L, Beck AJ, and Short RD. Characterization of plasma polymers of acrylic acid and propanoic acid. *Macromolecules* 29: 5172-5177 (1996).
- Petrak K and Pitts E. Permeability of oxygen through polymers. II. The effect of humidity and film thickness on the permeation and diffusion coefficients. *Journal of Applied Polymer Science* 25: 879-886 (1980).
- Pieracci J, Crivello JV and Belfort G. Photochemical modification of 10 kDa polyethersulfone ultrafiltration membranes for reduction of biofouling. *Journal of Membrane Science* 156:223-240 (1999).
- Ping ZH, Nguyen QT, Chen SM, Zhou JQ, and Ding YD. States of water in different hydrophilic polymers-DSC and FTIR studies. *Polymer* 42:8461-8467 (2001).

- Rabinow BE, Ding YS, McHalsky ML, Schneider JH, Ashline KA, Shelbourn TL, and Albrecht RM. Biomaterials with permanent hydrophilic surfaces and low protein adsorption properties. *Journal of Biomaterial Science Polymer Edition*. 6: 91-109 (1994).
- Radovich, JM. Composition of polymer membranes for therapies for end-stage renal disease. *Contributions to Nephrology* 113:11-24 (1995).
- Raghunath K, Rao KP, Nagarajan B, and Joseph KT. Grafting of poly(vinyl pyrrolidone) onto gelatin and its application as synthetic plasma expander. *European Polymer Journal* 21(2): 195-199 (1985).
- Ratner BD, Hoffman AS, Whiffen JD. The thrombogenicity of radiation grafted polymers as measured by the vena cava ring test. *Journal of Bioengineering* 2:313-23, (1978).
- Ratner BD, Chilkoti A, and Lopez GP. Plasma Deposition and treatment for biomaterial applications in *Plasma Deposition, Treatment and Etching of Polymers*. R d'Agostino (ed), Boston: Academic Press (1990) p.463-516.
- Ratner BD. New Ideas in biomaterials science-a path to engineered biomaterials. *Journal of Biomedical Materials Research* 27:837-850 (1993).
- Rinsch CL, Chen X, Panchalingam V, Eberhart RC, Wang J and Timmons RB. Pulsed radio frequency plasma polymerization of allyl alcohol: controlled deposition of surface hydroxyl groups. *Langmuir* 12: 2995-3002 (1996).
- Rinsch CL, Chen X, Panchalingam V, Savage CR, Wang YH, Eberhart RE, and Timmons RB. Film chemistry control during pulsed RF plasma polymerization of allyl alcohol and allyl amine. *Polymer Preprints* 36:95-96 (1995).
- Robinson BV, Sullivan FM, Borzelleca JF, and Schwartz SL. *PVP: a critical review of the kinetics and toxicology of poly(vinyl pyrrolidone)*. Chelsea, Michigan: Lewis Publishers (1990) p 1-28.
- Robinson S and Williams PA. Inhibition of protein adsorption onto silica by polyvinyl pyrrolidone. *Langmuir* 18: 8743-8748 (2002).

- Rovira-Bru M, Giralt F, and Cohen Y. Protein adsorption onto zirconia modified with terminally grafted polyvinyl pyrrolidone. *Colloid and Interface science* 235:70-79 (2001).
- Sagnella, S, Kwok J, Marchant RE and Kottke-Marchant, K. Shear-induced platelet activation and adhesion on human pulmonary artery endothelial cells seeded onto hydrophilic polymers. *Journal of Biomedical Materials Research* 57: 419-431 (1999).
- Sanborn, SL, Murugesan G, Marchant RE and Kottke-Marchant, K. Endothelial cell formation of focal adhesions on hydrophilic plasma polymers. *Biomaterials* 23:1-8 (2002).
- Schenck H, Simak P, and Haedicke E. Structure of polyvinyl pyrrolidone-iodine (povidone-iodine). *Journal of Pharmaceutical Sciences* 68(12):1505-1509 (1979).
- Seferis. JC. Chapter 7: Refractive indices of polymers in *Polymer Handbook 4<sup>th</sup> Edition*, J Brandrup, EH Immergut and EA Grulke (eds), New York: John Wiley and Sons, Inc. (1999). p.571.
- Sheth and Leckband D. Measurement of attractive forces between proteins and end-grafted poly(ethylene glycol) chains. *Proceedings of the National Academy of Science* 94: 8399-8404 (1997).
- Smith JN, Meadows J and Williams PA. Adsorption of polyvinyl pyrrolidone onto polystyrene lattices and the effect on colloid stability. *Langmuir* 12:3773-3778 (1996).
- Sodhi RNS, Sahi VP, and Mittelman MW. Application of electron spectroscopy and surface modification techniques in the development of antimicrobial coatings for medical devices. *Journal of Electron Spectroscopy and Related Phenomena* 121:249-264 (2001).
- Sodhi, RNS. Curve Fitting Procedure. Personal Communication (2003).
- Sofia SJ, Premnath V, and Merrill EW. Poly(ethylene oxide) grafted to silicon surfaces: grafting density and protein adsorption. *Macromolecules* 31(15): 5059-5070 (1998).



- Sun T and King HE. Aggregation behavior in the semidilute poly(N-vinyl-2-pyrrolidone)/water system. *Macromolecules* 29:3175-3181 (1996).
- Szleifer I. Protein adsorption on surfaces with grafted polymers: A theoretical approach. *Biophysical Journal* 72: 595-612 (1997a)
- Szleifer I. Protein adsorption on tethered polymer layers: effect of polymer chain architecture and composition. *Physica A* 244:377-388 (1997b).
- Takagishi T and Kuroki N. Interaction of polyvinyl pyrrolidone with methyl orange and its homologs in aqueous solution: Thermodynamics of the binding equilibria and their temperature dependences. *Journal of Polymer Science: Polymer Chemistry Edition* 11:1889-1900 (1973).
- Tang L, Wu Y and Timmons RB. Fibrinogen adsorption and host tissue responses to plasma functionalized surfaces. *Journal of Biomedical Materials Research* 42:156-163 (1998).
- Timmons; Richard B, Wang; Jenn-Hann Savage; Charles R. (Arlington, TX); Wu; Yuliang (Arlington, TX). Nonfouling wettable surface. US Patent # 6482531, 2002
- Tonelli AE. Conformational characteristics of poly(N-vinyl pyrrolidone). *Polymer* 23:676-680 (1982).
- Torchilin VP, Levchenko TS, Whiteman KR, Yaroslavov AA, Tsatsakis AM, Rizos AK, Michailova EV, and Shtilman MI. Amphiphilic poly-N-vinyl pyrrolidones: synthesis, properties and liposome surface modification. *Biomaterials* 22:3035-3044 (2001).
- Tsai W, Grunkemeier JM, and Horbett TA. Human plasma fibrinogen adsorption and platelet adhesion to polystyrene. *Journal of Biomedical Materials Research* 44:130-139 (1999).
- Tsai W, Grunkemeier JM, McFarland CD and Horbett TA. Platelet adhesion to polystyrene-based surfaces preadsorbed with plasmas selectively depleted in fibrinogen, fibronectin, vitronectin or von Willebrand's factor. *Journal of Biomedical Materials Research* 60:348-359 (2002).

- Tseng DY and Edelman ER. Effects of amide and amine plasma-treated ePTFE vascular grafts on endothelial cell lining in an artificial circulatory system. *Journal of Biomedical Materials Research* 42:188-198 (1998).
- Tseng R and Yasuda HK. Ex situ chemical determination of free radicals and peroxides on plasma treated surfaces. *Plasmas and Polymers* 7(1): 57-69 (2002).
- Tunney MM and Gorman SP. Evaluation of a poly(vinyl pyrrolidone)-coated biomaterial for urological use. *Biomaterials* 23:4601-4608 (2002).
- Unsworth LD. Grafted PEO chains to thiolated surfaces. Personal Communication (2001).
- van Gelder, JM; Nair, CH and Dhall, DP. Erythrocyte aggregation and erythrocyte deformability modify the permeability of erythrocyte enriched fibrin network. *Thrombosis Research* 82(1): 33-42 (1996).
- van Os MT, Menges B, Foerch R, Vancso GJ and Knoll W. Characterization of plasma-polymerized allyl amine using wave-guide mode spectroscopy. *Chemical Materials* 11:3252-3257 (1999).
- Vogler EA. Structure and reactivity of water at biomaterial surfaces. *Advances in Colloid and Interface Science* 74:69-117 (1998).
- Watts JF. *An Introduction to Surface Analysis by Electron Spectroscopy*. Oxford: Oxford University Press, 1990. p.10
- Whitesides GM and Laibinis PE. Wet chemical approaches to the characterization of organic surfaces: self-assembled monolayers, wetting and the physical-organic chemistry of the solid-liquid interface. *Langmuir* 6:87-96 (1990).
- Whittle JD, Short RD, Douglas CWI, and Davies J. Differences in the aging of allyl alcohol, acrylic acid, allyl amine and octa-1,7-diene plasma polymers as studied by X-ray photoelectron spectroscopy. *Chemistry of Materials* 12:2664-2671 (2000).

- Wickson BM, and Brash JL. Surface hydroxylation of polyethylene by plasma polymerization of allyl alcohol and subsequent silylation. *Colloids and Surfaces A: Physicochemical and Engineering Aspects* 156:201-213 (1999).
- Wiese KG, Heinemann DEH, Ostermeier D, and Peters JH. Biomaterial properties and biocompatibility in cell culture of a novel self-inflating hydrogel tissue expander. *Journal of Biomedical Materials Research* 54(2): 179-188 (2001).
- Williams DF. *Progress in Biomedical Engineering: Definitions in Biomaterials*. Elsevier (1987).
- Winters; S; Solen; K.A.; Sanders; C.G.; Mortensen; J. D.; Berry; G. Multifunctional thrombo-resistant coatings and methods of manufacture. US Patent 5,182,317 , 1993.
- Wittenbeck P and Wokaun A. Plasma treatment of polypropylene surfaces: characterization by contact-angle measurements. *Journal of Applied Polymer Science* 50:187-200 (1993).
- Wrobel AM. Aging process in plasma polymerized organosilicon thin films. *Journal of Macromolecular Science Chemistry A*: 22:1089-1100 (1985).
- Wu YJ, Timmons RB, Jen JS, and Molock FE. Non-fouling surfaces produced by gas phase pulsed plasma polymerization of an ultra low molecular weight ethylene oxide containing monomer. *Colloids and Surfaces B: Biointerfaces* 18:235-248 (2000).
- Xia J and Dubin PL. Dynamic and electrophoretic light scattering of a water-soluble complex formed between pepsin and poly(ethylene glycol). *Macromolecules* 26: 6688-6690 (1993).
- Yang; D, Stanslaski; J. L.; Wang; L; and Smith; S.R. Stent coating. US patent: 6,258,121 (2001).
- Yasuda, H. Plasma for modification of polymers. *Journal of Macromolecular Science-Chemistry A*10 (3): 383-420 (1976).

Yasuda, H and Lamaze CE. Polymerization in an electrodeless glow discharge: olefinic monomers. *Journal of Applied Polymer Science* 17:1519-1531 (1973).

Yasuda H. *Plasma Polymerization*. London, UK: Academic Press (1990), Chapters 6-10, p.72-369.

Yu XJ, and Brash JL. Measurement of protein adsorption using radioiodine labeling methods. in *Test Procedures for Blood Compatibility of Biomaterials*, S. Dawids,(ed.) Kluwer Academic Publishers, pp. 287-330 (1993).

## Appendix A: Estimation of the Vapour Pressure of NVP

The Clausius-Clapeyron equation can be used to estimate the vapour pressure at another temperature. The equation is in the form:

$$\ln\left(\frac{P}{P_o}\right) = \frac{-\Delta H_v}{R}\left(\frac{1}{T_o} - \frac{1}{T}\right) \quad (\text{A1})$$

when a vapour pressure at a particular temperature is known, this equation simplifies to:

$$\ln P = \frac{-\Delta H_v}{RT} + A \quad (\text{A2})$$

When the enthalpy of vapourization is unknown, a plot between the vapour pressures and the reciprocal of temperature (Table A1) determines the linear relationship and its parameters, the slope and intercept for NVP.

**Table A1 Vapour pressures and temperatures for N-vinyl pyrrolidone**

Pressure (mmHg)	Temperature (°C)	Temperature (K)	ln P	1/T (K <sup>-1</sup> )(x10 <sup>3</sup> )
0.114	25	298.2	-2.17	3.35
11	93	366.2	2.40	2.73
400	193	466.2	5.99	2.15

Using the data, Figure A1 below determines the Clausius-Clapeyron relationship.

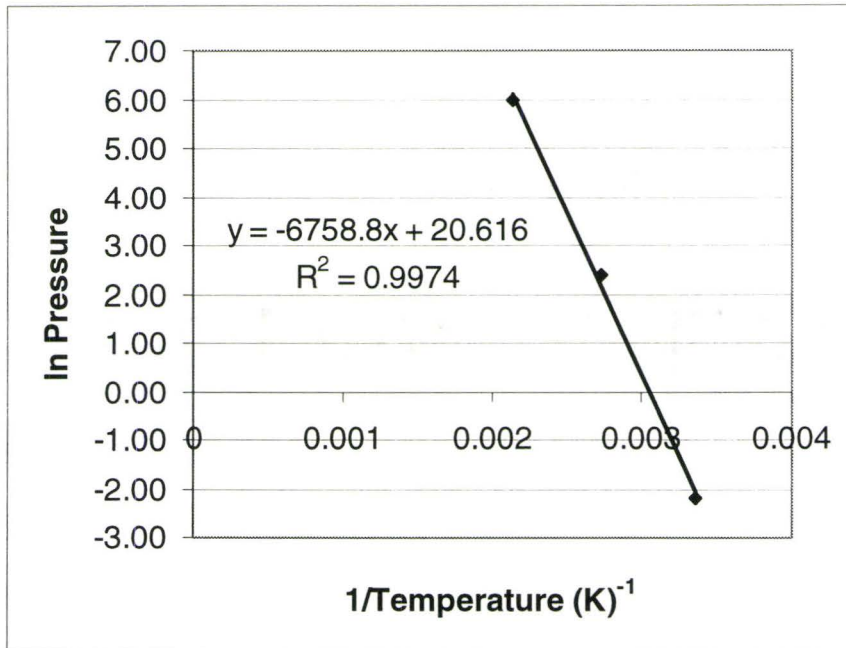


**Figure A1: Determination of the Clausius-Clapeyron relationship for N-vinyl pyrrolidone**

Thus the relationship for N-vinyl pyrrolidone using the above data is:

$$\ln P = -\frac{6760}{T} + 20.6 \quad (\text{A3})$$

To determine the vapour pressure at 50°C, the temperature is substituted for T below:

$$\ln P = \frac{-6760}{[50 + 273.2K]} + 20.6$$

$$P = 0.73 \text{ mmHg}$$

Compare this vapour pressure to one at room temperature of 25°C, this is a factor of:

$$= \frac{0.73}{0.114 \text{ mmHg/mmHg}}$$

$$= 6.4$$

## Appendix B: Preparation of Phosphate Buffered Saline

1.32 g of disodium hydrogen phosphate, 0.345 of sodium dihydrogen phosphate, and 8.5 g of sodium chloride were mixed with 1 L of Milli-Q water and the pH was adjusted to 7.4.

## Appendix C: Determination of Free Iodide Concentration by Trichloroacetic Acid (TCA) Precipitation of Fibrinogen

- Into 2 groups of 3 vials, place 0.9 mL of a 1% wt/v (in Milli-q water) bovine serum albumin (BSA) and 0.1 mL from a 1 in 10 diluted radioactive fibrinogen solution. 3 of the vials are referred to as Group A.
- To 3 of the vials (referred to as Group B), 0.5 mL of (TCA) was added. These vials were mixed with a vortex and left to stand for 10 minutes. After ten minutes, the vials were spun in a microcentrifuge for 1 minute.
- To a third set of vials, 0.5 mL of PBS buffer was added to each and 0.5 mL of the supernatant from the precipitated solutions (Group B) was added. These vials are referred to as Group C
- The vials from group A and C were counted in the gamma counter for 1 minute. The free iodide content was calculated as Equation C1.

$$\%FreeIodide = \frac{3 \times GroupC_{average}}{GroupA_{average}} \times 100 \quad (C1)$$